COMPLETE KINEMATIC AND KINETIC HAND FUNCTION: A METHOD, MAPPING AND MODEL

By

Joshua P. Drost

A DISSERTATION

Submitted to
Michigan State University
in partial fulfillment of the requirements
for the degree of

Engineering Mechanics—Doctor of Philosophy

2019

ABSTRACT

COMPLETE KINEMATIC AND KINETIC HAND FUNCTION:
A METHOD, MAPPING AND MODEL

By

Joshua P. Drost

Millions of people have reduced hand function; this loss of function can be due to injury, disease, or aging. Osteoarthritis is the leading cause of hand dysfunction in America, affecting over 60% of Americans over the age of 55. However, the current methods to quantify changes to hand function—such as questionnaires, goniometers, and dynamometry— are limited. In order to move towards personalized medicine and to design better devices for individuals with reduced hand function, it is critical to have an objective understanding of how hand function changes.

Therefore, the goals of this work were to 1) develop a method to quantify and visualize hand function in terms of kinematics (where the digits can reach) and kinetics (how the digits can apply force); 2) experimentally quantify the function of healthy fingers and develop a generalized linear mixed model (GLMM) to represent the finger function; and 3) track how hand function changes due to osteoarthritis and due to surgery.

First, a functional testing protocol was developed to calculate and visualize hand function. Motion capture was used to track finger and thumb postures over their ranges of motion and a multi-axis load cell with custom attachments was used to compute finger forces different at positions over their ranges of motion. The motion data were used to calculate the kinematic space of the digits, or everywhere each digit could reach. Then, the force data were transformed to the same coordinate space and mapped onto the kinematic spaces of each finger of each participant. Further, the functional data were normalized by the participants' hand sizes and mapped to create population models.

Next, the functional testing protocol was used to quantify finger function of forty-one healthy individuals. Maximum finger forces were affected by the fingers' joint angles (GLMM

p<0.001), and direction of the force (GLMM p<0.001). Those differences were used to develop a generalized linear mixed model to estimate heathy finger strength across the ranges of motion for all four fingers.

Then, the healthy participants' index finger function was compared to a population of participants with hand OA. The ranges of motion were smaller in participants with OA leading to an average 23% decrease in the kinematic space of the index finger. The OA group applied less force (Analysis of Variance p<0.001), using a smaller range of joint angles (ANOVA p=0.01) in a smaller range of directions (ANOVA p<0.001). The forces applied by the participants with OA also had reduced variation due to finger posture or force direction, as compared to healthy participants.

Finally, five patients were tested determine the effects of thumb suspensionplasty (removal of the trapezium followed by insertion of a suture wire between the first and second metacarpals). Participants were tested at three time points: before surgery, six weeks post-surgery, and again twelve weeks post-surgery. As expected, the suspensionplasty led to reduced pain in all patients; however, function was not consistently improved. Carpometacarpal joint ranges of motion were decreased due to the surgery, and the kinematic space of the thumb was similar after surgery to before surgery. The ability to apply forces, in terms of force magnitude, range of directions, and volume of space used to apply force, was not improved due to the surgery, but also did not lessen.

The ability to quantify motion and force data for each finger and map them together provides an improved understanding of the effects of treatments and rehabilitation and can lead to better informed device design. The models presented in this work can be used to compare an individual's function to normative function so clinicians can determine what function was lost and develop a treatment plan. Going forward, this process can be used to compare other populations, such as stroke or juvenile arthritis, to determine how function has changed, or compare to other surgeries to understand how different procedures lead to different outcomes for patients with severe OA.

ACKNOWLEDGMENTS

This dissertation is the finale of my work as a student at MSU, but I would not have been able to arrive here without the help and support of so many people.

First of all, I would like to thank my advisor, Dr. Tamara Bush, for nine years of mentoring and advice. I have learned almost everything I know about research from her and hope to one day be as inspiring of a mentor as she is. I would also like to thank my graduate committee—Dr. Grace Hong, Dr. Patrick Kwon, and Dr. Sara Roccabianca—for their support and input on my work. Dr. James Clarkson was an amazing clinical collaborator who always had new ideas for research. And I would not have made it through my graduate career without the help of Dr. Katy Colbry, Craig Gunn and the Mechanical Engineering office staff.

I had the honor of working with many incredible students, both graduate and undergraduate, while in the Biomechanical Design and Research lab. I am so grateful to the students who came before me and mentored me, and the students who came after me and I was able to mentor.

My wife, Tara, was an amazing support throughout my degree. I do not know how I would have made it without her love or the lunches she made me. Additional thanks to my family who constantly asked me when I would be done and encouraged me until I was.

And finally, I would like to thank my Lord and Creator. This work was done by His strength, for His glory.

TABLE OF CONTENTS

LIST OF TABLES ix

LIST OF FIGURES x

1 INTRODUCTION 1

2 FUNCTIONAL ABILITIES OF THE HAND AND CHANGES DUE TO OSTEOARTHRITIS: A LITERATURE REVIEW 4
- 2.1 Hand Anatomy 5
- 2.2 Osteoarthritis of the Hand 6
  - 2.2.1 Prevalence 6
  - 2.2.2 Treatments 7
- 2.3 Tools for Understanding Changes in Hand Function 9
  - 2.3.1 Questionnaires 9
  - 2.3.2 Task Based Tests 11
  - 2.3.3 Questionnaires and Task Based Tools 12
  - 2.4 Experimental Data and Models 12
  - 2.4.1 Kinematic Experiments and Models 13
  - 2.4.2 Kinetic Experiments and Models 15
  - 2.4.3 Task Based Experiments and Models 16
  - 2.4.4 Kinematic and Kinetics 17
- 2.5 Summary 18

3 MAPPING TOGETHER KINETIC AND KINEMATIC ABILITIES OF THE HAND 20
- 3.1 Introduction 21
- 3.2 Methods 22
  - 3.2.1 Participants 22
  - 3.2.2 Measurements 22
  - 3.2.3 Kinematic Range of Motion Measurements 23
  - 3.2.4 Force Measurements During Flexion and Extension 24
  - 3.2.5 Force Measurements During Adduction and Abduction 25
  - 3.2.6 Modeling the Kinematic Space 25
  - 3.2.7 Mapping Force Data to the Kinematic Space 26
  - 3.2.8 Population Force Spaces 27
  - 3.2.9 Statistical Analysis 27
- 3.3 Results 28
- 3.4 Discussion 30

4 DIFFERENCES IN FINGER STRENGTH OVER THE KINEMATIC SPACE, AN EXPERIMENTAL MODEL 33
- 4.1 Introduction 34
- 4.2 Methods 35
  - 4.2.1 Participants 35
  - 4.2.2 Experimental Data Collection 35
  - 4.2.3 Individual and Population Force Maps 37
  - 4.2.4 Statistical Differences Within and Between Fingers 39
  - 4.2.5 Generalized Linear Mixed Model 40
- 4.3 Results 42

4.3.1 Participants 42
4.3.2 Statistical Differences in Force Generation Within and Between Fingers 42
4.3.3 Generalized Linear Mixed Model..45
4.4 Discussion 46
4.4.1 Statistical Differences in Force Generation Within and Between Fingers 46
4.4.2 Generalized Linear Mixed Model..47
4.4.3 Limitations 48
4.4.4 Conclusions 48

5 QUANTIFYING FUNCTIONAL DIFFERENCES IN THE INDEX FINGER DUE TO OSTEOARTHRITIS 50
5.1 Introduction..51
5.2 Methods 52
5.2.1 Participants 52
5.2.2 Experimental Data Collection 52
5.2.3 Mapping the Motion and Force Abilities 53
5.2.4 Comparing Arthritic Population to a Healthy Population 55
5.3 Results 56
5.3.1 Participants 56
5.3.2 Functional Differences due to Osteoarthritis 56
5.3.3 Comparing Arthritic Individuals to a Healthy Population 58
5.4 Discussion 59
5.4.1 Functional Differences due to Osteoarthritis 60
5.4.2 Comparing Arthritic Individuals to a Healthy Population 61
5.4.3 Limitations 61
5.4.4 Conclusions 61

6 CHANGES IN THUMB FUNCTION DUE TO CARPOMETACARPAL JOINT SUSPENSIONPLASTY, A PILOT STUDY 63
6.1 Introduction..64
6.2 Methods 65
6.2.1 Participants 65
6.2.2 Clinical Methods 66
6.2.3 Range of Motion 66
6.2.4 Force Generation 67
6.2.5 Mapping Forces to the Range of Motion 68
6.2.6 Analysis 69
6.3 Results 70
6.3.1 Clinical Tests 70
6.3.2 Range of Motion 71
6.3.3 Forces...73
6.4 Discussion 73
6.4.1 Limitations 75
6.4.2 Conclusions 75

7 Conclusions...77

APPENDICES 79
Appendix A: 8.1 Protocol for quantifying thumb function. 80
Appendix B: MATLAB Codes...86

REFERENCES..107

LIST OF TABLES

Table 2.1: Radiographic OA prevalence and confidence intervals (Pereira et al., 2011).............7

Table 2.2: FIHOA is a shorter questionnaire than most with only ten questions. 10

Table 3.1: Notation used for analysis. 26

Table 4.1: Mean force and standard deviation by region for male and female participants (N). The regions that are blank are regions with too few force trials to be accurately averaged (n<7). 44

Table 4.2: Mean force angle (°) in the sagittal plane and standard deviation by region for male and female participants. The angle is measured as the angle from the vector normal to the palm. 44

Table 4.3: GLMM covariate estimates and significance when the digits were modeled separately (left) and when digits were modeled together (right)...45

Table 5.1: Mean and standard deviations of joint range of motion as well as maximum and minimum joint angles for the index finger joint for both the healthy and OA groups (°). Joint angles are measured from parallel with the palm, with negative angles being hyperextension..56

LIST OF FIGURES

Figure 2.1: Joints and Bones of Hand 5

Figure 2.2: Hand OA Prevalence in Framington Cohort Study (Haugen et al. 2011). Vertical axis is the percent of the sample with erosive and non-erosive hand OA per age group. 6

Figure 2.3: Example of one test from HAMIS, testing the total finger function. A higher grade shows less function. This is one of nine total tests and at the end the scores are added for the final grade (Sandqvist and Eklund, 2000a, 2000b) 11

Figure 2.4: Common clinical tools for testing range of motion and grip strength. Left: goniometer. Middle: power grip dynamometer. Right: pinch grip dynamometer. 13

Figure 2.5: Left: hand clamp set-up for finger strength. Right: thimble and handle set up for finger force collection testing (Cruz et al., 2005; Valero-Cuevas et al., 1998). 18

Figure 3.1: Locations of motion capture markers on hand and kinematic motions. Individual markers were placed on the wrist and rigid body marker clusters were placed on each phalanx and the back of the palm for a total of 67 markers. a) Reference, b) Flexion/extension of the MCP joints, c) Flexion/extension of the interphalangeal joints, d) Adduction/Abduction of the MCP joints. 23

Figure 3.2: Force Measurement procedure: A U-shaped bracket was placed in each of seven positions where the participant was asked to a) push and then b) pull. Adduction/abduction force measurement procedure: c) three positions to push and d) three positions to pull using different degrees of adduction and abduction. This procedure measured participants’ maximum forces in push and pull orientations while varying the finger posture (e & f). A multi-axis load cell was attached below the system. 24

Figure 3.3: Sagittal plane view of kinematic finger space with overlaid force vectors for the index finger. The displacements of the figure are measured from the center of the wrist. The greyscale background represents the range of orientations the distal phalanx can reach at the specific point and colored arrows represent the forces that were applied at each position with relative magnitudes. The transparent finger on the figures indicates the orientation of the image..........28

Figure 3.4: Sagittal plane view of kinematic finger spaces with overlaid force vectors for each finger of a single participant. 29

Figure 3.5: Sagittal projection of each index finger force for all participants. Displacements are normalized based on participant’s finger length. The orientation is the same as Figure 3, but the displacements are measured from the center of the first MCP joint...29

Figure 3.6: Average maximum force abilities across the four fingers for each trial with standard error. 29

Figure 3.7: Average index fingers forces with standard error for each trial. a) Flexion-Extension tests b) Abduction-Adduction tests 30

Figure 4.1: Figure 4.1: Experimental setup used to obtain range of motion and force abilities for the four fingers. (a) MCP flexion/extension, (b) IP flexion/extension, (c) MCP adduction/ abduction (d) flexion/extension pull force trial, (e) adduction/abduction push force trial.............37

Figure 4.2: Mapping together kinematic and kinetic finger function. Top: Individual force map shows the kinematic space of the index finger in grayscale, and the forces applied as colored arrows. Middle: The population force map of the participants (n= 41) shows all the forces applied by participants' index fingers for all finger postures. Bottom: Averaged force capability for regions within the kinematic space. Regions were numbered from full extension (1) to full flexion (10). 38

Figure 4.3: Definitions of finger posture and force direction. (a) Finger posture as defined by the flexion of the three joints of the finger. (b) Finger posture measured as the polar position of the fingertip in relation to the MCP joint. (c) Force direction was defined as the angle between the force vector and the vector normal to the fingertip in the sagittal plane. 39

Figure 4.4: Average force abilities over the range of motion for all four fingers for all participants. Each range of motion is subdivided into regions, and the color represents the average force in the region. The black regions are areas where to few force events (n<7) occurred for accurate averages. 43

Figure 5.1: Experimental setup to obtain range of motion and force abilities for the index finger. (a) MCP flexion/extension, (b) IP flexion/extension, (c) MCP adduction/ abduction, (d) flexion/extension pull force trial, (e) adduction/abduction push force trial 52

Figure 5.2: Force data mapped to the kinematic space. These maps are 2D representations of 3D data sets. The grey background represents the kinematic space of the finger. The colored arrows represent force actions in position, direction and magnitude. First an individual's force abilities are mapped to his or her kinematic space (left). Next, all individuals in a population are mapped together (center). Finally, the population's abilities are averaged over regions of the kinematic space (right). 54

Figure 5.3: Definitions of finger posture and force direction. (a) Finger posture measured as the region in the kinematic space. (b) Finger posture as defined by the flexion of the three joints of the finger. (c) Force direction was defined as the angle between the force vector and the vector normal to the fingertip in the sagittal plane. 55

Figure 5.4: Index finger forces mapped to the kinematic space. Top: Population maps of all force events. Bottom: Regional maps of average forces across the kinematic space. 57

Figure 5.5: Four female participants in the OA group compared to the healthy female population. The regional map in the background shows the healthy female data. The black outline describes the arthritic participant's kinematic space, a smaller kinematic space indicates reduced motion function. The colored arrows represent the force actions of that participant, forces with similar colors indicate the individual has healthy force function. 59

Figure 6.1: Motions to determine thumb kinematic space: a) flexion/extension of thumb metacarpophalangeal and interphalangeal joints; b) opposition to the pad of the 5th digit; c) palmar abduction; d) radial abduction...67

Figure 6.2: Thumb force measurement apparatus. a) Hand is rotated at 60° and thumb is pushing towards the ground. b) Hand is level with the ground and pulling toward the palm.......68

Figure 6.3: Force map of the thumb for a participant. The grey background represents the kinematic space of a participant's thumb, while the white background represents the kinematic space of a representative healthy participant. Both have been scaled by the participants' thumb lengths. The color scale represents the amount of force that was applied, with each vector representing a 2D projection of the direction of the force and position within the kinematic space where the force was applied. A semi-transparent thumb is overlaid on the figure to describe the orientation. 69

Figure 6.4: Changes to clinical measurements following surgery. A higher VAS score indicates higher pain. A higher DASH score indicates less hand function. 71

Figure 6.5: Change in range of motion and kinematic space due to surgery for each participant. Left: Flexion/extension differences. Middle: Adduction/abduction differences. Right: Change in volume of the kinematic space of the thumb. 72

Figure 6.6: Differences in force production for one participant and all participants. Top: Visualized force profiles over the range of motion for Participant 2 at each testing point. Bottom: Differences in magnitude of force, range of force directions and volume of force space between three time points. 73

Figure 6.7: Differences in force production for one participant and all participants. Top: Visualized force profiles over the range of motion for Participant 2 at each testing point. Bottom: Differences in magnitude of force, range of force directions and volume of force space between three time points. 74

Figure 8.1: Motion protocol for the thumb. a) Motion capture marker placement for the thumb. b) MCP and IP flexion and extension. c) Opposition to the pad of the fifth digit. d) Palmar and radial abduction........80

Figure 8.2: The CMC joint of the thumb has two degrees of freedom. Left: flexion is rotation around the second metacarpal. Right: abduction is rotation away from the second metacarpal 81

Figure 8.3: Kinematic space of the thumb. Left: Three dimensional view of the kinematic space. Right: Two dimensional projection looking from the wrist towards the fingers. A transparent thumb has been added to indicate orientation. 83

Figure 8.4: Thumb force measurement apparatus. a) Hand is rotated at 60° and thumb is pushing towards the ground. b) Hand is level with the ground and pulling toward the palm.......84

Figure 8.5: Force map of the thumb for an individual. The grey background represents the kinematic space of a participant's thumb. The color scale represents the amount of force that was applied, with each vector representing a 2D projection of the direction of the force and position within the kinematic space where the force was applied. 85

1 INTRODUCTION

Loss of hand function can be caused by many factors including injury, stroke, and arthritis. Osteoarthritis (OA), specifically, is one of the most common causes of changes to hand function, affecting over 60% of Americans over the age of 55. (Haugen et al., 2011; Zhang et al., 2002). A better understanding of how OA affects hand function will lead to improved diagnosis, treatment and products designed for individuals with hand OA.

Several approaches have been used to define hand function, however, most of these approaches are subjective (Dziedzic et al., 2005). For example, how well the individuals' hands are able to accomplish tasks of daily living is one approach to identifying function (Visser et al., 2015). Pain is another important part of hand function as pain limits joint use (Scott and Huskisson, 1976). Questionnaires are used to evaluate the ability to accomplish tasks of daily life or the amount of pain felt during those tasks (Dziedzic et al., 2005; Prodinger et al., 2016). While these tests are easy to administer, they are subjective and are not able to quantify the function that has been lost. Kinematics (movement) and kinetics (forces) have been used to define function: goniometers (protractors for joints) and dynamometers (grip force scales) are commonly used to measure joint ranges of motion and total grip strength. Unfortunately, these tools have significant shortcomings: goniometry measurements have high variability and dynamometers only measure whole hand strength in limited postures (Cook et al., 2007; Ellis and Bruton, 2002; Nicolay and Walker, 2005). Improved tools to measure the movement and strength capabilities of the hand would allow for a better understanding of the changes to function.

The overall goal of this work was to experimentally quantify the functional abilities (kinematic and kinetic) of the hand, then develop a visualization of and statistically model changes to function for populations and individuals. This was accomplished by computing and modeling the range of motion of the hand and the forces that were applied over that range of motion. Then, the developed protocol was used to understand how function changed in populations as a result of osteoarthritis and surgery. This work was completed through four specific aims:

Specific Aim 1 was to develop and demonstrate a method for measuring and mapping the kinematic and kinetic abilities of the hands together. To do this we developed an experimental method to obtain motion and strength measurements across the range of motion for the index finger and demonstrated the approach on the other three fingers. Then we created a population mapping of the range of motion abilities and strength abilities for both individuals and the entire test population.

Specific Aim 2 was to experimentally quantify finger forces of all four fingers over their individual movement (i.e. kinematic space); use a statistical modeling approach to understand what causes differences in the finger forces that can be applied by healthy participants over their kinematic spaces; and develop a statistical model to estimate the forces that can be produced by the fingers.

Specific Aim 3 was to objectively determine how index finger function is reduced as a result of osteoarthritis, specifically differences in motion and strength abilities.

Specific Aim 4 was to quantify how thumb CMC suspensionplasty affected the function of the thumb in terms of pain, range of motion, and strength. A stronger understanding of the changes in function due to mini-tightrope suspensionplasty will lead to more informed surgeons who can better select the right surgery for each patient.

This document is formatted as a literature review followed by four chapters that either have been, or will be, submitted to a journal for publication. Chapters are as follows:

Chapter 1: A literature review of functional abilities of the hand and changes due to osteoarthritis

Chapter 2: Mapping together kinetic and kinematic abilities of the fingers

Chapter 3: Differences in finger strength over the kinematic space, an experimental model

Chapter 4: Quantifying functional differences in the index finger due to osteoarthritis

Chapter 5: Changes in thumb function due to carpometacarpal joint suspensionplasty, a pilot study

Conclusions

Appendix: MATLAB codes

2 FUNCTIONAL ABILITIES OF THE HAND AND CHANGES DUE TO OSTEOARTHRITIS: A LITERATURE REVIEW

2.1 Hand Anatomy

There are 27 bones in the hand (Thompson and Netter, 2010). Eight carpal bones form the wrist and carpal tunnel. The palm of the hand is composed of the five metacarpal bones. Most distally are the phalanges, the first digit (thumb) has a proximal and distal phalange, and the second through fifth digits (fingers) have proximal, medial, and distal phalanges.

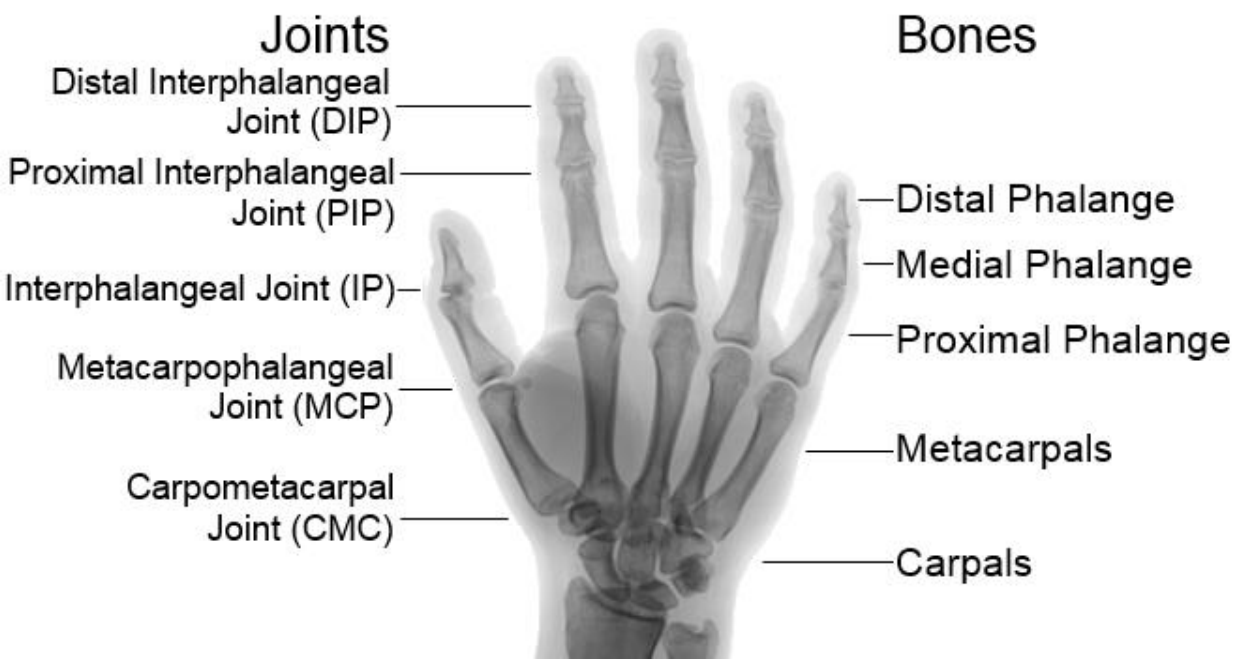

Figure 2.1: Joints and Bones of Hand

The carpals and metacarpals are connected by the carpometacarpal (CMC) joints which vary in amount and types of motion. The first CMC has significant motion and allows flexion, extension, adduction, abduction, and opposition. The second and third CMC joints are mostly fixed and allow little movement. The fourth and fifth CMC joints allow small amounts of flexion and extension motion, which is how the palm can be cupped. Metacarpophalangeal (MCP) joints connect the metacarpals and phalanges; the first MCP only flexes and extends, while the second through fifth MCP joints can also adduct and abduct (move side to side). Interphalangeal (IP) joints connect the phalanges and allow flexion and extension. The thumb has only one interphalangeal joint, while the fingers have two: a distal interphalangeal (DIP) joint and a proximal interphalangeal (PIP) joint. These bones and joints are shown in Figure 2.1.

2.2 Osteoarthritis of the Hand

2.2.1 Prevalence

Osteoarthritis (OA) is common among the aging population. OA occurs due to a breakdown of joint cartilage and the surrounding bone and results in swelling, pain, and stiffness (Haugen et al., 2016; Pereira et al., 2011; Thompson and Netter, 2010). The exact prevalence changes depending on how it is documented. OA can be radiographic (changes to joint can be seen in an x-ray) or symptomatic (the individuals has symptoms of pain and loss of function). Hand OA can also be defined as erosive or non-erosive; erosive hand OA involves bone changes and leads to more pain and synovitis, and is more aggressive than non-erosive OA (Haugen et al., 2016).

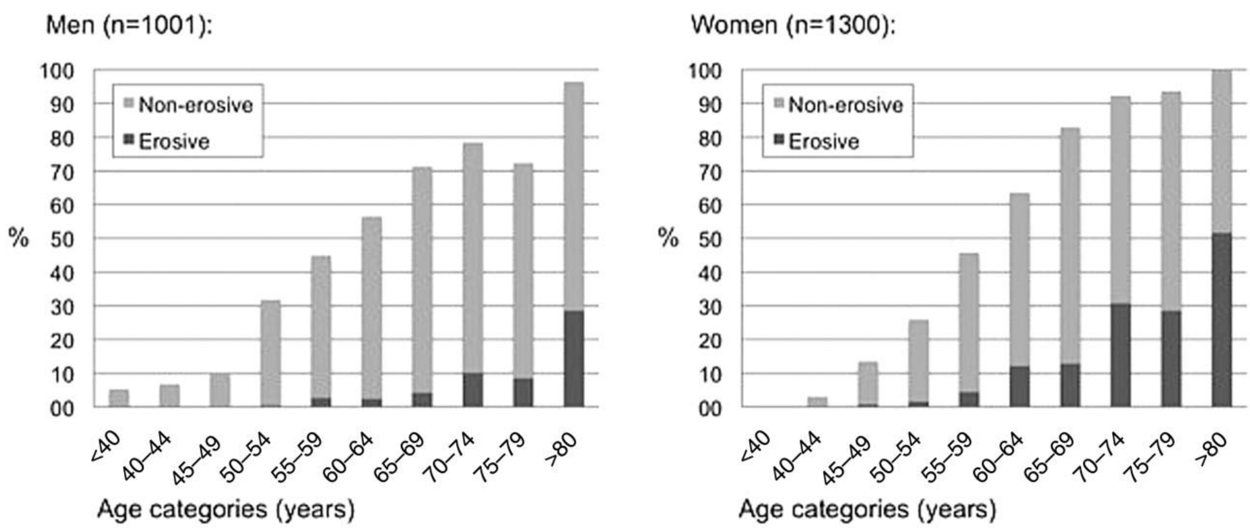

Figure 2.2: Hand OA Prevalence in Framington Cohort Study (Haugen et al. 2011). Vertical axis is the percent of the sample with erosive and non-erosive hand OA per age group.

Three main cohort studies have been conducted in the US focusing on hand osteoarthritis: 1) the Framington, 2) Rotterdam, and 3) Johnston County studies (Dahaghin et al., 2005; Haugen et al., 2011; Qin et al., 2017; Zhang et al., 2002). The Framington study included 2301 participants (1001 males mean age 59.2 years; 1300 women mean age 58.7 years) and found that 47.9% of males and 50.5% of females had radiographic OA in one joint of their hand (Figure 2.2). This drops down to 8.2% and 15.9% occurrence respectively for symptomatic hand OA in one joint, and 3.6% and 9.8% for erosive hand OA in one joint. (Haugen et al., 2011; Zhang et al., 2002). The Rotterdam study found similar results, where 67% of the women and 54.8% of the men had radiographic OA in at least one hand joint (Dahaghin et al., 2005).

Table 2.2: Radiographic OA prevalence and confidence intervals (Pereira et al., 2011).

Joint Site	OA Prevalence Women	OA Prevalence Men	OA Prevalence Total
Knee	27.3%	21.0%	23.9%
Hip	11.60%	11.50%	10.90%
Hand	43.30%	44.50%	43.30%

The Johnston County cohort study focused on the risk of developing hand OA and found that the overall lifetime risk of hand OA (i.e. that an individual will develop OA by 85 years old) is 39.8%. The chance is higher for females (47.2%) as compared to males (24.6%) (Qin et al., 2017).

Pereira *et al.* published a comprehensive literature review in 2011 which reviewed 72 prevalence studies that had been published prior to 2011. Between the twenty studies in the review, they estimated an average prevalence of 43.3% of women and 44.5% of men have some form of hand OA in at least one joint (Table 2.2). It is of note that the highest OA prevalence estimates were found in hand joints but the knee is the most studied joint, based on the number of publications they found in their review (Pereira et al., 2011).

2.2.2 Treatments

Several treatment approaches are available for hand OA. Towheed and Mahindra published a series of literature reviews of random controlled trials comparing different hand OA treatment methods (Lue et al., 2017; Mahendira and Towheed, 2009; Towheed, 2005). They found that medications such as NSAIDS (nonsteroidal anti-inflammatory drugs), systematics, inter-articular and topical drugs are common treatments, with NSAIDs being the most common medication (Mahendira and Towheed, 2009).

Exercise and therapy are common treatments for hand OA, seeking to improve strength and movement and reduce pain. Exercise and education have been shown to reduce the effects of arthritis and improve hand function in some studies (Bjurehed et al., 2017). However, other studies have indicated exercise did not show improvement in muscle strength and function or decreased pain (Magni et al., 2017). It should be noted that this review had strict inclusion criteria, only investigating five random controlled trials out of 42 found.

Surgery is an option in severe cases. Trapeziectomy, removal of the trapezium bone from the carpals, is the most common surgery to treat severe thumb CMC OA (Li et al., 2011). While in the short term these surgeries may lead to a reduction in pain and increase in function, there is not consistent proof that these procedures are effective over the long term (Vermeulen et al., 2011). Removal of the trapezium is often followed by reconstruction of many of the ligaments of the CMC joint, to provide support and movement to the thumb after surgery (Li et al., 2011).

Basal joint arthroplasty goes one step further: after removal of the bone, a synthetic joint is implanted to replace the thumb CMC joint. Often times this is a total joint implant made of metal, ceramic or polymer (Huang et al., 2015). However, these arthroplasty techniques can be controversial. Based on evidence arthroplasty can improve short term outcomes yet tend to do poorly in long term outcomes, as compared to trapeziectomy (Huang et al., 2015; Miller et al., 2018). Another approach is the mini tight rope method, which uses a strong thread to attach the base of the thumb metacarpal to the second metacarpal (Friebel et al., 2018). This is a newer approach, based on approaches in the knee and ankle (Eguchi et al., 2014; Storey et al., 2012). Early studies on the tightrope method have had favorable outcomes as compared to other thumb fixation methods in cadaveric tests and case studies (Assiotis and Giannakakis, 2017; Desai et al., 2016; Friebel et al., 2018; Hooke et al., 2016; Parry and Kakar, 2015).

There are other treatments that have shown improved quality of life for individuals with hand OA (Lue et al., 2017). Currently, multiple groups are developing soft robotic devices to assist with hand therapy to reduce function loss (Chu and Patterson, 2018). These devices allow a patient to continue treatments at home and without constant supervision of a therapist; as portability, patient outcomes and safety are improved they could become widely used (Chu and

Patterson, 2018). Splints and gloves have been used to support joints of the hand, typically the thumb CMC joint. Dietary supplements have been found to be effective, but not more so than medications. Leeching has also been shown to reduce pain and improve quality of life over a two-month period (Michalsen et al., 2008).

One issue with these treatments is the lack of objective measures used to understand their impact. There are many tools to measure hand function and changes, but most are subjective. Being able to objectively measure improvements due to treatment will allow for better treatment of hand OA and better patient outcomes.

2.3 Tools for Understanding Changes in Hand Function

2.3.1 Questionnaires

Questionnaires are the main tool used to diagnose changes in hand function (Dziedzic et al., 2005). They present many benefits over other tools: they are simple and easy to administer, they do not require any extra equipment, and the results are easy to understand. Many questionnaires are also in the public domain, so they do not cost anything to use (Dziedzic et al., 2005). The downside to these questionnaires is that they are entirely subjective: the results are based on the impressions and opinions of the patient. A 2005 literature review compared eighteen measurement tools for hand function (Dziedzic et al., 2005). Some tests were broad and could be used for any hand condition, while other tests were specific to the effects of hand OA on function and quality of life. Six tests (four questionnaires, two functional tests) will be specifically explained below as they are more commonly used clinically to understand hand function in individuals with arthritis.

The Michigan Hand Outcomes Questionnaire (MHOQ) is a 37-item questionnaire that takes approximately 10 minutes to complete. Patients answer questions about their overall hand function, activities of daily living, pain, work performance, aesthetics, and patient satisfaction with hand function. It has been translated into different languages and tested and validated all over the world (Chung et al., 1998).

The Visual Analog Scale (VAS) is the most widely used tool to understand pain associated with hand OA. The tool includes a 0-10 scale where 0 is “No Pain” and 10 is “Pain as Bad As It Could Be” (Scott and Huskisson, 1976). The patients mark on the scale how much pain they are in, which is then measured as a value between 0 and 10. While the test is highly subjective, it is easy to use (Visser et al., 2015).

AUSCAN (Australian Canadian Osteoarthritis Hand Index) is a 15 item questionnaire developed by a multinational team to measure the symptoms of hand OA and has been validated for test-retest reliability and consistency (Bellamy et al., 2002). AUSCAN provides comparable results to other questionnaires. Compared to other hand questionnaires developed specifically for OA, AUSCAN is one of the most applied and evaluated tools for hand OA. A major downside of AUSCAN is that it is not in the public domain, which limits its use (Visser et al., 2015).

Table 2.2 : FIHOA is a shorter questionnaire than most with only ten questions. (Dreiser et al., 2000)

1.	Are you able to turn a key in lock?
2.	Are you able to cut meat with a knife?
3.	Are you able to cut cloth or paper with a pair of scissors?
4.	Are you able to lift a full bottle with the hand?
5.	Are you able to clench your fist?
6.	Are you able to tie a knot?
7.	*For women:* Are you able to sew? *For men:* Are you able to use a screwdriver?
8.	Are you able to fasten buttons?
9.	Are you able to write for a long period of time?
10.	Would you accept a handshake without reluctance?

Scoring System: 0=possible without difficulty, 1= possible with slight difficulty, 2=possible with important difficulty, 3=impossible.

The Functional Index for Hand OA (FIHOA) is another questionnaire specifically for hand OA. What makes FIHOA unique is that it is short: a total of ten questions shown in Table 2.2 (Dreiser et al., 2000). It has been validated and compared to other similar questionnaires (Moe et al., 2010).

Each of these questionaires has different scales, outcomes and possible interpretations. Due to that it is difficult to compare results between the different tools. Prodinger *et al.* developed an algorithm to convert many of the common tools (including AUSCAN and FIHOA) to a common 0-100 scale (Prodinger et al., 2016).

2.3.2 Task Based Tests

Not all current tools are questionnaires; some are based on measuring the abilities of the fingers. The Jebsen–Taylor Hand Function Test (JTT) is a tool designed in 1969 to assess upper extremity function by measuring the time to complete seven tasks which is then compared to a set of normative values (Hackel et al., 1992). The JTT can determine upper extremity function and is objective, task based, and simple to administer. On the downside, it cannot tell specifically how function has been lost (changes to range in motion or strength), only that the function has been lost. There are differing opinions on the validity of this approach for determining treatment effectiveness; some researchers have compared it to other methods (the MHOQ) and found that time to finish tasks is not as repeatable as a questionnaire to measure loss of hand function (Davis Sears and Chung, 2010). It should be pointed out that the cited study was published by the researchers who developed the MHOQ.

Figure 2.3: Example of one test from HAMIS, testing the total finger function. A higher grade shows less function. This is one of nine total tests and at the end the scores are added for the final grade (Sandqvist and Eklund, 2000a, 2000b)

Finger Flexion	
Can bend fingers 2-5 around a pencil (5 mm diam). All fingers must be tight to the object.	0
Can bend fingers 2-5 around a piece of cutlery (15 mm diam)	1
Can bend fingers 2-5 around a handlebar (30 mm diam).	2
Cannot manage the previous item	3

Hand mobility in scleroderma (HAMIS) is a tool where participants are asked to perform nine tasks related to range of motion of the hand and graded for each task by the test administrator, which is combined to give the final grade (Sandqvist and Eklund, 2000a, 2000b). It is a hybrid quantitative and qualitative test, evaluating range of motion of the hand during daily tasks but is graded by the tester. An example of one of the tasks is shown in Figure 2.3 The other tests assess finger extension, abduction of the thumb, pinch grip, finger abduction/adduction, dorsal extension and volar flexion of the wrist, and pronation and supination. It was designed and validated for Scleroderma but has also been used for hand OA (Sandqvist and Eklund, 2000a, 2000b).

The JTT and HAMIS are the commonly used functional tests (Visser et al., 2015). There are other tests, such as the Moberg Pick-Up Test; while these tests are well developed, they are not used as often (Visser et al., 2015). Most commonly, function is measured using simple grip or pinch tests using dynamometers (Visser et al., 2015).

2.3.3 Questionnaires and Task Based Tools

Overall, the questionnaires are easy to administer and provide understandable results but are subjectively based on the participant. This makes it difficult to compare between participants and even can change based on the participants mood between testing events. The task-based JTT measures time to complete tasks; however, the results are less clear, and it is difficult to know if a slow time to complete tasks is due to hand disfunction or neurological reasons. HAMIS aims to relate how well a task is completed but does so by being subjectively based on the tester. An ideal tool for hand dysfunction would be easy to administer, objective, and output results towards understanding the individual's loss of function.

2.4 Experimental Data and Models

Significant research has been experimentally and computationally conducted to better understand aspects of hand function. Due to the complexity of the hand, most studies focus on only one aspect of function such as kinematics (ability to move hand and range of motion) or kinetics (ability to apply force, typically whole hand grip). Experimental data and computational models investigating strength and motion abilities of the hand are limited, there are even fewer that map the two together.

2.4.1 Kinematic Experiments and Models

The most common tools used to measure range of motion are goniometer (specialized protractors to measure joint angles), electro goniometers, and motion capture (Cook et al., 2007; McVeigh et al., 2016). Studies have shown that measuring range of motion with goniometry and electro-goniometry is related to functional disability (Bashardoust Tajali et al., 2016). Goniometry is most commonly used in clinical settings due to its simplicity, as shown in Figure 2.4 Left, yet has low interrater reliability and is significantly less accurate than motion capture (Cook et al., 2007; Ellis and Bruton, 2002). Other measurement tools have been used, such as wire tracing, composite finger flexion, visual assessment and angle sensing gloves, but they are either less accurate or more difficult to use (Dipietro et al., 2003; Ellis et al., 1997; Ellis and Bruton, 2002; McVeigh et al., 2016; Simone et al., 2005).

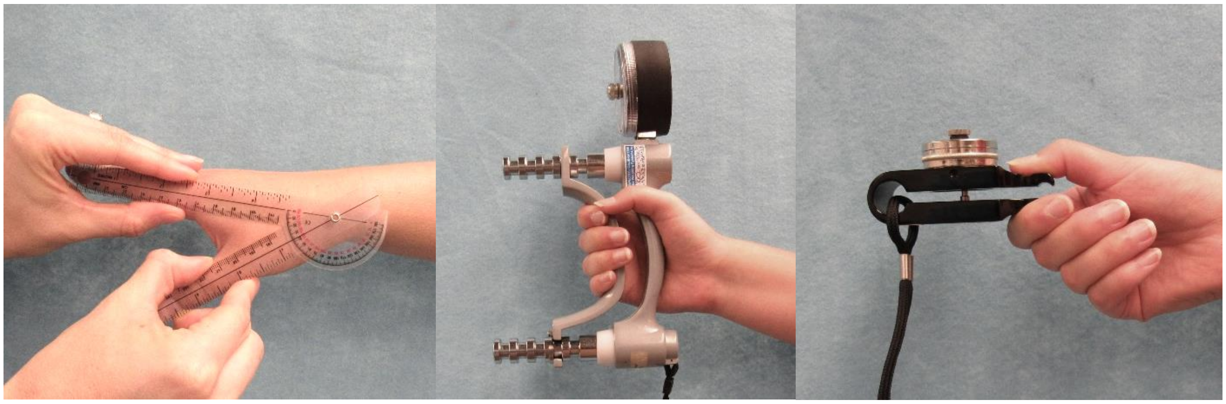

Figure 2.4: Common clinical tools for testing range of motion and grip strength. Left: goniometer. Middle: power grip dynamometer. Right: pinch grip dynamometer.

Several research groups have tested the Microsoft Kinect for motion capture. It is a one device system, and can be used for whole-body motion data (Sharp et al., 2015). The Microsoft team has built an in-house program that is able to match hand gestures. They found it to be consistent at determining complex postures (Sharp et al., 2015). However, the program is not available to the public, and can only match pre-taught gestures. Another team used particle-swarm optimization to determine hand posture in real time (Oikonomidis et al., 2011). However, these approaches have low accuracy and cannot measure precise movements of the hand and are better suited for whole body applications that do not require high accuracy (Galna et al., 2014; Mousavi Hondori and Khademi, 2014).

Other studies investigated total kinematic abilities of the hand and the functional space it uses to accomplish tasks. Hume *et al.* measured the range of motion of each finger using goniometry, and what subsection of that space is used for common activities similar to the activities in FIHOA described in Figure 2.3 (Hume et al., 1990). Leitkam *et al.* used motion capture to quantify the range of motion for each finger in terms of the number of ways to reach a position, the range of fingertip orientation angles at each position and the theoretical range in force application directions at each point (Leitkam et al., 2015, 2014). These tools were also used to analyze how different shaped objects could best be interacted within 3D space. Coupier *et al.* conducted similar research using optimized marker placement (Coupier et al., 2016).

Nataraj *et al.* studied the index finger and thumb, and developed a model that could determine the joint centers of those digits with minimal markers (Nataraj and Li, 2013). Cerveri *et al.* developed a computer program that could be calibrated to specific individuals to assist in real time position measurements of their hands (Cerveri et al., 2007). Viegas *et al.* conducted a wide range of work measuring maximal ranges of cadaver motion. Specifically, this work focused on different carpal bones and metacarpal joints and compared different bone shapes to different patterns of motion. This allowed them to understand motion within the palm, or cupping of the hand, which was not often included in hand models (Nanno et al., 2007; Peh et al., 1999; Viegas et al., 1993, 1991). Recent work focused on building models for prosthetic devices. These models use muscle activation as an input and finger position as an output (Blana et al., 2017).

Motion tests that have been conducted are wide ranging in terms of hand movements that have been studied. However, they focus solely of kinematic function and do not include any kinetic function.

2.4.2 Kinetic Experiments and Models

To investigate the force abilities of the hand, many researchers have evaluated grip strength which is typically tested through cylindrical objects containing load cells or dynamometers (Figure 2.4 Middle and Right). Nicolay *et al.* investigated the effects of hand size, gender, and handedness on grip strength (Nicolay and Walker, 2005). They found that the dominant hand was typically stronger than the non-dominant hand but fatigued faster. Hand strength is also highly correlated with hand and arm size: larger fingers, palms, and forearms relate to higher grip forces (Nicolay and Walker, 2005). Freund *et al.* tested whole hand power grip (e.g. holding a dumbbell or beverage) and measured the amount of force each finger contributed during the whole hand grip (Freund et al., 2002). Shivers *et al.* found that there was an optimal grip distance of 55 mm for applying force for a cylinder (Shivers et al., 2002). Young *et al.* evaluated breakaway strength, or the maximum force that could be applied to an object before it slipped out of the hand, and used bars at different orientations and with different friction coefficients to determine the common breakaway force of human – the amount of force required for an object to slip out of the hand (Young et al., 2010). Li found that wrist angle significantly affected the amount of force that could be applied by the fingers and that there was an optimal wrist position to apply forces with the fingers (Li, 2002).

Many authors have also researched finger synergy, or how multiple fingers interact while applying force. Multiple fingers apply force more efficiently and accurately due to shared muscle groups used to move fingers (Martin et al., 2011). Multiple fingers applying load together will individually apply loads in slightly different directions but the resultant of the finger will be in the desired direction (Gao et al., 2005). However, individual fingers apply lower individual forces and have lower individual accuracy during complex tasks (Danion et al., 2003). Other studies have investigated how nerves affect muscle strength, and the effects on shear forces (Kapur et al., 2010; Quaine et al., 2012; Yokogawa and Hara, 2002).

Other researchers used computer models and optimization approaches to determine joint and tendon loads during power grip; while these models are computationally strong, they are based in simulation and not validated with significant experimental data (An et al., 1985, 1983; Fok and Chou, 2010; Sancho-Bru et al., 2001; Wu et al., 2008). Serbest *et al.* developed a simulation model to calculate joint torques at different hand positions without external measuring devices; however, their model was not compared to experimental data (Serbest et al., 2016). Similarly, Qiu and Kamper created an anatomic model of joint contact forces during arthritis (Qiu and Kamper, 2014). Wohlman *et al.* compared their model to force data from two pinch positions (Wohlman and Murray, 2013). These models are computationally strong but are based on limited experimental data.

While there has been significant work conducted on hand strength specific to whole hand grip or individual positions, there is a gap in the research investigating forces at multiple finger postures. Most grip studies measure whole hand force in one or two positions. The synergy/enslaving studies help understand how fingers apply forces in relation to each other but are typically more focused on the nerve effects on the hand, not kinematics and kinetics. These studies do not describe the total force abilities of individual fingers across the complete kinematic range of movement.

2.4.3 Task Based Experiments and Models

There are many studies on specific tasks, such as typing or tasks of daily life, and how the hand moved and applied force during them. For example, researchers investigated playing the piano and clarinet (Angelaki and Soechting, 1993; Bella and Palmer, 2011; Hofmann and Goebl, 2016), opening weighted doors (Sanford et al., 2014), baseball pitching (Kinoshita et al., 2017) and opening jars (Fair et al., 2008). Lee and Jung measured how people interacted with objects (different sized cylinders), showing the effects of grip type, object size and weight on the hand posture (Lee and Jung, 2016). Bae and Armstrong developed a model of how humans grasped and interacted with specific objects based on experimental data (Bae and Armstrong, 2011). Howard *et al.* researched how people accomplished occupational tasks involving large objects, exploring how whole body forces are applied through the hand during a task (Howard et al., 2014).

Task based research has its benefits: it is directly relatable to specific actions in people's lives and can provide understanding of those specific situations. However, these tests have narrow outcomes and cannot be used to extrapolate other motions or actions. Non-task-based studies have the potential to be used to understand a broader area of tasks.

2.4.4 Kinematic and Kinetics

There are a couple research groups that have studied force abilities at different positions within the range of motion. Kamper and his team used a clamp and cast set up to measure hand forces; the participant's hand was placed in a cast to fix its position and orientation, and the fingertip was clamped to a load cell (Figure 2.5 Left). The participant then applied force in six directions. These data were used to understand the abilities of individuals after strokes, and to investigate neuromuscular control (Cruz et al., 2005; Kamper et al., 2006; Seo et al., 2010). A similar testing setup was also used with cadavers to understand tendon impact on forces (Lee et al., 2008) and to measure the effects of hand exoskeletons (Hoffmann et al., 2015). These publications focus on a small number of positions (typically five) and a small number of healthy participants (less than five).

Valero Cuevas investigated finger force ability in multiple positions using a thimble and handle set up (Figure 2.5 Right). This work primarily investigated the different muscle control abilities for different positions and focused on Parkinsons Disease. (Valero-Cuevas, 2005; Valero-Cuevas et al., 1998; Venkadesan and Valero-Cuevas, 2008). Sancho-Bru *et al.* developed a model that used forces in hand and arm ligaments to simulate hand movement, however, this model could not simulate force application.

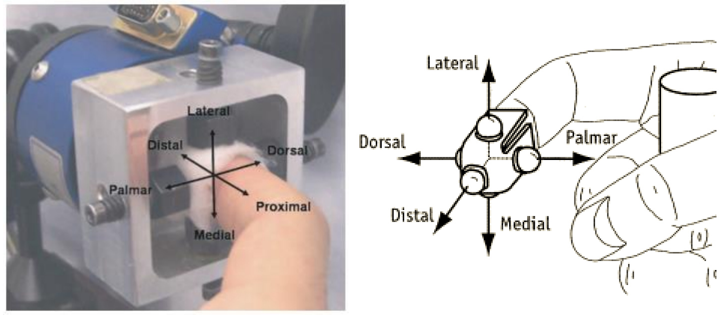

Figure 2.5: Left: hand clamp set-up for finger strength. Right: thimble and handle set up for finger force collection testing (Cruz et al., 2005; Valero-Cuevas et al., 1998).

In terms of evaluation of changes due to aging and arthritis, Bohannon *et al.* published a review identifying baseline hand grip dynamometer data for twelve age groups (five-year sections starting at 20 years) and found that grip strength stayed consistent until around 50 years, where it starts slowly declining (Bohannon et al., 2006). Vieluf *et al.* showed that older individuals had lower grip force capabilities; however, they also tended to overcompensate and use higher forces than younger individuals when performing a task (i.e. grasping a glass of water or a key) (Vieluf et al., 2013). Leitkam *et al.* showed that hand OA caused a decrease in the range of motion of the hand and decreased ability to orient the finger and apply different directions of load (Leitkam and Bush, 2015). Other grip and pinch studies showed that older participants were able to apply 25-30% less force on average compared to college age participants. While differences in force can be related to aging, other work has shown that OA causes further and different loses to hand function, however the exact amount is not consistent between different tests and seems to be dependent on test setup and extent of OA within the test group (Bagis et al., 2003; Villafañe et al., 2014).

2.5 Summary

There is a gap in current research that is important for understanding the abilities and function of the hand. While several researchers have developed models associated with the hand, there are limited experimental models that include *both motion and force abilities* of the hand for all finger postures, and the work that has been published either has a small number of participants, a small number of postures or only the index finger. This is the gap in the research we aim to fill.

3 MAPPING TOGETHER KINETIC AND KINEMATIC ABILITIES OF THE HAND

Drost, Joshua P., Hyokyoung G. Hong, and Tamara Reid Bush. "Mapping together kinetic and kinematic abilities of the hand." Journal of biomechanical engineering 142.2 (2020).

3.1 Introduction

Models of the hand are necessary to understand functional loss due to injury or disease such as stroke or osteoarthritis; identify the effects of recovery as a result of treatment, therapy, and rehabilitation; and to support device designs (Blana et al., 2017; Bullock et al., 2012). In order to determine where in the hand function has been lost and to identify the magnitude of loss, it is important to have an assessment of what constitutes “normative” functional abilities of the hand, so deviations from “normative” can be quantified.

Some work has been conducted to measure and model the kinematic abilities of the fingers and hand, predominantly on individuals with reduced function. Researchers have measured joint range of motion using different tools, such as goniometry, electro-goniometry and motion capture (Bashardoust Tajali et al., 2016; Cook et al., 2007; McVeigh et al., 2016). Others studied grasp using dynamometry, pinching, and pressure sensors during object interaction and tasks of daily living (Bae and Armstrong, 2011; Bohannon et al., 2006; Nataraj and Li, 2013; Smaby et al., 2004). However, limited data sets are available for normative force abilities over the range of motion of the fingers. Previous studies by the authors investigated the complete ranges of motion for the fingers of healthy and arthritic individuals (Leitkam et al., 2015, 2014; Leitkam and Reid Bush, 2015). Investigators have researched grip or strength abilities, focusing on one or two finger postures (Freund et al., 2002; Nicolay and Walker, 2005). Finger forces have been measured using a handle and thimble setup to understand the connection between nerve activations and muscle contractions in the forearm (Valero-Cuevas, 2005; Valero-Cuevas et al., 1998; Venkadesan and Valero-Cuevas, 2008). One group investigated index finger forces at different positions for stroke victims and included six participants as healthy controls (Cruz et al., 2005; Kamper et al., 2006; Seo et al., 2010). Other researchers worked on anatomical and mechanical models of the hand estimating forces over the range of motion based on tendons and muscles; a limitation to these studies is that they incorporated only one or two force positions for validation or used hands from cadavers (An et al., 1985, 1979; Fok and Chou, 2010; Sancho-Bru et al., 2001; Wohlman and Murray, 2013). Data sets including both force and motion over an array of finger postures for healthy individuals do not currently exist in published literature, and are critical for a complete understanding of functional abilities of the fingers. To obtain these data sets, first a method to collect these data must be developed and tested.

The long-term goal of this project is to model the functional abilities (i.e. motion and strength together) of the hand for use in clinical assessment. The specific goal of this research was to develop and demonstrate a method for measuring and mapping the kinematic and kinetic abilities of the hands together. To do this we developed an experimental method to obtain motion and strength measurements across the range of motion for the index finger, and demonstrated the approach on the other three fingers. Then we created a population mapping of the range of motion abilities and strength abilities for both individuals and the entire test population. Finally, we statistically analyzed the population mapping for an initial understanding of how the position within the range of motion and directions of the applied force affected the magnitude.

3.2 Methods

3.2.1 Participants

Thirty-six healthy individuals participated in this study. The index finger was tested for sixteen participants (seven female, nine male, mean age 25.6 years, SD 6.1 years). Additionally, all four fingers were evaluated for twenty participants (ten female, ten male, mean age 21.1 years, SD 0.9 years). All participants were right hand dominant and all tests were conducted on the right hand. All individuals consented to participate in this study which was approved by the university's human research board.

3.2.2 Measurements

First, anthropometric data of the participants' hands were collected using an electronic caliper (Starrett Model 723) including: overall hand length, width, and span; distance to the wrist and the distal and lateral distances to the metacarpophalangeal (MCP) joints of each digit from the center of the palm; and the length of each distal, medial, and proximal phalanx.

Finger posture and motion data were measured using a seven-camera motion capture system and reflective markers (Qualisys, Gothenburg, Sweden). A total of 67 markers were attached to the right hand and wrist (Figure 3.1). Three markers were placed on the proximal side of the wrist. Clusters of four markers were attached on the center of the back of the hand and at the center of each phalanx. Loads applied by the finger were collected using a multi-axis load cell (Advanced Mechanical Technology, Inc., Watertown, MA, USA). Four markers were attached to the load cell to determine the location and orientation of the load cell relative to the hand. To remove possible effects of fatigue, the order of the force tests was randomized for each participant.

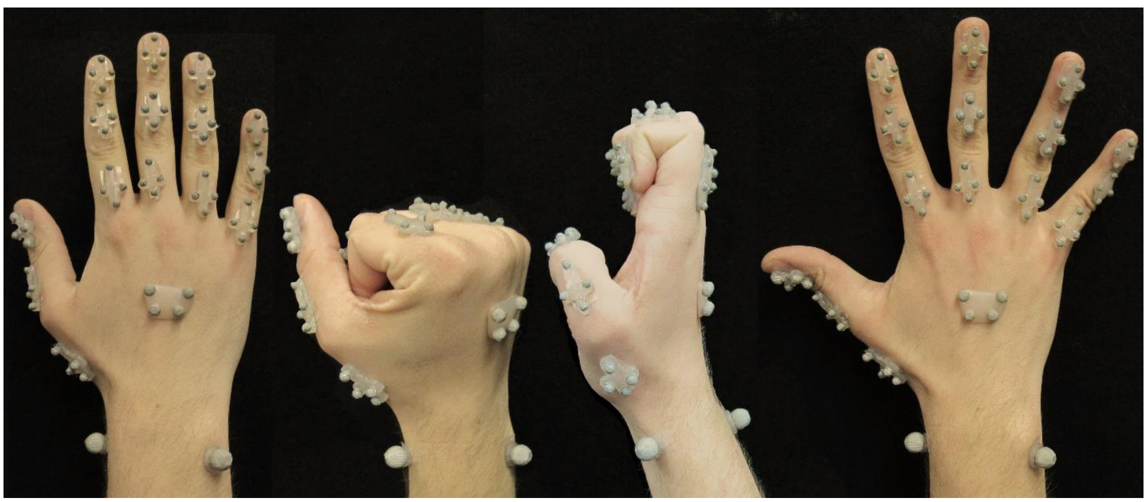

Figure 3.1: Locations of motion capture markers on hand and kinematic motions. Individual markers were placed on the wrist and rigid body marker clusters were placed on each phalanx and the back of the palm for a total of 67 markers. a) Reference, b) Flexion/extension of the MCP joints, c) Flexion/extension of the interphalangeal joints, d) Adduction/Abduction of the MCP joints.

3.2.3 Kinematic Range of Motion Measurements

The kinematic abilities of the participant's fingers were determined by gathering three movements (Figure 3.1). These motions were used to develop the kinematic space (the full range of motion of the hand) and were also used in our prior work (Leitkam and Reid Bush, 2015). The three motions were as follows. 1) Flexion/extension of the MCP joints were measured by the participant hyper extending the MCP joints then fully flexing the MCP joints with the 2^{nd}-5^{th} digits touching the proximal palm. 2) Flexion/extension of the interphalangeal joints were measured by the participant hyper extending the digits then fully flexing the interphalangeal joints with the 2nd-5th distal phalanges touching the proximal phalanges. 3) Adduction/abduction of the MCP joints were measured by the participant separating all fingers then having the participant maximally separate the digits.

3.2.4 Force Measurements During Flexion and Extension

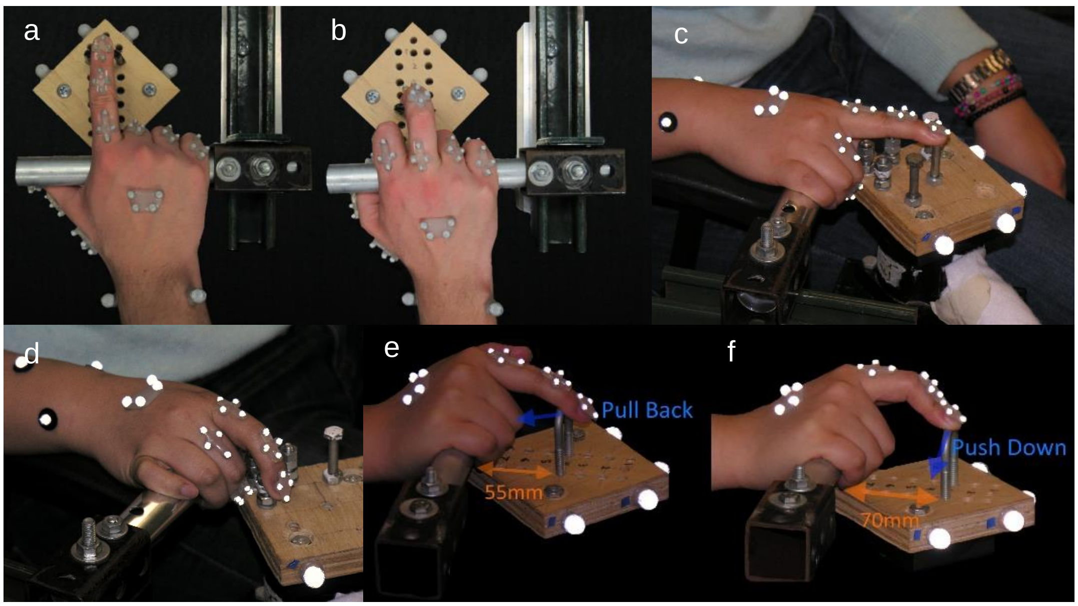

Figure 3.2: Force Measurement procedure: A U-shaped bracket was placed in each of seven positions where the participant was asked to a) push and then b) pull. Adduction/abduction force measurement procedure: c) three positions to push and d) three positions to pull using different degrees of adduction and abduction. This procedure measured participants' maximum forces in push and pull orientations while varying the finger posture (e & f). A multi-axis load cell was attached below the system.

Force data were collected through thirteen force trials to measure forces at different amounts of flexion/extension of the index finger. To accomplish this, a "U shaped" bracket attached to the load cell was used as the interface point where the participant pushed or pulled to apply maximum force (Figure 3.2 a-b). The bracket was manually placed in seven positions along a line starting 100 mm from a handle grasped by the participant and then moving towards the participant at 15 mm increments to a final position of 10 mm from the handle. Changes in positioning of the bracket resulted in changes in finger flexion/extension. The participant started at the furthest position that could be reached with the finger being tested; this may not have been the 100-mm position if the participant's finger did not reach this distance.

At each position the participant was asked to use only the pad of the finger to apply two types of maximal load: 1) *push* down normal to the palm on the bracket (Figure 3.2 a); and 2) *pull* towards the wrist on the bracket (Figure 3.2 b). Note: Pulling forces were not measured at the full extension position as the fingertip could not wrap around the bracket to pull.

During each test the participant was asked to rest his/her palm on a handle and grip the handle with the remaining fingers. The purpose of the handle was to isolate forces to the fingers and restrict the use of the arm in the application of the forces.

3.2.5 Force Measurements During Adduction and Abduction

Force measures were also conducted for adduction and abduction. While in maximum extension, forces were generated at three positions: 1) a neutral position (i.e., no abduction or adduction), 2) finger adduction and 3) finger abduction (Figure 3.2 c-d). These three positions were repeated at a mid-flexion position which was located halfway between the handle and the maximum extension position. The forces at maximum extension were measured by asking the participant to push perpendicular to the palm with maximum force on each of the three positions (Figure 3.2 c). Flexion positions were measured by asking the participant to pull towards the wrist with maximum force on each of the three positions (Figure 3.2 d).

3.2.6 Modeling the Kinematic Space

The kinematic space of the finger consisted of all the points in space that could be reached by the pad of the index fingertip and was based on prior work by the authors (Leitkam and Reid Bush, 2015). Briefly, maximum and minimum joint angles were determined from the three kinematic motions tested. Fingertip posture (the 3D x, y, z coordinates in space of the fingertip) was calculated at every unique integer combination of joint angles within the ranges of motion for that digit. Then those postures were rounded to a 2.5 mm grid value; at each cell on the grid, the number of points represented the number of joint angle combinations that allowed the finger to reach that cell.

Table 3.1: Notation used for analysis.

t	Time
$\boldsymbol{F}$	Force Vector
$\boldsymbol{\hat{n}}$	Direction of Force
$\boldsymbol{f}$	Position of Fingertip
$\boldsymbol{R}$	Rotation Matrix
$\boldsymbol{\hat{e}^F}$	Coordinate System of Load Cell
$\boldsymbol{\hat{e}^P}$	Coordinate System Centered at Palm
$\boldsymbol{\hat{e}^M}$	Coordinate System Centered at MCP
L	Finger Length
$\boldsymbol{u}$	Distance from Center of Palm to MCP

3.2.7 Mapping Force Data to the Kinematic Space

The maximum force generated by each finger was computed for each participant for each of the trials. The force vector data, $\boldsymbol{F}(t) = [F_x(t), F_y(t), F_z(t)]$ was given in the local coordinate system of the load cell ($\boldsymbol{\hat{e}}^F$). From this, the magnitude of the force vector $|\boldsymbol{F}(\boldsymbol{t})|$ was calculated and the maximum force $|F_{max}|$ and its time (t_{max}) were found by using the average of 25 time samples, 12 frames before and after the maximum force (collected at 360 Hz). The direction of the maximum force $\boldsymbol{\hat{n}^F}$ relative to the local load cell coordinate system $\boldsymbol{\hat{e}^F}$ was determined using:

$$\boldsymbol{\hat{n}^F} = \frac{\boldsymbol{F}(t_{max})}{|F_{max}|} \tag{1}$$

The motion capture data were based on a local coordinate system $\boldsymbol{\hat{e}^P}$ that was located in the center of the palm and oriented with the x-axis pointing laterally, the y-axis pointing distally, and the z-axis pointing normal to the palm, extending out of the palm. These data were used to determine the posture of the fingertip $\boldsymbol{f^P}(t)$ as well as the transformation matrix between the load coordinate system $\boldsymbol{\hat{e}^F}$ and the motion coordinate system $\boldsymbol{\hat{e}^P}$, represented as a rotation matrix $\boldsymbol{R}$ so that:

$$\hat{\boldsymbol{e}}^{\boldsymbol{P}} = \boldsymbol{R}\hat{\boldsymbol{e}}^{\boldsymbol{F}} \tag{2}$$

Next, the kinematic data file and force data were synchronized. The time of the maximum force t_{max} was used to find the posture of the finger $\boldsymbol{f_{max}}$ and the direction of the force in terms of $\hat{\boldsymbol{e}}^{\boldsymbol{P}}$was found using:

$$\hat{\boldsymbol{n}}^{\boldsymbol{P}} = \boldsymbol{R}\hat{\boldsymbol{n}}^{\boldsymbol{F}} \tag{3}$$

Force vectors were then mapped onto the kinematic space using the fingertip posture and the direction and magnitude of the forces.

3.2.8 Population Force Spaces

After the motion and force plots were created for individual participants, a group plot was created for our sample. This population force space was created to compare the force abilities of the finger with respect to the finger posture within the range of motion. To remove differences in hand size between participants, the finger posture coordinates were normalized based on finger length: the local coordinate system was translated so that the origin was in the center of each participant's MCP joint and scaled so that a unit vector in each primary direction was the length of the participant's index finger.

$$\hat{\boldsymbol{e}}^{\boldsymbol{M}} = \frac{\hat{\boldsymbol{e}}^{\boldsymbol{P}} + \boldsymbol{u}}{L} \tag{4}$$

Where $\boldsymbol{u}$ was the distance vector between the center of the palm and the MCP, and L was the length of the finger, both of which were obtained through physical measurements; $\hat{\boldsymbol{e}}^{\boldsymbol{M}}$ was the scaled coordinate system centered at the MCP. After translating and scaling the coordinate system, the force vectors for all participants were then plotted together based on posture, direction, and magnitude of the force vector.

3.2.9 Statistical Analysis

Statistical analysis was used to provide an initial understanding of how the direction of the force and the location within the range of motion affected the maximum force that could be applied. Analysis of covariance (ANCOVA), multivariate analysis of covariance (MANOVA) and multiple linear regressions were used to determine statistical differences in maximum force data relating to force direction and finger posture. To eliminate any confounding effects, sex was controlled in our analysis. Thus, the force data were examined based on three hypotheses: fingertip posture affects the maximum force that can be applied; direction of the applied force affects the maximum force that can be applied; and maximum force varied among fingers.

3.3 Results

The kinematic space with mapped force data for a single participant is presented in Figure 3.3. While the data are three-dimensional (i.e., ab/adduction and flexion/extension), these data have been projected onto a 2D sagittal plane for the ease of viewing. The greyscale background indicates the angular range of fingertip orientations that are possible at each point in the kinematic space. The force arrows represent the force vectors for each test position projected onto the sagittal plane with the color of the vector indicating force magnitudes. Additionally, the plots are shown for all four fingers from a single participant (Figure 3.4).

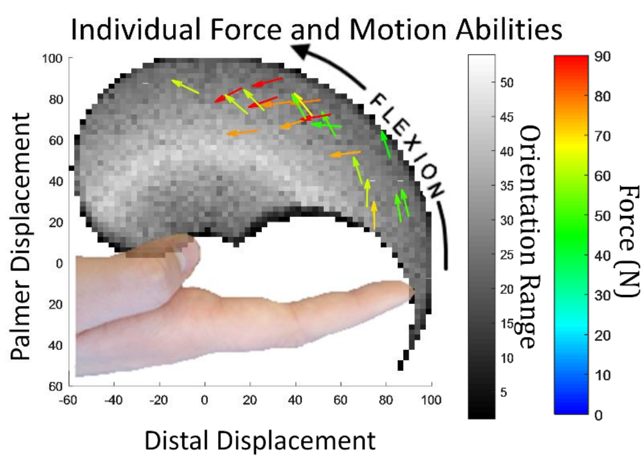

Figure 3.3: Sagittal plane view of kinematic finger space with overlaid force vectors for the index finger. The displacements of the figure are measured from the center of the wrist. The greyscale background represents the range of orientations the distal phalanx can reach at the specific point and colored arrows represent the forces that were applied at each position with relative magnitudes. The transparent finger on the figures indicates the orientation of the image.

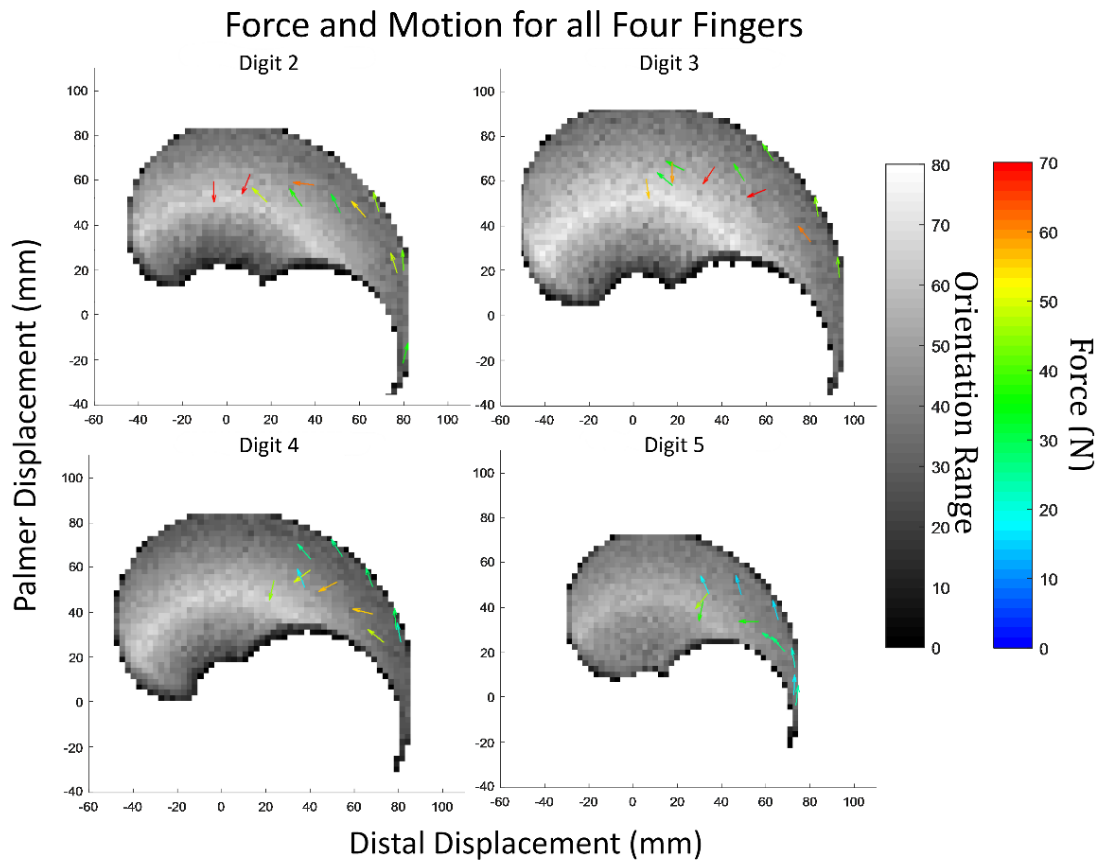

Figure 3.4: Sagittal plane view of kinematic finger spaces with overlaid force vectors for each finger of a single participant.

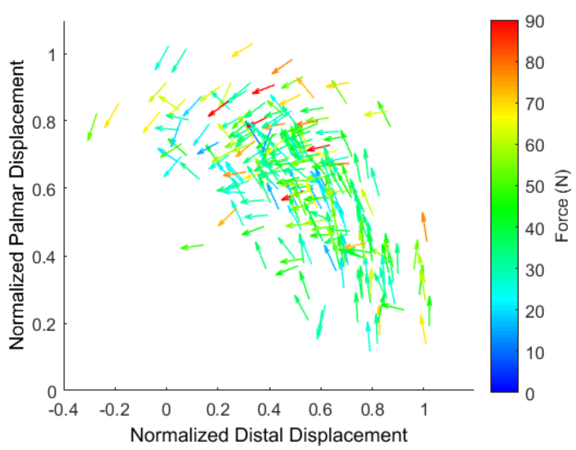

Figure 3.5: Sagittal projection of each index finger force for all participants. Displacements are normalized based on participant's finger length. The orientation is the same as Figure 3, but the displacements are measured from the center of the first MCP joint.

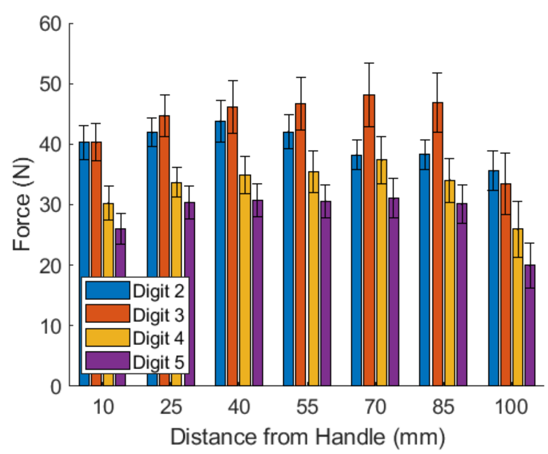

Figure 3.6: Average maximum force abilities across the four fingers for each trial with standard error.

Statistical analysis of the applied forces showed fingertip posture in the kinematic space significantly affected the amount of force applied (ANCOVA, p=0.01). Forces near the center of the range of motion tended to be higher than forces at the edge of the kinematic space (Figure 3.7). Also, maximum forces decreased with abduction and increased with adduction. This difference was statistically significant (MANOVA p=0.011).

Direction of the force significantly affected the amount of force applied (multiple linear regression p<0.001). Forces in the pull directions were higher than forces in the push directions.

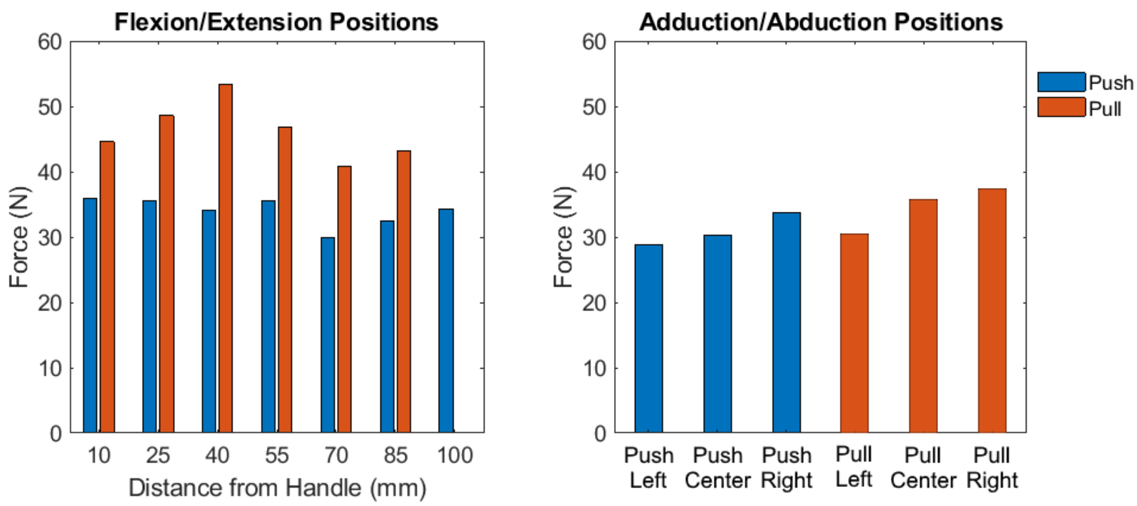

Figure 3.7: Average index fingers forces with standard error for each trial. a) Flexion-Extension tests b) Abduction-Adduction tests

There were also differences in maximum force production among fingers (Figure 3.6). The second and third digits applied significantly more forces than the fourth and fifth digits at all test positions (MANOVA p<0.001).

3.4 Discussion

The goal of this research was to develop and demonstrate a method for measuring and mapping the kinematic and kinetic abilities of the hands together. This new method significantly advances our ability to collect and analyze force data associated with the hand. Further, the data presented here provides a normative data set for the fingers including both motion and forces, and how the position within the range of motion and the direction of the applied force affect the amount of force that can be applied. These data are not currently available elsewhere.

Other methods to measure forces include dynamometers, which are the primary means of clinical analysis (Bohannon et al., 2006; Nicolay and Walker, 2005). However, these systems focus on measurement of specific types of grasp and there is little variation in finger posture permitted and individual finger data cannot be collected. Researchers have also measured finger forces with a cast and clamp device (Cruz et al., 2005; Kamper et al., 2006; Seo et al., 2010; Valero-Cuevas, 2005; Valero-Cuevas et al., 1998). However, data were predominantly conducted on a stroke population, data sets from a healthy population were not the focus of that work (Cruz et al., 2005; Kamper et al., 2006; Seo et al., 2010). Our method does not require finger clamping, can be used on individual fingers, and provides an array of finger postures.

The statistical results indicate that both the finger posture and the direction of the applied force affect the amount of force that can be applied. These differences show the importance in collecting functional data at multiple positions over the range of motion and in multiple directions. Also, the maximum amount of force that can be applied differs among fingers, indicating that assessment of fingers should be performed individually. Future work will model these differences to create a complete model of forces over the range of motion for the healthy hand. We will use this model clinically to compare participants with reduced hand function before, during and after therapy or surgery to determine quantitatively how function has changed, as well as validating future mechanical and simulation models (An et al., 1985, 1979; Fok and Chou, 2010; Sancho-Bru et al., 2001; Wohlman and Murray, 2013).

A limitation of this method is that data collection in full flexion (when the fingertips are near the palm) is not well covered. The use of a smaller, hand-held load cell could be added to the protocol to expand our data set to cover this region in the kinematic space. However, very few tasks are conducted with the fingers in full flexion; so, when relating the forces to functional tasks and prioritizing the kinematic space, our method covers the region most used by individuals

(Leitkam et al., 2015). Additionally, while more positions could provide additional data points for force, there is a tradeoff; more positions increase the testing time and could increase fatigue, particularly in older participants with reduced hand function. Another limitation is that the protocol discussed in the methods requires more time than is often available in a clinical setting. As we move towards using this method and model clinically, a simplified setup will be developed.

Testing the thumb will require a separate protocol as its movement abilities are different. However, once force and motion data are obtained from the thumb, the same mathematical analysis techniques can be used to process and map the data.

The authors have also conducted initial tests to confirm that the protocol can be completed by individuals with osteoarthritis (OA) of the hand. Future work will use this approach to test a population of severe OA participants to quantify their initial abilities and follow them through hand surgery to determine if functional changes occur.

This work demonstrates a unique protocol, apparatus, and method permitting the gathering of force data and mapping them to finger postures. These data were also combined to demonstrate a population map of normative force abilities for the index finger. This work fills a critical need in the realm of hand function and assessment.

4 DIFFERENCES IN FINGER STRENGTH OVER THE KINEMATIC SPACE, AN EXPERIMENTAL MODEL

4.1 Introduction

Finger strength is an important component of overall hand function. Applying forces with the fingers is required to control objects and accomplish tasks of daily living (Fowler and Nicol, 1999; Polygerinos et al., 2015; Vieluf et al., 2013). However, hand strength can be reduced due to many conditions, such as aging, injury, osteoarthritis, or stroke (Bagis et al., 2003; Cruz et al., 2005; Ranganathan et al., 2001; Villafañe et al., 2014). It is necessary to understand how finger strength changes so that clinicians have the most information possible when treating patients. Also, quantitative data sets provide designers more understanding of hand function to develop products for people with reduced hand function.

Clinically, hand strength is measured using dynamometers, which measure whole hand grip or a single pinch grip (Bagis et al., 2003; Bohannon et al., 2006; Nicolay and Walker, 2005; Shivers et al., 2002). This is a helpful measurement for clinicians, as it is fast and gives a single force value. However, previous work has shown both finger posture and the direction in which the force is applied affect the magnitude of the forces that are generated (Cruz et al., 2005; Drost et al., 2019; Fowler and Nicol, 2001; Yokogawa and Hara, 2002). Tools that only measure forces in one position and one direction do not fully measure function of the fingers.

Researchers have developed other methods to measure finger strength. Many of these methods tested finger forces in different directions, but in only one or two finger postures (Freund et al., 2002; Li et al., 2003; Valero-Cuevas et al., 1998). These methods did not identify the differences in force capabilities over the full range of motion for each finger. To understand how hand strength fully changes due to aging, osteoarthritis, stroke or other complications, it is imperative that strength changes be measured for all fingers at many positions over the kinematic space of the fingers (the entire volume that can be reached by each finger). Other tests quantified finger strength in multiple positions but focus on small healthy samples of fewer than ten participants (Cruz et al., 2005; Kamper et al., 2006; Seo et al., 2010; Yokogawa and Hara, 2002). Larger populations of participants are required for a complete understanding of finger function.

To quantify changes in finger strength and identify where patients have reduced function, it is also necessary to have a normative model representing healthy finger force ability to use as a baseline. A few researchers have focused on estimating force abilities through models and simulations. These models focus on an array of topics including: tendon loads during power grip (Fok and Chou, 2010); force application and joint torques at different finger postures (Qiu and Kamper, 2014; Serbest et al., 2016; Wu et al., 2008); and thumb force during key and pinch grips (Wohlman and Murray, 2013). These simulations estimate the abilities of the hand based on anatomy and mechanics. However, there is a lack of robust experimental data sets to validate these models.

Therefore, the goals of this work were to: 1) experimentally quantify finger forces of all four fingers over their individual movement (i.e. kinematic space); 2) use a statistical modeling approach to understand what causes differences in the finger forces that can be applied by healthy participants over their kinematic spaces; and 3) develop a statistical model to estimate the forces that can be produced by the fingers. This work will provide a complete data set of finger forces that can be applied over the kinematic space for use in comparing individuals with reduced finger function and to validate future computational models and mechanical simulations.

4.2 Methods

4.2.1 Participants

For this study, 41 healthy individuals who had no hand injuries or loss of finger function participated. All participants in this study were right hand dominant, and only the right hands of participants were tested. Each participant consented to the study which received University Institutional Review Board approval.

4.2.2 Experimental Data Collection

Both motion and force data were obtained as part of the experimental protocol. To obtain motion data, a seven-camera motion capture system (Qualisys, Gothenburg, Sweden) collected coordinate data (x,y,z) of 54 reflective markers positioned on the hand (Figure 4.1).

Simultaneously, a multi-axis load cell (Advanced Mechanical Technology, Inc., Watertown, MA, USA) with a custom force application attachment measured the finger forces applied by each participant. Reflective markers were also attached to the load cell to determine the location and orientation of the load cell relative to the hand.

Full range of motion of the joints of each finger were computed through the collection of data from three different hand movements: maximum metacarpophalangeal joint (MCP) flexion and extension, similar to making a fist (Figure 4.1a); maximum flexion and extension of both interphalangeal joints (IP) (Figure 4.1b); and adduction and abduction of MCP joints by spreading the fingers (Figure 4.1c). These range of motion data were used to determine each finger's kinematic space: the fingertip coordinates were calculated for all possible combinations of joint angles using a procedure previously published by the authors (Leitkam et al., 2015, 2014).

Next, maximum forces were collected in nineteen positions that spanned the fingers' kinematic spaces. To start, the participant gripped a handle to isolate the force production to the fingers and remove any contribution from the elbow and shoulder. Additionally, to reduce variance in forces due to the participants' body postures, the testing setup was adjusted so all participants sat upright with their arms alongside their torsos, elbows at 90° flexion, and wrists straight. Maximum forces at different finger postures due to changes in flexion/extension of the index finger were collected using a bracket mounted to the load cell (Figure 4.1d). The bracket was placed in seven positions along a line starting at 10mm from the handle and moving in 15mm increments to 100mm from the handle. At maximum extension, the participant was asked to push with maximum force towards the ground. At every other position, the participant was asked to push on the bracket towards the ground, and then pull towards the wrist with maximum force using the pad of their finger (pulling was not possible in maximum extension).

Maximum forces during abduction and adduction were measured in six positions (Figure 4.1e). Three of the positions were at maximum extension, where the participant was asked to push with maximum force towards the ground at a center position, an adducted position, and an abducted position. The other three were at a mid-range flexion of the finger joints, where the participant was asked to pull with maximum force towards the wrist at a center position, an adducted position, and an abducted position. The order of the force trials was randomized between participants to remove potential effects due to fatigue.

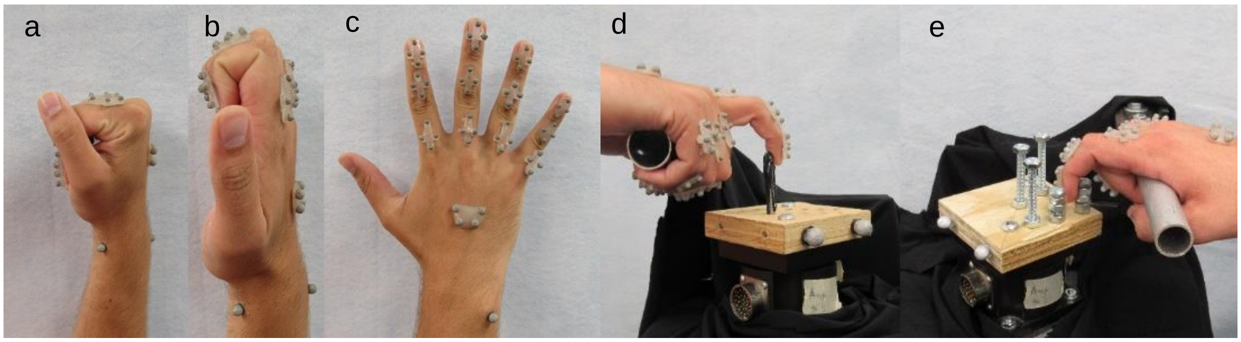

Figure 4.1: Experimental setup used to obtain range of motion and force abilities for the four fingers. (a) MCP flexion/extension, (b) IP flexion/extension, (c) MCP adduction/ abduction (d) flexion/extension pull force trial, (e) adduction/abduction push force trial

For all participants, forces were collected from the index finger. Additionally, a subset of the population participated in testing of all four fingers (n=20); however, to reduce testing time and limit participant fatigue, the adduction/ abduction positions were removed from the protocol for this group.

4.2.3 Individual and Population Force Maps

In order to understand how force production changed over the kinematic space, the collected force data were mapped to the kinematic space. This mapping was accomplished by transforming the data sets to the same coordinate system so the force and motion abilities could be overlaid. These maps are 3D data sets projected onto the sagittal plane for viewing in this document. Three sets of maps were developed: individual maps detailing each participant's abilities, population maps combining all the abilities of the tested population, and regional maps which showed the average abilities for different regions of the kinematic space. These will each be explained in detail.

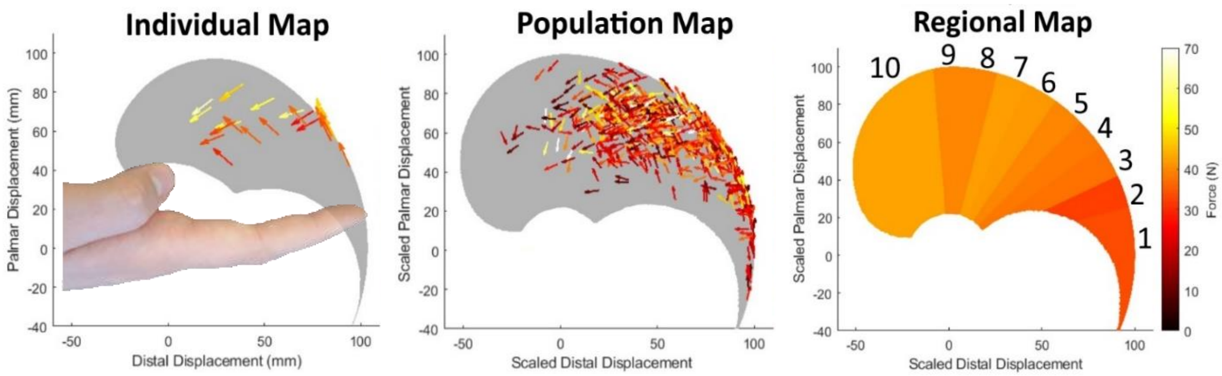

Figure 4.2: Mapping together kinematic and kinetic finger function. Left: Individual force map shows the kinematic space of the index finger in grayscale, and the forces applied as colored arrows. Middle: The population force map of the participants (n= 41) shows all the forces applied by participants' index fingers for all finger postures. Right: Averaged force capability for regions within the kinematic space. Regions were numbered from full extension (1) to full flexion (10).

First, each participant's force actions were mapped onto the participant's functional finger space to determine an individual's force abilities over their finger's range of motion. Briefly, the kinematic space and the collected force data were transformed to the same coordinate system at the base of the digit's MCP joint, and the force data was analyzed by the finger posture, direction of the force and force magnitude (Drost et al., 2019). The data were three-dimensional but projected onto the sagittal plane for ease of viewing (Figure 4.2, Left). The greyscale background visualizes the kinematic space of the finger for a given participant. The colored arrows show the force actions and key information; specifically, the magnitude of the force, the direction the force was applied, and the position within the space. The origin for these plots is the center of the individual's MCP joint.

Next, the individual maps were combined into population maps (Figure 4.2, Middle). These maps were created to compare all the force actions within the tested participant group. To compare between participants, the individual spaces were scaled by dividing the (x,y,z) coordinates by the participant's finger length. Then the spaces were transformed and mapped together, with the origin being the MCP joints of the fingers. A population map was developed for each finger.

Finally, the population maps were averaged into regional maps (Figure 4.2, Right). The regional maps were created as a means to compare between fingers and to visually compare an individual's abilities to a population. They were calculated by subdividing the kinematic space of each finger into polar segments originating at the MCP joint (with 0° being parallel with the palm). Regions 2-9 were each 10° arcs: starting at 10° from parallel with the palm and going to perpendicular with the palm (90°). Fewer participants applied forces in Regions 1 and 10, so these regions were larger to increase the number of force trials in the regions. Then, the average and standard deviations of the forces were calculated for all the forces within each region. Also, the mean and standard deviations of the angle of the force vector in the sagittal plane were calculated for each region to understand the directions used to apply forces. The force angle was defined by the vector normal to the palm (Figure 4.2 positive y-axis). These data were analyzed for each finger with all participants, then for each finger split by sex.

4.2.4 Statistical Differences Within and Between Fingers

Analysis of Variance (ANOVA) with Tukey post hoc test and Generalized Linear Mixed Modelling (GLMM) were used to determine statistical differences in the strength abilities of the fingers. These data were analyzed in terms of five parameters: force magnitude, finger posture, force direction, the finger used to apply the force, and the sex of the participant.

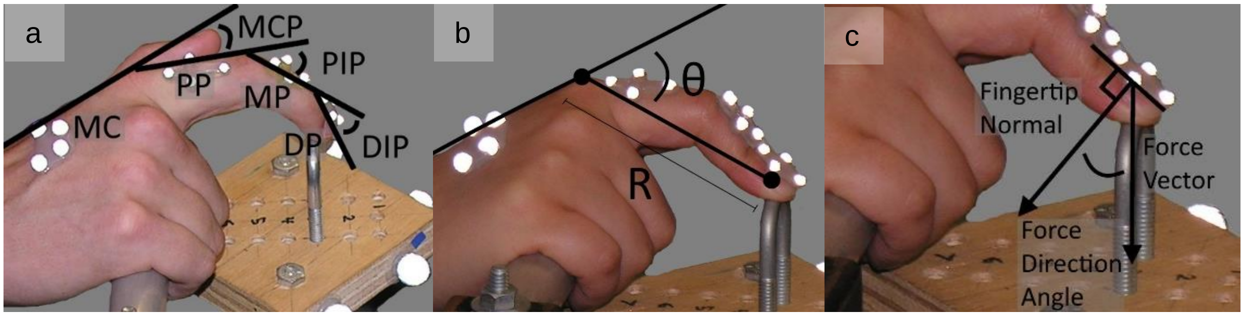

Figure 4.3: Definitions of finger posture and force direction. (a) Finger posture as defined by the flexion of the three joints of the finger. (b) Finger posture measured as the polar position of the fingertip in relation to the MCP joint. (c) Force direction was defined as the angle between the force vector and the vector normal to the fingertip in the sagittal plane.

Multiple mathematical approaches to define the posture of the finger were used in statistical analysis to understand the relationship between finger posture and force application.

1) **Region of kinematic space** where the force was applied (Figure 4.2, Bottom). This definition was used to compare participants statistically with only one variable (i.e. one of the 10° sections of the kinematic space). While no two participants applied forces at the same (x,y,z) coordinate in space, most participants applied forces in at least seven of the ten regions.

2) **Finger joint angles**, specifically the flexion of the MCP, PIP and DIP joints (Figure 4.3a). This definition was used to define the system anatomically.

3) **Polar location of the fingertip** in the sagittal plane of the finger (Figure 4.3b). This definition was used to test if the finger strength was related to the fingertip position regardless of the joint angles needed to reach that posture. Since the finger can be approximated as a series of hinge joints that move in rotations, polar coordinates were used instead of Cartesian coordinates to compute finger posture. R was the scalar distance to the midpoint of the distal phalange from the MCP joint. To compare between participants with different finger lengths, R was scaled by dividing by each participant's finger length. θ was defined angle of flexion where 0° was fully extended, parallel with the palm (Figure 4.3b).

Force direction was defined as the angle between the force vector generated at the fingertip and the vector normal to the fingertip in the sagittal plane (Figure 4.3c). In this definition, a force with a positive direction was produced by flexing the MCP joint and extending the IP joints, while a negative force was produced by MCP joint extension and IP joint flexion.

The force data of the four fingers were examined based on three hypotheses:

1. Different fingers applied different amounts of maximum force.
2. Finger posture affected the maximum force magnitude that could be applied. This was evaluated using each of the three methods of defining posture: kinematic regions, joint angles, and polar fingertip coordinates.
3. Direction of the applied force affected the maximum force magnitude that could be applied.

4.2.5 Generalized Linear Mixed Model

After examining the force data for significant effects, GLMM was used to create a continuous model of force over the range of motion. This approach used inputs of both fixed effects and random effects. Fixed effects are inputs that stay the same for all participants in the population, which for this model were fingertip position (R, θ), joint angles (MCP, PIP, DIP), and force direction. Sex was also included as a fixed input. As part of model selection, second order terms of the covariates were tested to understand the parabolic nature of the covariates. Similarly, covariate interactions, which are multiplicative terms that address how the effects of one covariate change due to another covariate, were tested but not included in the final model as they were not significant.

In this study, participants were considered a random effect to control for the strength differences between individuals. As some participants could apply more force than others, using a random variable helped compare between participants. This was accomplished by giving each participant a subject number (s). Random effects were used to reduce error in the model (ε).

$$Force = A_1 + A_2 * Direction + A_3 * MCP + A_4 * PIP + A_5 * DIP + A_6 * MCP^2 + \ldots \\ A_7 * PIP^2 + A_8 * DIP^2 + A_9 * Sex + s + \varepsilon \tag{5}$$

$$Force = A_1 + A_2 * Direction + A_3 * MCP + A_4 * PIP + A_5 * DIP + A_6 * MCP^2 + \ldots \\ A_7 * PIP^2 + A_8 * DIP^2 + A_9 * Sex + A_{10} * Digit + s + \varepsilon \tag{6}$$

For the models in this work, joint angles (MCP, PIP, DIP) were chosen to define the posture of the finger as the statistical analysis found that the most significant postural effects on the strength abilities of the fingers came from joint angles. Adduction/Abduction of the MCP joints was not included as it was not tested on all fingers. Force direction and participant sex were also included in the models. For the models, the force was included in Newtons, the angles (MCP, PIP, DIP, direction) as radians, and the rest (sex, digit) were categorical (either 0 or 1).The models outputs were the covariate coefficients (A_i) which estimated the relationship between the covariates and the force that was applied.

Two statistical models of the hand were developed to estimate the strength abilities of the four fingers using finger joint angles. First, each finger was modeled separately (Equation 1) to understand each finger as a separate digit able to apply force independently of the other fingers. Second, all four digits were modeled together (Equation 2), with digit number as a categorical covariate. This model was created as the anatomical and mechanical background of the fingers are using similar flexor and extensor muscle groups in the forearm.

4.3 Results

4.3.1 Participants

The group of participants in the study included 41 heathy participants (21 female, 20 male, mean age 23.0 years, SD 10.6 years) split into two sub-groups: 21 participants (11 female, 10 male, mean age 28.3 years, SD 10.0 years) completed the test on the index finger only with adduction/abduction positions, and 20 participants (10 female, 10 male, mean age 21.1 years, SD 0.9 years) completed the flexion-extension positions for all four fingers.

4.3.2 Statistical Differences in Force Generation Within and Between Fingers

There was a significant difference in the amount of force applied between the four fingers (ANOVA $p<0.001$). Specifically, the second and third digits applied significantly more force than the fourth and fifth digits (Tukey post hoc test $P<0.001$). Males applied more force than females with each finger (ANOVA $p<0.001$).

Finger posture significantly affected the force that can be applied. This was tested three ways: range of motion regions, joint angles, and polar fingertip position. There were significant differences in force production by region of the kinematic space when controlling for digit and force direction (ANOVA $p<0.001$). Specifically, regions one through three (most extended) applied significantly less force than regions six through eight (mid flexion). This was also true comparing each digit separately. The means and standard deviations of the magnitude of force that could be applied are shown in Table 4.1.

When defining the posture as joint angles, maximum force production was significantly affected for all three joints (GLMM $p<0.001$). Each joint angle significantly affected the force that was applied when comparing the digits together; however, the PIP had no significant effect on the fourth or fifth digits. (Table 4.3). For each joint the relationship was second order (i.e. MCP^2) showing that the relationships were parabolic. As the estimates were negative, that denotes that higher forces were produced when the joints were flexed.

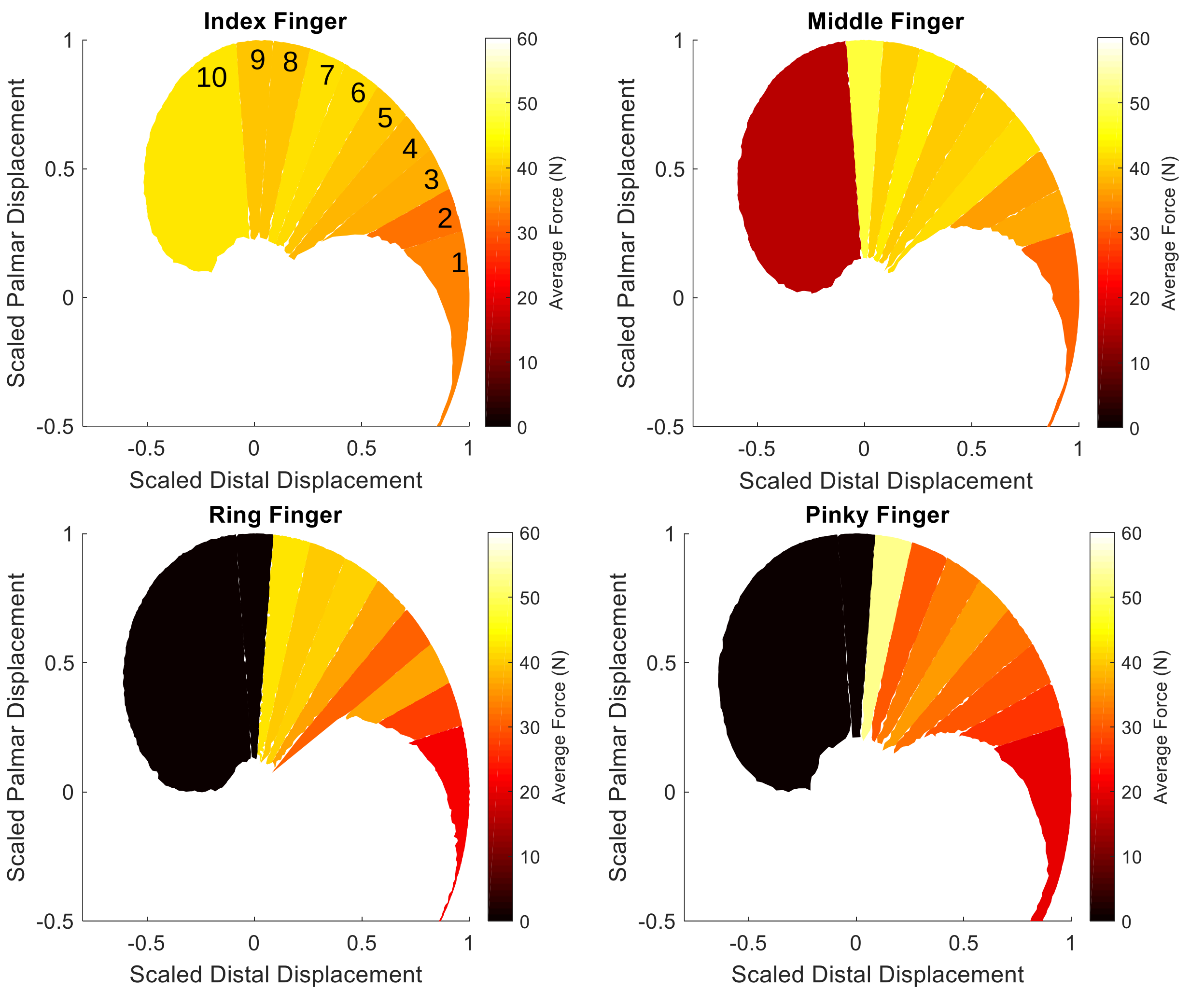

Figure 4.4: Average force abilities over the range of motion for all four fingers for all participants. Each range of motion is subdivided into regions, and the color represents the average force in the region. The black regions are areas where to few force events (n<7) occurred for accurate averages.

Fingertip position as defined by (R, θ) was not a consistent method for comparing finger posture to force production between fingers. When all the fingers were compared together, the distance from the MCP joint (R) had a second order relationship with the maximum force (GLMM $p < 0.001$) and θ had no significant effect on the force (GLMM). Yet, when the second digit was compared separately θ was significant, and R was not significant. Therefore, while finger posture effects force production, fingertip position as defined by (R, θ) did not affect fingers similarly.

Table 4.1: Mean force and standard deviation by region for male and female participants (N). The regions that are blank are regions with too few force trials to be accurately averaged (n<7).

	Male				Female			
	Digit 2	Digit 3	Digit 4	Digit 5	Digit 2	Digit 3	Digit 4	Digit 5
Region 1	40.1±22.1	37.0±18.4	21.7±9.5	22.1±8.5	28.8±6.8	28.6±8.6	20.3±7.4	18.2±5.0
Region 2	34.9±20.3	37.6±14.3	30.8±14.8	33.9±13.5	29.0±9.3	36.3±16.7	24.3±9.0	19.8±6.0
Region 3	40.0±19.2	38.0±17.1	46.7±20.9	34.5±17.5	34.4±10.5	33.2±7.7	28.2±14.8	23.6±10.2
Region 4	40.8±19.7	47.4±21.5	33.8±15.1	35.4±16.1	33.5±10.8	31.9±14.4	27.1±11.3	25.3±12.4
Region 5	44.2±25.1	44.9±23.6	47.8±22.8	45.6±24.2	32.7±14.1	35.8±13.4	24.6±10.5	25.3±8.7
Region 6	46.8±23.2	44.0±20.4	48.4±22.0	40.7±16.1	34.8±16.2	34.0±14.8	31.5±15.2	27.2±12.3
Region 7	48.2±20.8	50.4±29.6			31.4±19.1	35.6±14.7	28.6±09.6	
Region 8	46.4±28.5	55.1±21.0			34.6±24.3	29.4±17.9		
Region 9	45.7±28.3	46.2±21.5			33.4±25.2			
Region 10	59.6±28.6				27.6±19.7			

Table 4.2: Mean force angle (°) in the sagittal plane and standard deviation by region for male and female participants. The angle is measured as the angle from the vector normal to the palm.

	Male				Female			
	Digit 2	Digit 3	Digit 4	Digit 5	Digit 2	Digit 3	Digit 4	Digit 5
Region 1	26.0±50.1	35.0±54.0	3.9±72.0	1.9±59.6	15.9±53.3	20.1±56.6	-4.5±23.8	6.2±68.9
Region 2	27.1±51.6	34.2±57.9	14.2±76.1	21.0±55.8	28.7±53.8	33.6±66.7	9.5±54.0	27.4±57.9
Region 3	30.8±58.4	42.3±58.1	35.7±72.3	26.7±63.2	40.2±55.4	36.0±56.9	28.6±64.2	33.2±69.1
Region 4	54.5±61.2	60.9±55.1	32.6±73.0	30.6±64.6	49.2±63.6	47.0±57.8	44.3±69.2	41.5±71.0
Region 5	67.2±62.6	57.6±59.9	50.3±72.7	50.6±68.4	68.1±60.2	67.2±62.4	47.4±64.7	74.9±70.5
Region 6	79.2±55.7	83.7±54.8	88.8±56.5	53.0±61.0	89.6±50.4	98.8±53.6	70.0±69.4	114.4±75.3
Region 7	93.9±57.1	107.6±42.1			63.6±55.0	81.6±40.5	82.4±71.7	
Region 8	109.3±45.1	126.3±35.7			121.2±42.5	122.8±40.2		
Region 9	131.2±34.9	131.9±29.2			112.2±34.4			
Region 10	173.6±66.1				181.1±35.3			

Direction of the force significantly affected force magnitude (GLMM $p<0.001$). The angle of the force vector in 3D space varied by region (ANOVA $p<0.001$), as shown in Table 4.2. To control for the relationship between the kinematic space region and the force vector, force direction was calculated as the angle between the force vector and the vector normal to the fingertip. By calculating direction from the fingertip, direction was not related to the region in space, but significantly affected the force that could be applied. This was true for all digits, both compared separately and together (Table 4.3).

4.3.3 Generalized Linear Mixed Model

Two statistical models of the hand were developed to estimate the strength abilities of the four fingers using finger joint angles: modelling each digit separately (Table 4.3 left) and modeling them combined (Table 4.3 right). Each model included the estimates of the covariates tested, and the covariates' significance. The separate model showed slight differences in how the covariates affected force between the fingers, such as sex affecting digits four and five more than digits two and three. In the combined model, the coefficient for digit three was not significant. This was due to the fact that the second and third digits did not apply significantly different forces.

Table 4.3: GLMM covariate estimates and significance when the digits were modeled separately (left) and when digits were modeled together (right)

Estimates	Digit 2	Digit 3	Digit 4	Digit 5
Intercept	20.4	23.3	12.7	4.66
Direction	5.23	4.12	3.70	4.67
MCP	3.06	3.77	19.7	17.3
PIP	3.87	1.57	2.30	1.34
DIP	2.09	4.94	7.09	5.82
MCP^2	-2.40	-3.83	-14.9	-15.3
PIP^2	-1.86	-3.56	-1.31	-1.41
DIP^2	0.63	1.83	1.09	2.13
Sex Male	9.23	9.34	13.8	14.1

P Value	Digit 2	Digit 3	Digit 4	Digit 5
Intercept	0.000	0.000	0.001	0.144
Direction	0.000	0.000	0.000	0.000
MCP	0.193	0.377	0.002	0.001
PIP	0.016	0.346	0.504	0.738
DIP	0.032	0.000	0.000	0.000
MCP^2	0.006	0.070	0.012	0.000
PIP^2	0.047	0.000	0.523	0.649
DIP^2	0.005	0.007	0.007	0.000
Sex Male	0.065	0.049	0.001	0.000

Name	Estimate	P Value
Intercept	30.5	0.000
Direction	5.14	0.000
MCP	8.55	0.000
PIP	3.30	0.000
DIP	7.54	0.000
MCP^2	-0.85	0.168
PIP^2	-1.42	0.006
DIP^2	1.60	0.000
Digit 3	-0.94	0.222
Digit 4	-12.4	0.000
Digit 5	-18.5	0.000
Sex Male	9.64	0.036

The relationship between the joint angles and the max force that can be applied is second order, indicating a parabolic relationship. As the coefficients are negative for the MCP and PIP joints, these parabolas have a maximum indicating a peak angle. Therefore, the MCP and PIP joints have an optimal region of force production.

Each model included the participant number as a random variable. For the individual models the standard deviations of the random effects were 15.3 N for digit 2, 14.3 N for digit 3, 8.50 N for digit 4 and 7.27 N for digit 5. For the combined model the standard deviation of finger force was 14.1 N.

4.4 Discussion

The goals of this work were to: 1) experimentally quantify finger forces of all four fingers over their individual movement (i.e. kinematic space); 2) use a statistical modeling approach to understand what causes differences in the finger forces that can be applied by healthy participants over their kinematic spaces; and 3) develop a statistical model to estimate the forces that can be produced by the fingers.

This work is a substantial contribution to the study of hand function. Force data are currently not available across the range of motion for all four fingers, and previous experimental studies have not linked the force data to the finger posture. This work is also novel in that we have developed a new approach for presenting, viewing and analyzing data that represents combined kinematic and kinetic finger function. Future work can use the regional maps of populations to compare to individuals and determine the magnitude of kinematic and kinetic function the individual has lost compared to a healthy population.

4.4.1 Statistical Differences in Force Generation Within and Between Fingers

Each finger applied the highest average force in one of the middle regions (flexed posture), and lower forces on the fully extended regions (Figure 4.4). Both the MCP and PIP joints had an optimal region of force production for all fingers, which led to finger postures where the tip of the finger was in the middle regions of the kinematic space. This optimal region is related to the optimal diameters for grip, which have been discussed by other authors (Kong and Lowe, 2005; Ruiz-Ruiz et al., 2002; Shivers et al., 2002).

Participants applied greater force with pull forces than push forces. This is likely an anatomical relationship, where the direction of the force was related to the muscles used to apply the force. Previous work investigated the effects of different muscles on force capabilities at different positions and directions (Kamper et al., 2006; Qiu et al., 2009; Yokogawa and Hara, 2002). Our work adds to the existing literature by developing a model that identifies the differences due to force direction for all four fingers. The work presented by the authors is a substantial advancement to the available body of literature. Here, all fingers were evaluated with optimal locations and force magnitudes obtained, where previous studies focus solely on the index finger.

There were also significant differences in how forces were applied between the four fingers. The index and middle fingers applied more force than the ring and pinky fingers. This finding is supported by other research and is due to the shared flexor and extensor muscles in the forearm (Martin et al., 2011). Additionally, while the index finger applied forces over the entire kinematic space, participants applied less forces in the flexed regions of the kinematic space with the other fingers. This could be due to the second digit being used commonly for precise tasks, and the other three fingers being more commonly used for grasping objects, rather than precise tasks.

The average finger force and average direction used to apply force for ten regions of the kinematic space were computed and identified. These data sets are separated by fingers and by sex to represent all fingers of both males and females. This is one of the most comprehensive data sets that is currently available in terms of positions tested, including all four fingers, and separated by sex. These data can be used in future anatomical and mechanical models of the fingers for testing and validation.

4.4.2 Generalized Linear Mixed Model

Finger force production was affected by both finger posture and force direction. The GLMM model was developed to estimate how posture and direction affected finger force application. The coefficient estimates presented in this work are valuable in that they can predict the amount of force that can be produced for any finger, at any posture, in any direction. Predicting forces across many postures and directions has applications in product design. Maximum finger force that can be applied across the kinematic space can lead to products developed to be used in the optimal kinematic regions. The data sets can inform robotics designers how to create biomimetic hands that replicate human grip. Soft finger exoskeleton devices for rehabilitation can be developed to limit forces to what is within average force ranges to prevent injuries.

Similarly, this model can be used in the future for personalized medicine. These data can be used to compare patients to an average healthy individual. By collecting forces over the range of motion and estimating a healthy individual's force in the same postures and directions, the individual's abilities can be compared to the estimated magnitudes of the forces they could produce if they were healthy. Comparing the patient's forces would show which regions of the kinematic space have lost more function than others and help clinicians decide what treatments or therapies to use. Function can also be tracked throughout rehabilitation to determine when the patient has reach average levels of function. Long term, similar research on patients going through treatment could lead to a predictive model to simulate how treatment will affect the range of motion and strength abilities of the hand.

4.4.3 Limitations

As this work was a statistical model, the relationships between the covariates in this model were arbitrary and not based in anatomic relationships, which could help limit model error. This work was also an initial population model focusing on a small sample size of mostly young individuals. Future work will test more participants and increase the range of ages tested. Additionally, adduction/abduction of the fingers was not included in the model, the work primarily focused on finger flexion and extension.

4.4.4 Conclusions

There is currently a lack of published experimental research that identifies finger forces over the range of motion and relates the amount of force the fingers can produce to the posture of the finger. This work presented a comprehensive data set of finger force and directions used to apply force for ten regions of the kinematic space, and how they differed between the fingers and between males and females. Similar data is not available elsewhere. Future work can use these data to validate future anatomical and mechanical models of the fingers. This work also developed a novel method of visualizing and interpreting function that can be used to better understand how a patient's function has changed.

There is also a lack of experimental models of finger forces. Our GLMM model showed how the amount of force that can be applied by the finger's changes based on the finger posture and the direction of the force. Future work can use this model to compare individuals with reduced hand function and understand how finger strength changes due to conditions such as osteoarthritis or stroke. This model can also be used to design products based on how much force the hand is able to produce at many different places, or in prosthetics where it is important to mimic the strength abilities of humans.

5 QUANTIFYING FUNCTIONAL DIFFERENCES IN THE INDEX FINGER DUE TO OSTEOARTHRITIS

5.1 Introduction

Osteoarthritis (OA) affects an estimated 27 million people in the United States (Lawrence et al., 2008). In particular, OA of the hand affects more than 26% of adults in America and 60% of Americans over the age of 55 (Dahaghin et al., 2005; Zhang et al., 2002). Hand OA results in decreased hand strength as well as decreased mobility leading to a significantly lower quality of life (Bagis et al., 2003; Villafañe et al., 2014). For example, loss of hand function can result in difficulties in daily activities such as opening packages, getting dressed and cutting food (Altman, 2014; Hill et al., 2010).

Clinically, changes in hand function are measured using questionnaires, goniometry, and dynamometry (Bagis et al., 2003; Bohannon et al., 2006; Nicolay and Walker, 2005; Shivers et al., 2002). While these tests are quick and easy to perform, they are also limited. Questionnaires are subjective and can be affected by mood; goniometry has high interrater error; and dynamometry measures the strength of all the combined fingers in only one or two postures which does not take into account differences due to posture or force direction or individual finger force (Bashardoust Tajali et al., 2016; Cruz et al., 2005; Drost et al., 2019; Fowler and Nicol, 2001; Yokogawa and Hara, 2002). These methods provide a limited understanding of changes in hand function; a quantitative and complete understanding of hand function and associated changes would lead to better personalized care and device design.

It is important to understand how finger function, specifically motion and force abilities, changes due to arthritis as one in two individuals will suffer from functional loss due to OA. Previously, research has shown that osteoarthritis leads to a reduction in the kinematic spaces of the digits, or everywhere the digits can reach (Leitkam et al., 2014; Leitkam and Bush, 2015). Other work has shown that OA leads to a decrease in grip strength of the hand and how stroke affects force over the kinematic space (Cruz et al., 2005; Kamper et al., 2006; Seo et al., 2010). However, there is limited research that has quantified the finger strength changes over the kinematic space of the fingers due to OA. A better understanding of how finger forces change over the kinematic space of the finger will help designers better develop products for people with reduced hand function from OA (Bullock et al., 2012).

Therefore, the goal of this work was to objectively determine how the function of the index finger is reduced as a result of osteoarthritis, specifically differences in motion and strength abilities.

5.2 Methods

5.2.1 Participants

For this study two participant groups were tested. The first group was denoted as “healthy participants”. This group did not have hand OA nor hand injuries (n=41). The second group, termed the “OA group”, was comprised of participants with doctor diagnosed hand OA (n=17). All participants in this study were right hand dominant, and only right hands were tested. Each participant consented to the study prior to participating in accordance with the Institutional Review Board requirements.

5.2.2 Experimental Data Collection

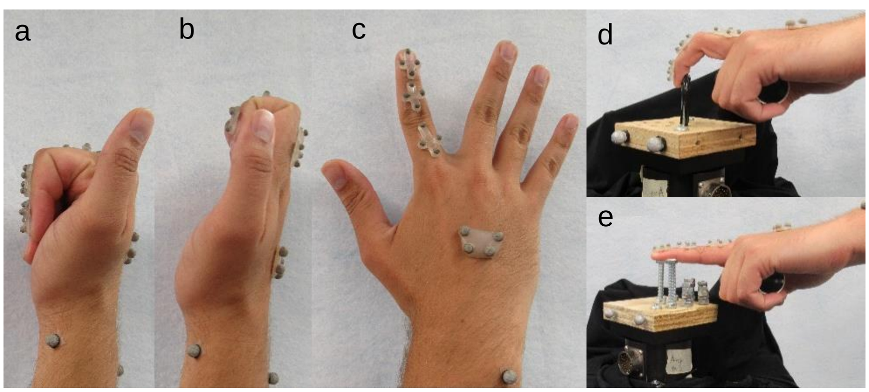

Figure 5.1: Experimental setup to obtain range of motion and force abilities for the index finger. (a) MCP flexion/extension, (b) IP flexion/extension, (c) MCP adduction/ abduction, (d) flexion/extension pull force trial, (e) adduction/abduction push force trial

Joint ranges of motion of the index fingers for each participant were computed from three finger movements: flexion and extension of the metacarpophalangeal (MCP) joint (Figure 5.11a); flexion and extension of both the proximal interphalangeal (PIP) and distal interphalangeal (DIP) joints (Figure 5.1b); and adduction and abduction of MCP joints (Figure 1c). During these motions a seven-camera motion capture system (Qualisys, Gothenburg, Sweden) collected coordinate data (x,y,z) of 18 reflective markers positioned on the hand; these were used to calculate finger posture (Figure 5.1). The joint range of motion data were used to determine the kinematic space for each participant's index finger, or the entire volume that the finger could reach. To do this, the location of the fingertip was calculated for all possible combinations of joint angles, creating the three-dimensional kinematic space (Leitkam et al., 2014).

Maximum forces were measured at 19 positions throughout the index finger's kinematic space. A multi-axis load cell (Advanced Mechanical Technology, Inc., Watertown, MA, USA) measured the loads while the motion capture simultaneously collected the locations of the reflective markers. Markers were also attached to the load cell to determine the location and orientation of the load cell relative to the hand and permit alignment of the force and motion data (Figure 5.1).

For all trials, the participant gripped a support bar to limit changes in wrist motion and prevent force generation from the other body segments. Additionally, all participants sat with their arms vertical, elbows at 90°, and wrists flat to limit force differences due to position of the arm. First, differences in forces related to the finger flexion were investigated (Figure 5.1d). A bracket was placed in seven positions at 15 mm intervals ranging from 10 mm from the handle to 100 mm from the handle. At each position, the participant was asked to push towards the ground with maximum force then pull towards the wrist with maximum force. Next, differences in forces related to finger adduction/abduction were investigated (Figure 1e). The participant was asked to push towards the ground at three positions at full finger extension (adducted, middle, abducted), then pull towards the wrist at three positions at mid flexion (adducted, middle, abducted). To avoid fatigue, the order of the tests was randomized between participants.

5.2.3 Mapping the Motion and Force Abilities

In order to understand how force production changed over the kinematic space, the collected force data were mapped to the kinematic space (Figure 5.2). This process of transforming the data sets to the same coordinate system and overlaying the force and motion abilities is described in previous published work by the authors (Drost et al., 2019). Briefly, each individual's abilities were mapped by aligning the coordinate systems of the kinematic space and the force trials; these individual maps visualize how finger function changes between participants. Next, the individual maps were combined into healthy and arthritic population maps. The (x,y,z) coordinates of these maps were normalized by the finger length.

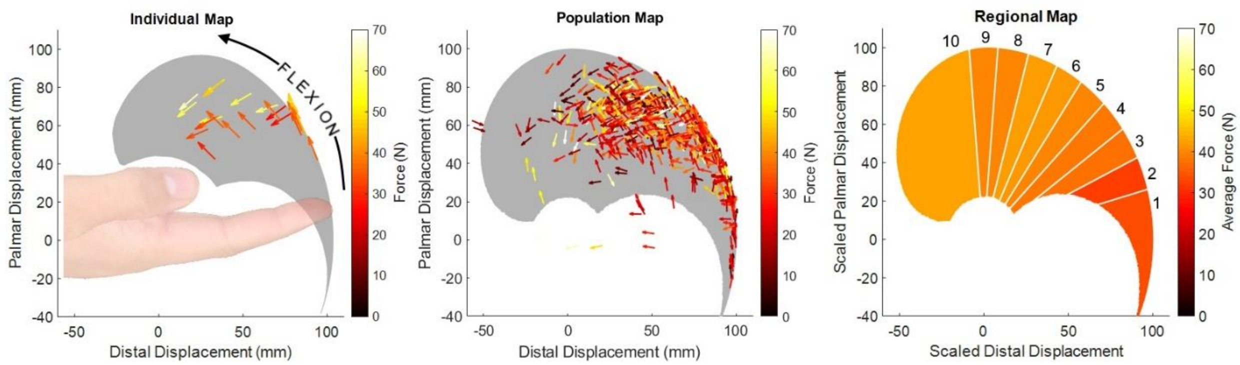

Figure 5.2: Force data mapped to the kinematic space. These maps are 2D representations of 3D data sets. The grey background represents the kinematic space of the finger. The colored arrows represent force actions in position, direction and magnitude. First an individual's force abilities are mapped to his or her kinematic space (left). Next, all individuals in a population are mapped together (center). Finally, the population's abilities are averaged over regions of the kinematic space (right).

Finally, the collected data were computed to form regional maps (Figure 5.3a). These regional maps were created as a means for comparison between the healthy and arthritic populations and to compare an individual to a population. Regional maps were calculated by subdividing the kinematic space of each finger into polar segments across the range of motion and averaging the force magnitudes for each section. Regions 2-9 were each 10° arcs ranging from 10° from parallel with the palm all the way to 90° from the palm. Most healthy participants applied forces between 10° and 90° from parallel with the palm. Additionally, regions 1 and 10 were designed to be larger to increase the number of force trials in the regions, as fewer participants applied forces in these regions.

To compare between an individual and a population, each arthritic participant's individual force map was transformed onto the population's regional map. Similar to mapping the population maps, the coordinates for the individual map were normalized by the participant's finger length to compare individuals regardless of finger length. Then the individual's kinematic space and force data were overlaid on the regional map for comparison (i.e. to compare a participant from the OA group to the healthy population).

5.2.4 Comparing Arthritic Population to a Healthy Population

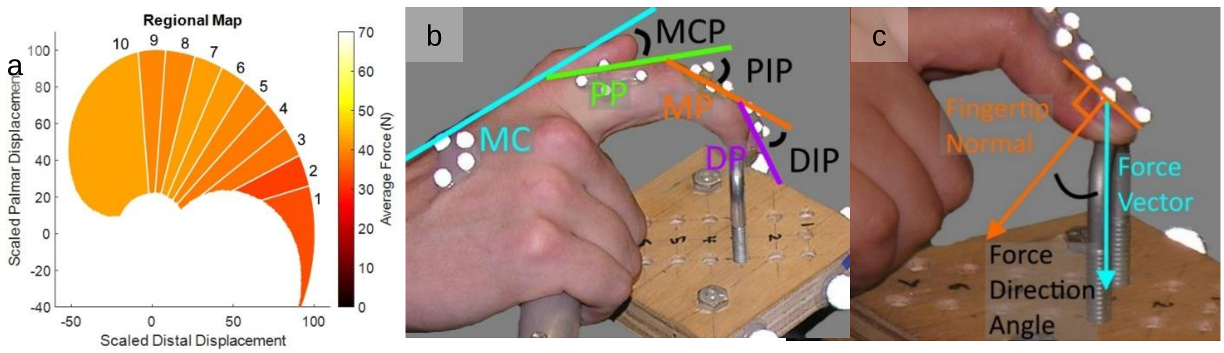

Figure 5.3: Definitions of finger posture and force direction. (a) Finger posture measured as the region in the kinematic space. (b) Finger posture as defined by the flexion of the three joints of the finger. (c) Force direction was defined as the angle between the force vector and the vector normal to the fingertip in the sagittal plane.

Analysis of Variance (ANOVA) with a Tukey post hoc test and Generalized Linear Mixed Modelling (GLMM) were used to determine how OA affected the functional abilities of the fingers. Differences in index finger function due osteoarthritis were examined based differences in the range of motion and kinematic spaces of the participants, as well as the differences in the magnitude of force that could be applied.

To understand the relationship between finger posture and force generation, three key factors were considered. 1) Region of kinematic space where the force was applied (Figure 3a). Regions were used to compare participants statistically with only one variable. 2) MCP, PIP and DIP joint angles were compared to understand differences based on finger posture (Figure 3b). 3) The direction the force was applied, defined as the angle between the force vector and the vector normal to the fingertip in the sagittal plane (Figure 3c). Each of these factors was statistically analyzed to determine how they affected finger function, and how those effects change due to OA. To eliminate any confounding effects from age and gender, those variables were controlled for in our statistical analysis.

5.3 Results

5.3.1 Participants

Two groups of participants were tested as part of this study. The healthy group was split into two sub-groups: 21 healthy participants (11 female, 10 male, mean age 28.3 years, SD 10.0 years) completed the whole test; 20 healthy participants (10 female, 10 male, mean age 21.1 years, SD 0.9 years) completed only the flexion-extension positions. The second subgroup was added to increase the sample size of the healthy population. The OA group of 17 participants with hand osteoarthritis (15 female, 2 male, mean age 74.2 years, SD 5.2 years) completed the whole test.

5.3.2 Functional Differences due to Osteoarthritis

As expected, participants in the OA group had a significantly smaller ranges of motion. The motion was smaller in the OA group for the MCP joint (ANOVA $p<0.001$) and DIP joint (ANOVA $p<0.001$), but not the PIP joint (ANOVA $p=0.742$). Ranges of joint motion for each group are presented in Table 1. After normalizing by finger length, the volume of the kinematic space of the OA group was on average 21% smaller as compared to the healthy group (ANOVA $p=0.003$).

Table 5.1: Mean and standard deviations of joint range of motion as well as maximum and minimum joint angles for the index finger joint for both the healthy and OA groups (°). Joint angles are measured from parallel with the palm, with negative angles being hyperextension.

	Healthy Group			OA Group		
	Range	Minimum	Maximum	Range	Minimum	Maximum
MCP	115.8±17.7	-29.5±11.1	86.3±11.4	95.5±17.9	-21.1±13.0	74.5±11.5
PIP	116.5±17.2	-5.8±13.4	110.7±7.8	114.7±18.1	-6.9±17.4	107.8±5.6
DIP	89.8±12.6	-3.7±11.6	86.0±6.0	71.1±18.7	-6.2±15.4	64.8±12.9

Participants in the OA group applied less force than participants in the healthy group (ANOVA $p<0.001$). The OA group also used a smaller range of joint angles and a smaller volume of space to apply forces (Figure 4). Smaller ranges of motion were used to apply forces in the MCP and PIP joints (ANOVA $p=0.01$). The DIP joint did not show a significant difference due to

OA. This led to a smaller volume of space used to apply forces by the OA group participants (ANOVA p<0.001).

Range of force directions used were different between groups. The participants in the OA group used a smaller range of force directions to apply forces in regions 1-5 (ANOVA p<0.001). However, the range of directions used by participants in the OA group was not significantly different for regions 6-8 when compared to the participants in the healthy group. Therefore, the range of directions used to apply forces in extended positions decreased due to OA.

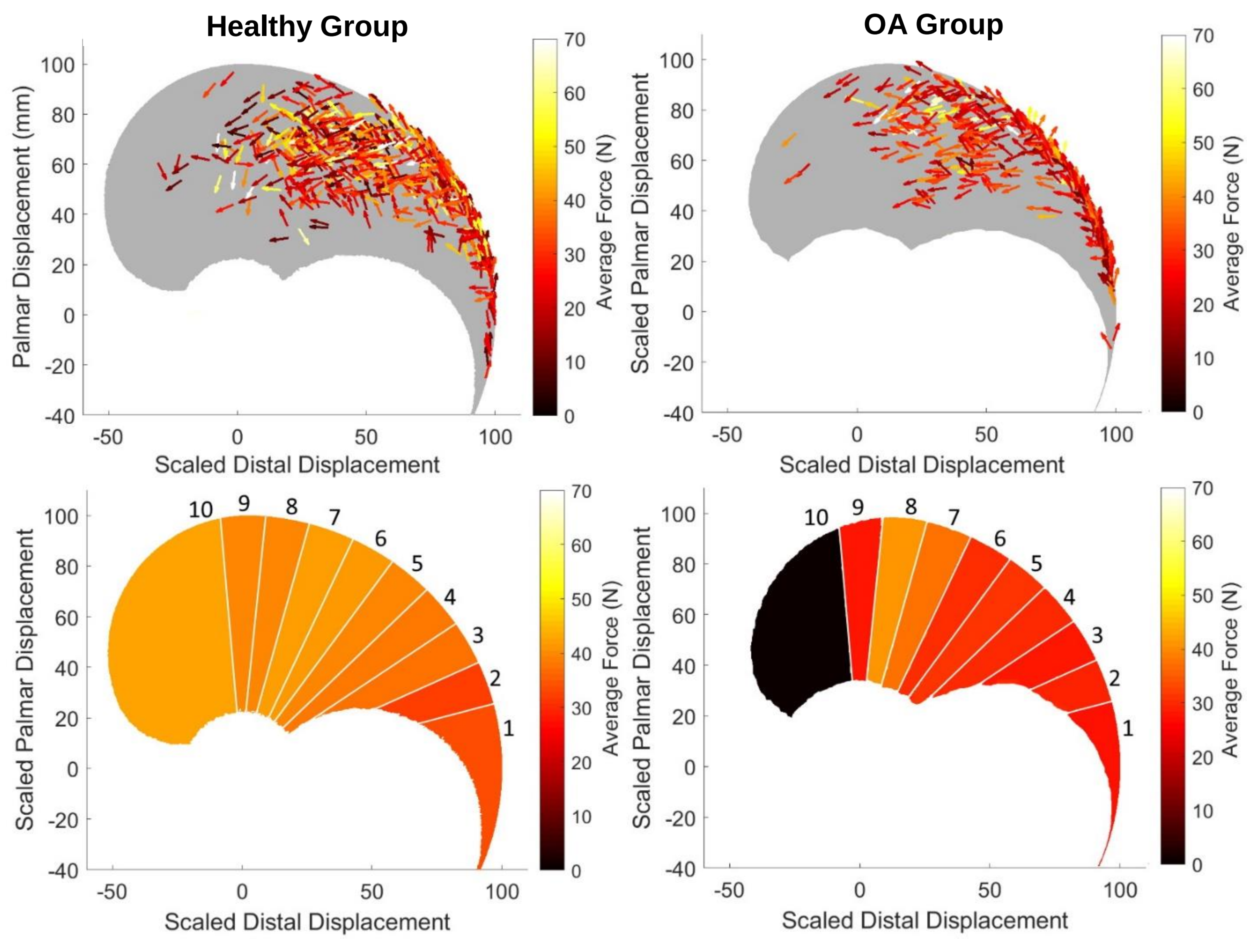

Figure 5.4: Index finger forces mapped to the kinematic space. Top: Population maps of all force events. Bottom: Regional maps of average forces across the kinematic space.

Additionally, there was less variance in the forces that were applied by participants in the OA group. The healthy group applied forces with significant differences between regions of the range of motion (regions 1-3 were different than regions 5-7 with p<0.01), while the OA group only had one pair of regions that were significantly different (regions 3 and 8 are different with $p=0.047$). There were also less differences in how force was applied due to joint angles. While healthy participant's forces changed based on the joint angles (GLMM $p<0.001$ for all three joints), the OA group's forces were only significantly affected by the MCP joint (GLMM $p=0.031$) and the forces were not significantly affected by the PIP joint (GLMM $P=0.793$) or DIP joint (GLMM $p=0.512$).

Maximum forces applied by participants in the healthy group were significantly affected by force direction angle (GLMM $p<0.001$), but forces applied by participants in the OA group were not (GLMM $p=0.933$). Forces applied by participants in the OA group changed less than participants in the healthy group due to the force direction angle and the location within the range of motion; overall, the OA group participants applied a similar maximum force between most trials.

5.3.3 Comparing Arthritic Individuals to a Healthy Population

The regional maps were also used to understand the degree of reduction of a participant's finger function. The visualizations in Figure 5 show four female participants in the OA group (colored arrows and black outline) that exemplify different ranges of reduced motion and force abilities compared to a regional map of healthy female participants (colored regions). The black outline describes the individual's kinematic space. Participants C and D had reduced kinematic spaces, while the participants A and B had kinematic spaces similar to the healthy group. The colored arrows represent the participant's strength abilities. A large difference in color between the arrows and the shaded regions implies that the individual's strength has decreased (participants B and C). Additionally, the area covered by the arrows represents the space used to apply forces: force arrows spread over the range of motion (such as participant A) show the participant is able to use a larger portion of the kinematic space to apply forces than force arrows grouped together (such as participant B). Using a smaller portion of the range of motion to apply indicates that the participant has a smaller functional area where forces can be applied and that more function has been lost.

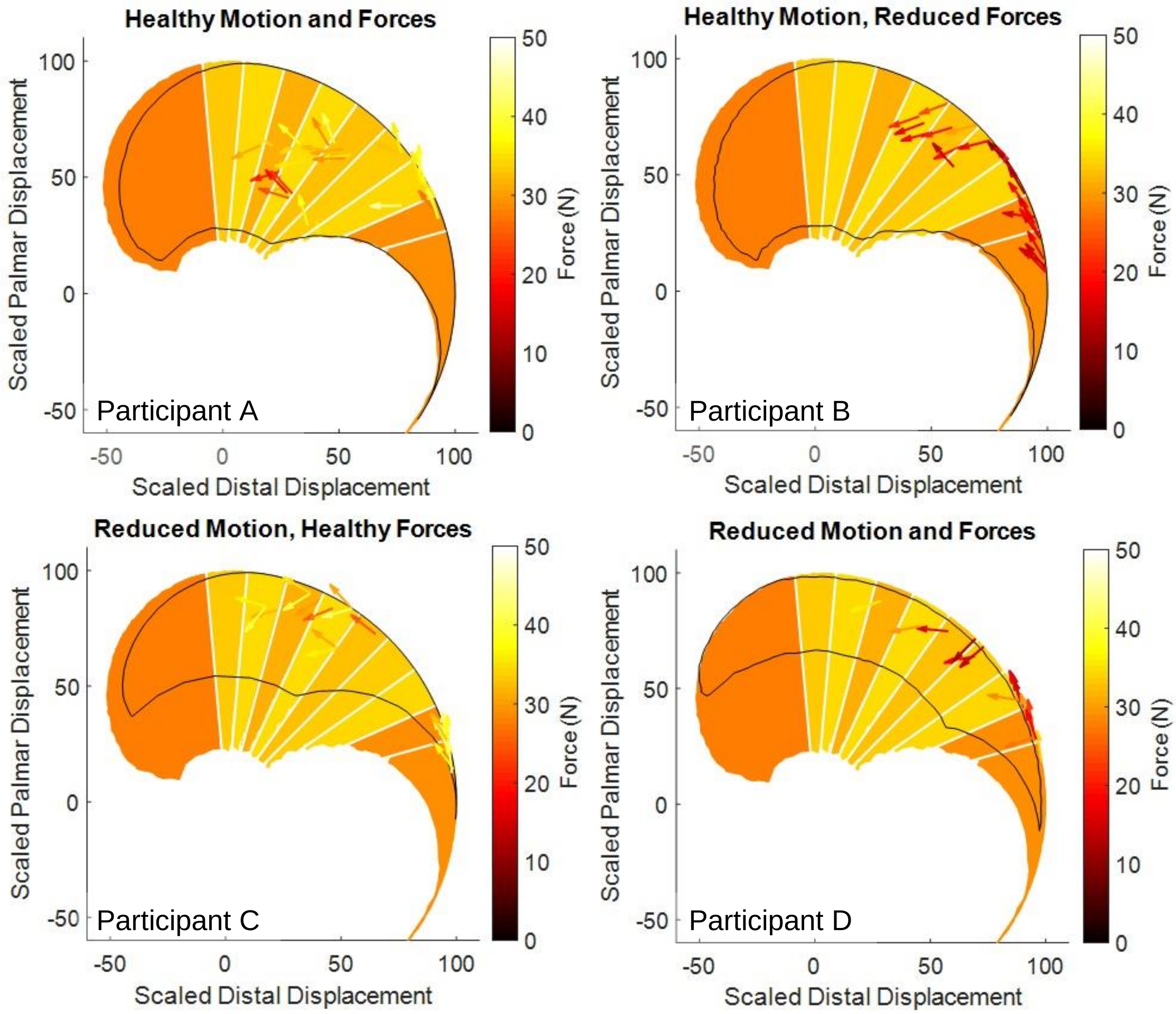

Figure 5.5: Four female participants in the OA group compared to the healthy female population. The regional map in the background shows the healthy female data. The black outline describes the arthritic participant's kinematic space, a smaller kinematic space indicates reduced motion function. The colored arrows represent the force actions of that participant, forces with similar colors indicate the individual has healthy force function.

5.4 Discussion

Therefore, the goal of this work was to objectively determine how index finger function is reduced due to osteoarthritis, specifically differences in motion and strength abilities. The work presented here is an important contribution to the understanding of how finger function changes due to osteoarthritis. While previous research concluded that OA leads to a reduction in grip strength and motion abilities (Leitkam et al., 2014; Leitkam and Reid Bush, 2015; Seo and Armstrong, 2008), there is limited research discussing how the forces change over the range of motion. Specifically, while healthy participants showed changes in force over the range of motion, participants with OA applied similar forces over the majority of the range of motion. This indicates that more function was lost in certain regions of the kinematic space and the optimal force region was much smaller for individuals with OA. It is important to understand how forces are applied over the kinematic space to best design devices for participants with reduced function, products should be designed for the smaller optimal space. Additionally, this work introduces a novel method of displaying and comparing function. These visualizations can be used to treat patients and develop personalized medicine to improve hand function.

5.4.1 Functional Differences due to Osteoarthritis

Arthritis significantly changed finger function. As expected, participants with arthritis had a smaller range of motion and applied less force that those in the healthy group, which agrees with reported literature (Bagis et al., 2003; Zhang et al., 2002). Participants with arthritis performed the motions in a smaller volume of space and used a smaller range of joint angles to apply forces in a smaller range of directions. Other studies have suggested that force and motion functions are related (Drost et al., 2019; Yokogawa and Hara, 2002), by limiting both the 3D space that the finger can apply force and the range of directions for that forces can be applied in arthritis significantly limits hand function.

Participants the OA group applied similar forces across their range of motion. The participants in the healthy group had higher forces in the central regions, showing an increase in force capabilities in the more flexed regions. However, this was not seen in the arthritic participants, where there was only one region that was significantly different from the other regions. The arthritic forces were also not as affected by the finger joints or direction of the force.

Therefore, hand OA affects the relationship between finger posture and strength. Certain regions of the kinematic space lost more function than others due to OA. The reason for this is not clear based on this study; this could be a physical or anatomical change where there is a maximum load that the finger can bear at all points. There could be a pain barrier, where only a low amount of force can be applied before there is pain. Or, the limit could be psychological, and the participants were only comfortable applying a certain amount of force.

These differences in function are important to understand for device design. Portions of the optimal region were lost due to osteoarthritis, and the optimal region for participants with OA was much smaller. Devices for individuals with reduced motion should focus on the areas where there is still significant function.

5.4.2 Comparing Arthritic Individuals to a Healthy Population

The mappings discussed in this work are a novel method to quickly and visually compare a participant to a healthy population. This procedure could be used for diagnosis of lost function, and to understand if a patient is symptomatic for OA. It could also be used to modify treatment for personalized medicine: a participant with healthy forces but reduced motion may benefit from different treatment than participants with normal motion and reduced forces. Future work will investigate which treatments are best for which conditions.

Going forward this method can be used to compare different treatments or surgeries to understand how function is changed. While many of these treatments are able to reduce pain, it is also important to restore function, and this method would be able to discern which treatments best restore function to the hand.

5.4.3 Limitations

There was a difference in the ages of the healthy and OA groups and the OA group was mostly female. Age and gender were controlled for during statistical analysis to account for these biases; however, the differences between the tested groups is a potential limitation of this work.

5.4.4 Conclusions

In conclusion, arthritis led to participants applying lower forces, over a smaller range of their kinematic space, and in a smaller range of directions. Arthritic participants also had smaller differences in the amount of force that was applied due to finger posture and direction of force. These changes in function are important. Devices for individuals with arthritis should focus on the optimal area of OA function, and treatments for OA should be compared to better understand how they affect function. Although trends in function were exhibited, it is also important to understand how each individual's function has changes to personally treat each patient.

6 CHANGES IN THUMB FUNCTION DUE TO CARPOMETACARPAL JOINT SUSPENSIONPLASTY, A PILOT STUDY

6.1 Introduction

Osteoarthritis is the leading cause of loss of hand function in America affecting over 60% of Americans over the age of 55 (Haugen et al., 2011; Zhang et al., 2002). While all the joints in the hand can be affected by OA, the carpometacarpal (CMC) joint of the thumb is the most commonly impacted (Thompson and Netter, 2010). The thumb CMC joint is necessary for grasping, pinching and manipulating objects; due to this, the thumb CMC is one of the most used joints in the hand. Loss of thumb function has been estimated to remove 40% of the function of the hand (Swanson, 1964).

Treatment of CMC OA depends on the level of severity (Lue et al., 2017; Mahendira and Towheed, 2009; Towheed, 2005). In patients with mild symptoms, such as minor pain and joint stiffness, exercise and medications are used to improve strength, range of motion, and to control pain (Bjurehed et al., 2017). For moderate OA, which includes pain while applying force and reduced range of motion, splints are used to support the thumb and limit loading through the joint (Mahendira and Towheed, 2009). However, in severe cases, where the pain is constant and range of motion is greatly diminished, surgery is an option to reduce pain and restore quality of life (Li et al., 2011).

The most common surgery for osteoarthritis of the thumb CMC joint is a trapeziectomy, which is removal of the trapezium (Li et al., 2011). Trapeziectomy lessens the pain in the joint; however, this also removes mechanical stability from the thumb, changing the method of force transduction. To provide support and increase the range of motion of the thumb after surgery, a trapeziectomy can be followed by reconstruction of the ligaments of the CMC joint or arthroplasty, where a synthetic joint is implanted to replace the thumb CMC joint (Huang et al., 2015; Li et al., 2011; Vermeulen et al., 2011).

A newer arthroplasty approach is the mini-tightrope method, also called suspensionplasty, which uses a suture wire to attach the base of the thumb metacarpal to the second metacarpal (Friebel et al., 2018). Formerly, suspensionplasty was used in the knee and ankle to increase bone support (Eguchi et al., 2014; Storey et al., 2012). Benefits of the suture wire method discussed in previous studies include that the surgery did not require tissues to be harvested from the hand during surgery and there was a shorter time between surgery and when the participant was able to start moving the operated joint (Igoe et al., 2014; Khalid and Jones, 2012). Suspensionplasty in the thumb CMC joint has also shown favorable outcomes as compared to other thumb fixation methods in cadaveric tests and case studies (Assiotis and Giannakakis, 2017; Desai et al., 2016; Friebel et al., 2018; Hooke et al., 2016; Parry and Kakar, 2015).

The assessments that have been conducted thus far focused on post-surgery patient questionnaires or cadaver bone movement, not *in vivo* functional improvements (Assiotis and Giannakakis, 2017; Desai et al., 2016; Hooke et al., 2016; Parry and Kakar, 2015). In order to understand the full benefits of thumb CMC suspensionplasty, it is critical to understand how the surgery affects both pain and function. Comparing kinematic (movement) and kinetic (strength) function before and after the surgery would allow patient outcomes to be assessed objectively.

Therefore, the goal of this work was to quantify how thumb CMC suspensionplasty affected the function of the thumb in terms of pain, range of motion, and strength. A stronger understanding of the changes in function due to mini-tightrope suspensionplasty will lead to more informed surgeons who can better select the right surgery for each patient.

6.2 Methods

6.2.1 Participants

For this study five participants (2 male, 3 female, mean age 63 years ± 5.4 years) who were scheduled for mini-tightrope suspensionplasty were tested at three time points: 1) prior to surgery; 2) six weeks after surgery and rehabilitation when the participant could apply force with the thumb, but was not fully healed; and 3) twelve weeks after surgery and rehabilitation when the thumb is considered fully healed and the participant could apply full forces. All participants gave written consent before each test point in accordance with the university's Institutional Review Board.

6.2.2 Clinical Methods

To compare the clinical outcomes of this surgery, each participant completed two questionnaires and took a dynamometer test. The first questionnaire was the Disabilities of the Arm, Shoulder and Hand (DASH) questionnaire (Hudak et al., 1996). The DASH has been used to measure subjective hand function in clinical settings and asked participants to rate different tasks of daily living from 1 (no difficulty) to 5 (very difficult) (Hudak et al., 1996; Igoe et al., 2014; Vermeulen et al., 2011). A high DASH score shows less function. The second questionnaire was the Visual Analog Scale (VAS) to measure pain; the VAS has participants mark a line on a 100mm scale from no pain to most possible pain, and that mark is measured with a caliper (Scott and Huskisson, 1976). This method has been validated as an objective measure for pain (Visser et al., 2015). The final clinical test used for this project was a Jamar Dynamometer test (Sammons Preston, Bolingbrook, Illinois, USA). Participants performed the power grip three times at the second grip size and the pinch grip three times.

6.2.3 Range of Motion

Kinematic function was computed using data from a motion capture system (Qualisys, Gothenburg, Sweden). Eighteen markers were attached to the hand and thumb (Figure 6.1). Clusters of four markers were placed on the middle of the dorsal side of the thumb phalanges and metacarpal, as well as a cluster on the center of the dorsal side of the palm. These clusters were used to calculate the position and rotations on each segment of the thumb relative to the palm. Two additional markers were placed at the wrist on the ulnar and radial styloids.

Three motions were used to calculate the entire thumb space (Figure 6.2). 1) Flexion and extension of the interphalangeal (IP) and metacarpophalangeal (MCP) joints. 2) Opposition to the pad of the fifth digit, where participants were asked to oppose first with the largest arc they could make with their thumbs, then to slide their thumbs distally along the pads of the fingers. This motion measured the range of abduction across the range of flexion and extension. 3) Palmar and radial abduction of the thumb.

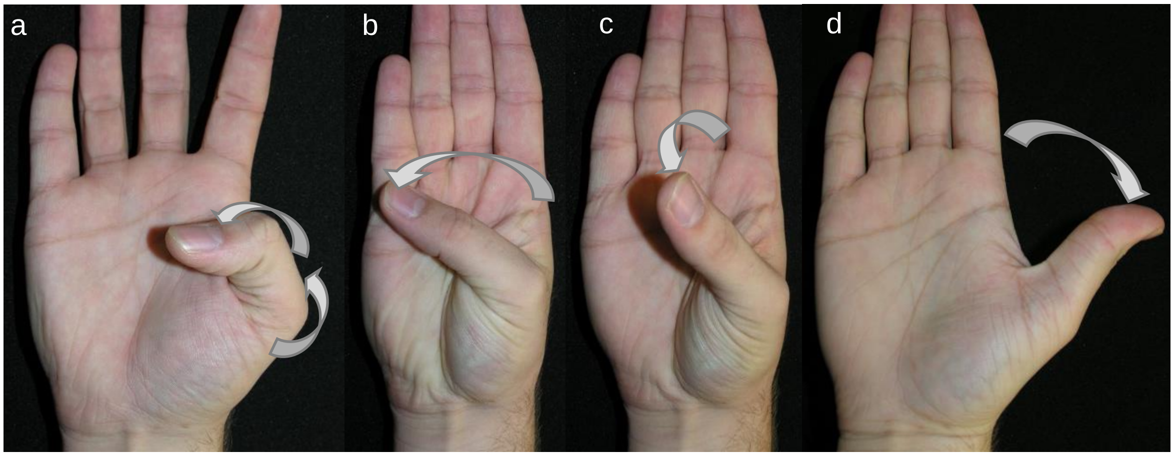

Figure 6.1: Motions to determine thumb kinematic space: a) flexion/extension of thumb metacarpophalangeal and interphalangeal joints; b) opposition to the pad of the 5th digit; c) palmar abduction; d) radial abduction.

Next the total kinematic space of the thumb, everywhere the thumb can reach, was computed. The thumb was analyzed with four degrees of freedom: IP joint flexion/extension, MCP joint flexion/extension, CMC joint abduction/adduction (movement away from the second metacarpal), and CMC flexion/extension (movement around the second metacarpal). Using the three motions, the range of motion for each thumb joint was calculated by comparing the maximum and minimum joint angles obtained through the three motions. The posture of the thumb, defined as the (X,Y,Z) coordinates of the tip of the thumb, was calculated for each combination of joint angles to give a cloud of (X,Y,Z) coordinates that the thumb could reach. The volume that encompassed all the calculated postures was the total kinematic space of the thumb.

6.2.4 Force Generation

Force generation over the range of motion of the thumb was measured using a six-axis load cell (Advanced Mechanical Technology, Inc., Watertown, MA, USA) along with the motion capture system. For all tests, the participants sat with their arms vertical, their elbows at 90°, and hands supported on a hand rest to limit differences in force from body posture. The hand rest limited force production to within the thumb and was positioned to give a neutral wrist angle. In order to collect forces at different flexions of the thumb, the hand rest was rotated in four positions with respect to the ground: 0°, 30°, 60°, and 90°. At each rotation the participant applied forces at two positions: adducted close to the palm and abducted at the furthest position the participant could reach (Figure 6.2). Then at each position, the participant applied forces in two directions: pushing down towards the ground and pulling in towards the palm. Each force action was performed twice. Therefore, each participant completed 32 force events: four rotations, two positions (adduction and abduction), two directions (push and pull), and two trials in each combination.

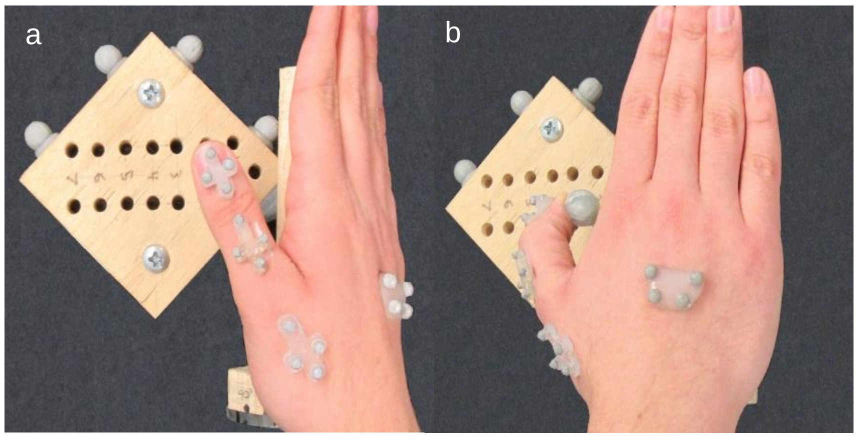

Figure 6.2: Thumb force measurement apparatus. a) Hand is rotated at 60° and thumb is pushing towards the ground. b) Hand is level with the ground and pulling toward the palm.

6.2.5 Mapping Forces to the Range of Motion

In order to understand how force production changed over the kinematic space before and after surgery, the collected force data were mapped to the kinematic space. This process of transforming the data sets to the same coordinate system and overlaying the force and motion abilities was originally developed for the fingers and then adapted for the thumb (Drost et al., 2019).

To do this, the force actions were analyzed to determine the time, direction, and magnitude of the applied force. Motion capture data were analyzed to determine to position of the fingertip and joint angles at the time of maximum force. The force vectors (comprised of the position of the fingertip, force direction, and magnitude of the force) and kinematic space (total 3D space the finger can reach) were both transformed to be in the same coordinate system with the origin at the MCP joint of the finger. This allowed the force abilities to be mapped to the kinematic abilities.

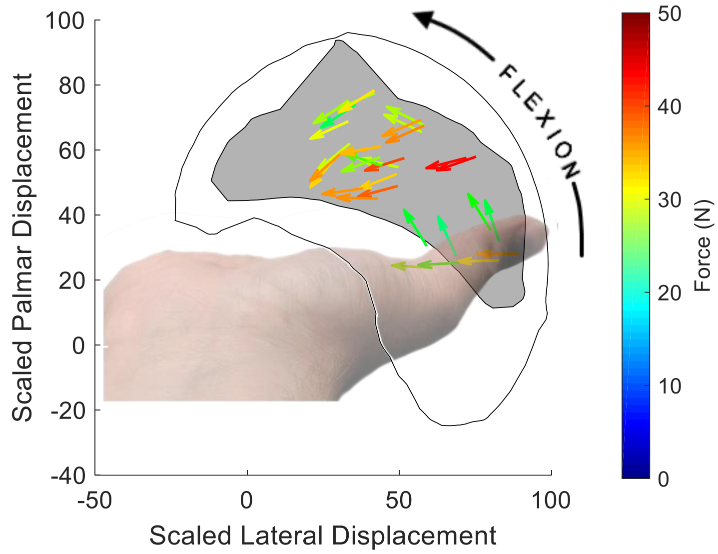

Figure 6.3: Force map of the thumb for a participant. The grey background represents the kinematic space of a participant's thumb, while the white background represents the kinematic space of a representative healthy participant. Both have been scaled by the participants' thumb lengths. The color scale represents the amount of force that was applied, with each vector representing a 2D projection of the direction of the force and position within the kinematic space where the force was applied. A semi-transparent thumb is overlaid on the figure to describe the orientation.

To do this, the force actions were analyzed to determine the time, direction, and magnitude of the applied force. Motion capture data were analyzed to determine to position of the fingertip and joint angles at the time of maximum force. The force vectors (comprised of the position of the fingertip, force direction, and magnitude of the force) and kinematic space (total 3D space the finger can reach) were both transformed to be in the same coordinate system with the origin at the MCP joint of the finger. This allowed the force abilities to be mapped to the kinematic abilities.

6.2.6 Analysis

Differences in clinical measures, range of motion, and force abilities between the three time points (pre-surgery, six weeks post-surgery, and twelve weeks post-surgery) were compared using repeated measures analysis of variance (RMANOVA). Clinical tests were statistically compared (RMANOVA) to understand how the pain, DASH score and grip strength changed due to surgery.

Changes to kinematic function were tested using two criteria: joint range of motion and volume of the kinematic space. The ranges of motion of the CMC joint, both in flexion/extension and adduction/abduction, were compared to understand how the individual motions of the thumb changed due to surgery. This was calculated as the difference between the maximum and minimum angles over the kinematic space. Volume of the kinematic space was compared to assess how removal of the trapezium affected the space the thumb could reach.

Differences in thumb strength between the three time points were assessed by three criteria. First, the magnitudes of the maximum forces were compared to understand strength changes. Second, the ranges of directions in the that were used to apply forces in the transverse plane of the hand were compared to determine if the change in mechanical structure of the thumb affected the directions in which forces could be produced. Third, the force application space, or the volume of the kinematic space used to apply forces, was compared to understand how surgery altered the usable kinematic space of the thumb.

6.3 Results

6.3.1 Clinical Tests

Pain was significantly reduced due to this surgery (RMANOVA p=0.046). For most participants, pain was greatly reduced six weeks following the surgery, however all participants mentioned a continued stiffness in the thumb joints (Figure 6.4). At twelve weeks the pain had further decreased in all patients.

Changes to DASH scores were participant dependent and showed no significant differences within the group. The DASH measures the participant’s perceived function with a higher score representing less function. Most participants had decreased function after six weeks; however, after twelve weeks some participants improved, while others did not. Notably, both participants who had higher DASH scores after twelve weeks were male.

Dynamometry showed a decrease in grip force after six weeks, which was significant for the pinch grip (RMANOVA p=0.032) and close to significant for the power grip (RMANOVA p=0.062). After twelve weeks both grip forces were similar to before surgery.

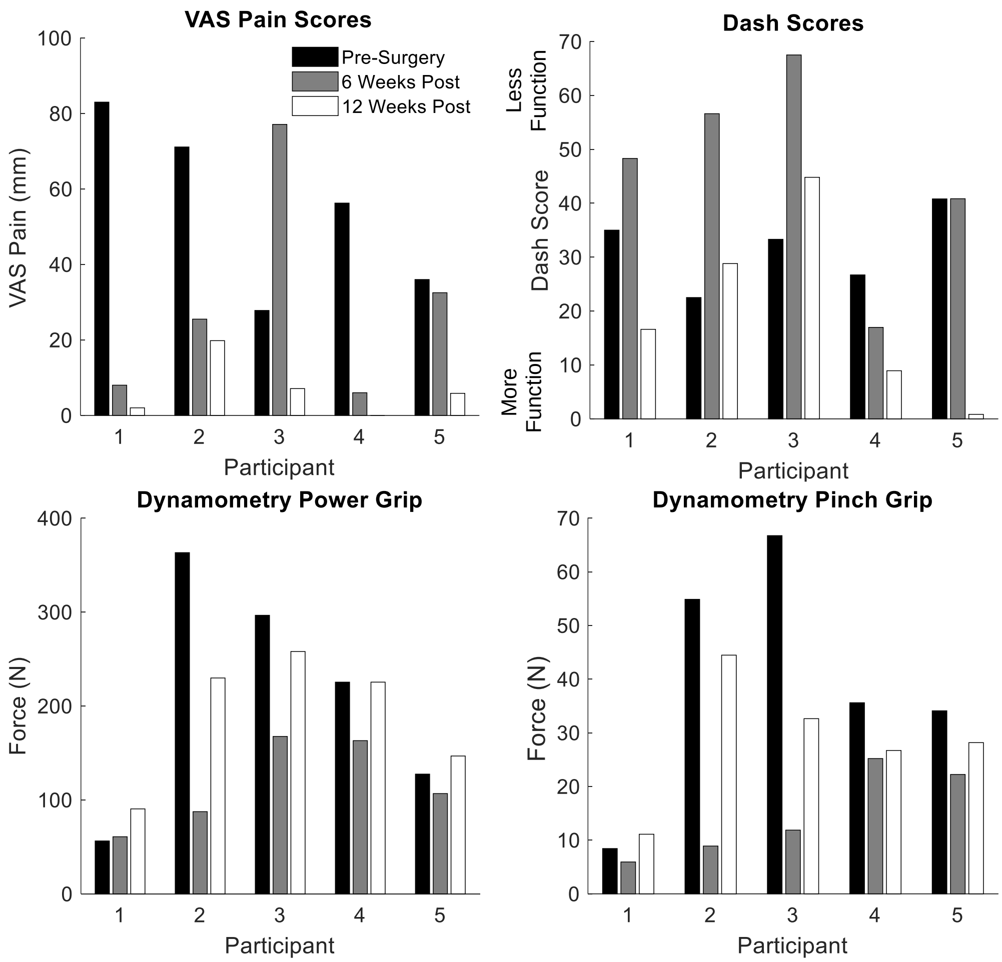

Figure 6.4: Changes to clinical measurements following surgery. A higher VAS score indicates higher pain. A higher DASH score indicates less hand function.

6.3.2 Range of Motion

The kinematic abilities of the thumb changed due to surgery, both in joint range of motion and in the kinematic space.

Joint range of motion changed for both CMC flexion/extension and abduction/adduction (Figure 6.5). For both, the range of motion was measured as the maximum angle to the minimum angle. There was a significant decrease in the range of CMC flexion/extension (RMANOVA p=0.016) at both 6 and 12 weeks with participants continuing to have poor range of motion. While the change in CMC adduction/abduction was not significant, most participants had a smaller range of motion at both test points following surgery.

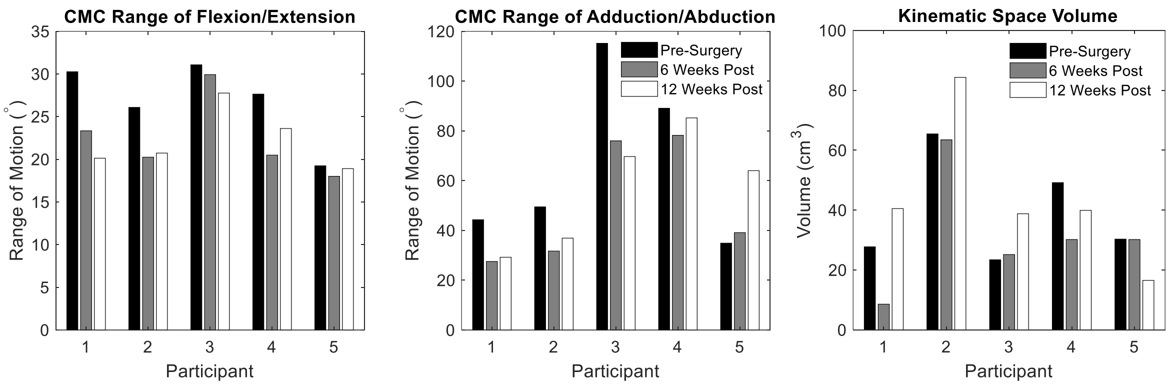

Figure 6.5: Change in range of motion and kinematic space due to surgery for each participant. Left: Flexion/extension differences. Middle: Adduction/abduction differences. Right: Change in volume of the kinematic space of the thumb.

Range of motion of the CMC joint decreased following surgery, but the volume of the kinematic space did not. This difference is due to the range of motion measuring the maximum and minimum angles that can be attained for flexion/extension and adduction/abduction; however, the range of abduction is not consistent over the range of flexion. While the maximum range of motion values deceased, the total range the CMC could move did not. The MCP and IP joints also contribute to the kinematic space and help the thumb reach the volume.

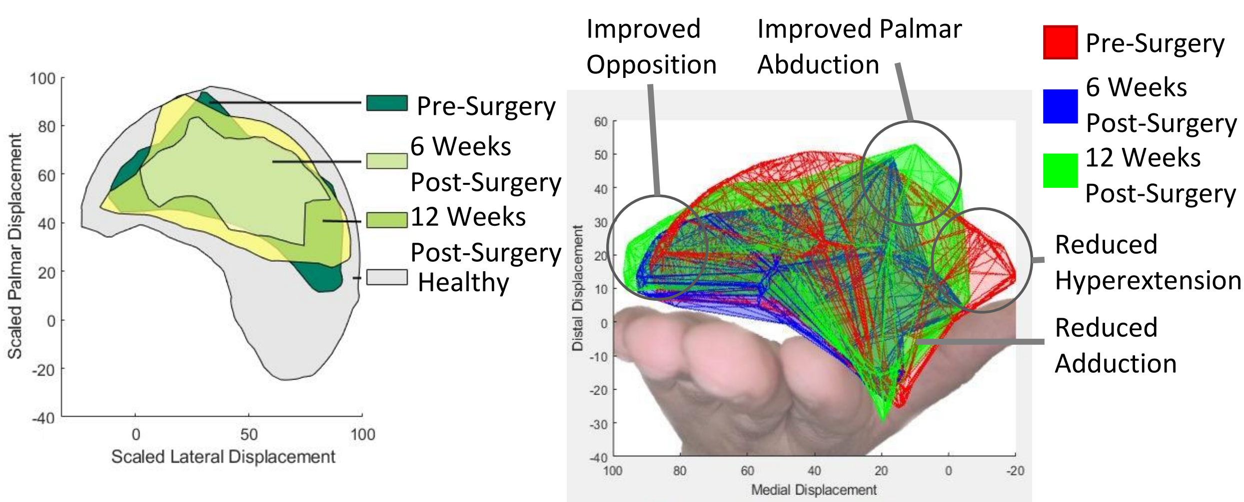

Figure 6.6: Visualization of changes to the range of motion. Left: Changes to the kinematic space of Participant 2 as a 2D projection. Right: Kinematic space differences in Participant 3 shown as a 3D space (right).

6.3.3 Forces

Forces were compared between tests using three criteria: magnitude of force relating to the strength of the thumb; the range of directions in which forces were applied; and the volume of space used to apply forces.

Force magnitudes were significantly lower after six weeks (RMANOVA p=0.012) then similar to before surgery after twelve weeks. The range of directions used to apply forces was similar for all three test times (RMANOVA p=0.510). There were no significant changes in the volume of space used to apply forces, as the changes were not consistent between participants.

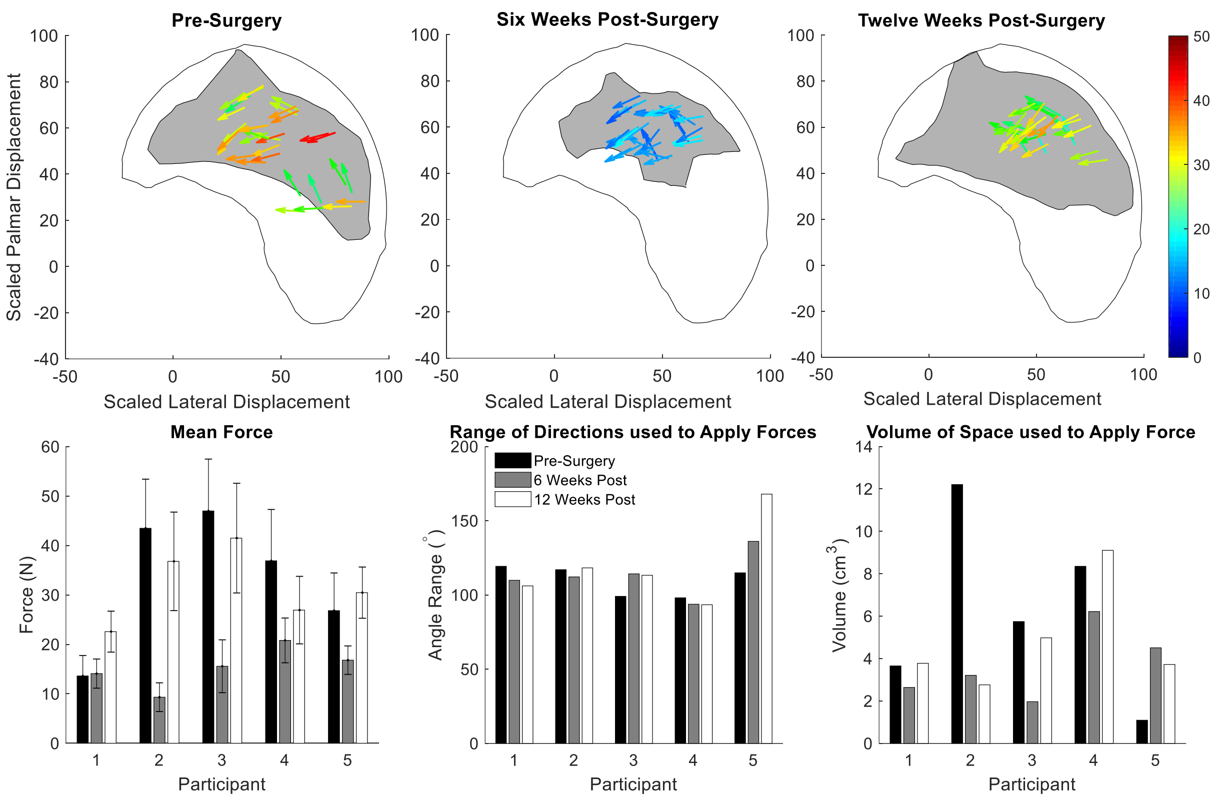

Figure 6.6: Differences in force production for one participant and all participants. Top: Visualized force profiles over the range of motion for Participant 2 at each testing point. Bottom: Differences in magnitude of force, range of force directions and volume of force space between three time points.

6.4 Discussion

The goal of this work was to quantify how thumb CMC suspensionplasty affected the function of the thumb in terms of pain, range of motion, and strength. Five participants were tested before surgery, six weeks after surgery, and twelve weeks after surgery. All participants saw a decrease in pain due to surgery; however, function was not consistently improved as the DASH scores, kinematic space volumes, and force results were not significantly changed.

There were differences in how the patients responded to the surgery. Participant 3 reported worse pain six weeks after the surgery than before the surgery. At twelve weeks, some participants had higher forces and increased volume of kinematic space used to apply forces as compared to before the surgery, while others did not. This could be due to differences between participants or due to differences in the surgery.

The purpose of suspensionplasty is to stabilize the thumb following trapeziectomy by connecting the metacarpal of the thumb to the metacarpal of the index finger. This limits the movement of the base of the metacarpal and allows force to be transferred from the thumb to the hand, wrist, and arm. However, there are currently no specific guidelines for the location of the anchor in the second metacarpal or the tightness of the suture wire. A suture wire that is too tight would be painful and restrict motion, while a loose suture wire would limit the force that can be transferred through the thumb. Previous research recommended attaching the anchor approximately halfway up the second metacarpal, so as to prevent bone subsidence and long term complications (Yao and Song, 2013). Future research is needed to determine the optimal location of the second metacarpal anchor position to both assist in force transference and lead to long term hand benefits.

For this test, both joint range of motion (which is used clinically) and the kinematic space (a novel method of quantifying thumb function) were compared. Range of motion of the CMC joint decreased following surgery, but the volume of the kinematic space did not. This shows that the tools currently used in clinical settings do not fully describe changes to hand function. Understanding how the kinematic space changes is important to know how the thumb can be used. The kinematic space visualizations in this work described how the kinematic space had changed to show specific functional changes due to the surgery (i.e. increased opposition, decreased hyperextension). Future work will investigate the tasks of daily living to relate the regions of the kinematic space to the activities of daily living to create a metric of which portions of the kinematic space are most needed and should be prioritized.

This novel method of quantifying changes in function can also be used in future work to compare different surgical treatments. Currently, it is difficult to compare between surgeries as most surgeries have been shown to reduce pain and the functional outcomes are qualitative or provide limited understanding of the functional changes of the hand. The procedures used in this work provide a method to compare between surgeries to understand the functional outcomes of different surgeries. Future work will test larger populations of participants through different surgeries to understand the differences in functional outcomes between the surgeries to give hand surgeons more data about the surgeries they are diagnosing.

6.4.1 Limitations

In this work, a pilot group of five participants were tested to demonstrate the potential of quantifying changes in function. This sample size is small for statistical power. Future work will test a larger cohort to determine more significant differences due to the mini-tightrope surgery. Also, 12 weeks is long enough to understand short term benefits, but not long-term benefits of the surgery. Future work will follow up with these patients to see the long term effects of surgical intervention on function.

6.4.2 Conclusions

Overall, mini-tightrope suspensionplasty led to reduced pain in all patients; however, function was not consistently improved among the participant group. CMC joint range of motion was decreased due to the surgery. The kinematic space of the thumb was similar to before the surgery. Similarly, the ability to apply forces in terms of force magnitude, range of directions, and volume of space used to apply force was not significantly different following surgery.

It is important to understand how surgery affects the hand, both in terms of pain and function. Ideally, an optimal surgery would both decrease pain and improve function of the hand.

Mini-tightrope suspensionplasty reduces pain but does not improve function. Going forward, this process can be used to compare other surgeries to understand how different surgeries lead to different changes in function to best treat patients with severe OA.

7 Conclusions

The overall goal of this work was to experimentally quantify the functional abilities (kinematic and kinetic) of the hand, then develop a visualization of and statistically model changes to function for populations and individuals.

First, a unique protocol, apparatus, and method was developed to gather force data for each digit and map them to the kinematic spaces of the digits. These data were also combined to demonstrate a population map of normative force abilities for the index finger. This work fills a critical need in the realm of hand function and assessment. While several researchers have developed tools associated with the hand, there are limited objective tools that include *both motion and force abilities* of the hand for all finger postures. The functional testing protocol that was developed as part of this research is a novel and important method to understand function of the fingers.

Second, the functional testing protocol was used to model and visualize the function of healthy participants. This work presented a comprehensive data set of finger force and directions used to apply force for ten regions of the kinematic space, and how they differed between the fingers and between males and females. Similar data is not available elsewhere. Future work can use these data to validate anatomical and mechanical models of the fingers. This work also developed a novel method of visualizing and interpreting function that can be used to better understand how a patient's function has changed. Future work can use the developed generalized linear mixed model to compare individuals with reduced hand function and understand how finger strength changes due to conditions such as osteoarthritis or stroke. This model can also be used to design products based on how much force the hand is able to produce at many different places, or in prosthetics where it is important to mimic the strength abilities of humans.

Third, the functional testing protocol was used to objectively determine differences due to osteoarthritis of the index finger. Osteoaarthritis led to participants applying lower forces, over a smaller range of their kinematic space, and in a smaller range of directions. Arthritic participants also had smaller differences in the amount of force that was applied due to finger posture and direction of force. These changes in function are important. Devices for individuals with arthritis should focus on the remaining optimal area, and treatments for OA should be compared to better understand how they affect function. This work also used regional force maps to compare participants with reduced hand function to a healthy population. By understanding what function has been lost, clinicians can develop personalized treatments for each patient.

Finally, changes in function due to thumb surgery were investigated. Overall, mini-tightrope suspensionplasty led to reduced pain in all patients; however, function was not consistently improved among the participant group. CMC joint range of motion was decreased due to the surgery. The kinematic space of the thumb was similar to before the surgery. Similarly, the ability to apply forces in terms of force magnitude, range of directions, and volume of space used to apply force was not significantly different following surgery. It is important to understand how surgery affects the hand, both in terms of pain and function. Ideally, an optimal surgery would both decrease pain and improve function of the hand. Going forward, this process can be used to compare other surgeries to understand how different surgeries lead to different changes in function to best treat patients with severe OA.

In conclusion, by developing a new method for collecting, visualizing and modeling function of the hand, this work objectively quantified the function of a healthy population and how hand function changed both for a population with OA and individuals going through surgery. Understanding how hand function has changed will lead to improved treatment of patients and personalized medicine as well as enhanced products for individuals who have lost hand function.

APPENDICES

Appendix A

8.1 Protocol for quantifying thumb function.

8.1.1 Overview

Chapter 3 is a published work which described the protocol for quantifying and visualizing the function of the fingers, and described the math used in the data mapping. Since the publication of Chapter 3, an adjusted protocol was developed for the thumb. This appendix describes the procedure used for the thumb.

8.1.2 The Kinematic Space

The kinematic space is the total volume of space the thumb can reach and was calculated by finding all possible thumb joint angle combinations and the resultant thumb postures. To do this, motion capture was used to collect the movements of the thumb (Figure 8.1). Clusters of four markers were placed on the center of the palm, on the thumb metacarpal, and on both thumb phalanges. Single markers were placed on the radial and ulnar styloids of the wrist.

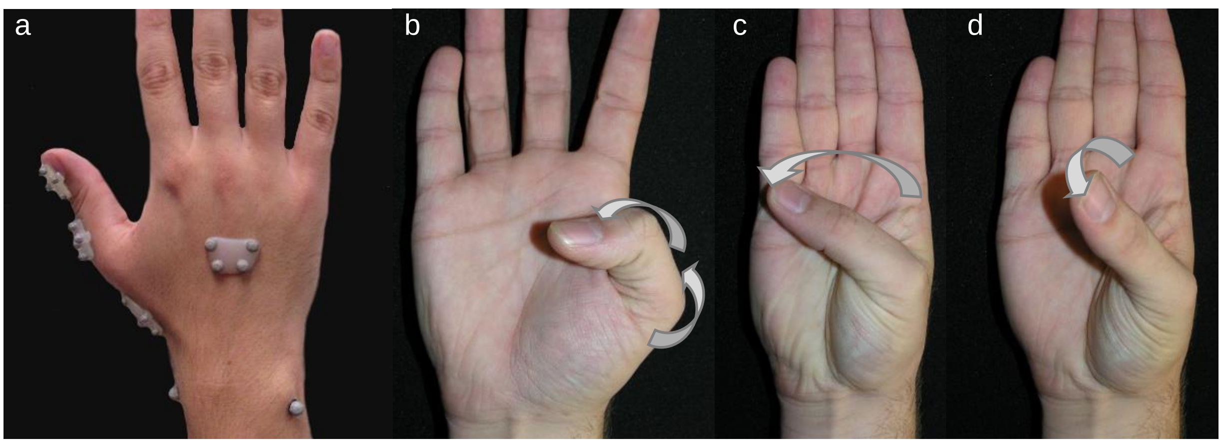

Figure 8.1: Motion protocol for the thumb. a) Motion capture marker placement for the thumb. b) MCP and IP flexion and extension. c) Opposition to the pad of the fifth digit. d) Palmar and radial abduction.

Three motions were used to calculate the entire thumb space (Figure 8.1). 1) Flexion and extension of the interphalangeal (IP) and metacarpophalangeal (MCP) joints. 2) Opposition to the pad of the fifth digit, where participants were asked to oppose first with the largest arc they could make with their thumbs, then to slide their thumbs distally along the pads of the fingers. This motion measured the range of abduction across the range of flexion and extension. 3) Palmar and radial abduction of the thumb.

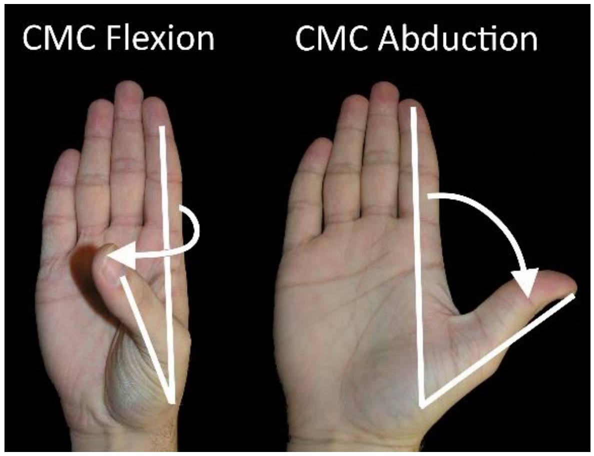

Figure 8.2: The CMC joint of the thumb has two degrees of freedom. Left: flexion is rotation around the second metacarpal. Right: abduction is rotation away from the second metacarpal.

The thumb was analyzed with four degrees of freedom. The IP joint is a hinge joint and has one degree of freedom in in flexion/extension. The MCP joint is also a hinge joint with a degree of freedom in flexion/extension. While the thumb MCP can move in adduction/abduction, the amount of motion in this direction is small and was not included in this analysis. The carpometacarpal (CMC) joint is a saddle joint and has unique movement compared to the other joints in the hand. This work analyzed it with two primary degrees of freedom: abduction, which is movement away from the second metacarpal, and flexion, which is movement around the second metacarpal (Figure 8.2). Opposition of the thumb is a special motion that uses all four degrees of freedom. Using the three motions, the range of each degree of freedom was calculated by comparing the maximum and minimum joint angles reached through the three motions.

However, the range of abduction were not consistent across the range of flexion. Therefore, the ranges of abduction were calculated across the range of flexion, so that for each value of flexion the minimum and maximum abduction values were known.

Similarly, the axes of rotation of the IP and MCP joints changed across the range of motions, specifically due to the flexion and abduction of the CMC joint. The three-dimensional axes of rotation were calculated for both joints at each combination of flexion and abduction by calculating the angular velocity vector of each joint.

$$\vec{\omega} = \frac{\vec{r} \times \vec{v}}{|r|^2} \quad (7)$$

To calculate angular velocity, the proximal and distal markers from the clusters on the phalanges were compared. The vector from the proximal to the distal marker was defined as $\vec{r}$, and the change in this marker over time was $\vec{v}$. A unit vector in the direction of ω was defined as the axis of rotation.

Next the posture of the thumb was calculated throughout the range of motion of each joint of the thumb. Latin hypercube sampling was used to generate a list of 10,000 random joint combinations from within the range of the degrees of freedom (CMC Fl, CMC Ab, MCP Fl, IP Fl). For each angle combination, if the CMC abduction angle was within the possible range for the chosen CMC flexion angle, the finger posture was calculated from that combination of joint angles. The thumb CMC joint was treated as (0,0,0).

First, the vector of the thumb metacarpal ($\overrightarrow{MC}$) was calculated using spherical coordinate conversion, (Equations 6-9).

$$MC_x = MC_{length} * \sin(CMC\ Ab) * \cos(CMC\ Fl) \quad (8)$$
$$MC_y = CM_{length} * \cos(CMC\ Ab) \quad (9)$$
$$MC_z = MC_{length} * \sin(CMC\ Ab) * sin(CMC\ Fl) \quad (10)$$
$$\overrightarrow{MC} = (MC_x, MC_y, MC_z) \quad (11)$$

To find the vector of the proximal phalange ($\overrightarrow{PP}$), the axis of rotation for the MCP joint was computed from the relationship found previously. That axis of rotation and the selected MCP joint angle were used to calculate the rotation matrix for the MCP joint using the axis angle equation, where u is an axis of rotation and θ is the rotation around that axis (Equation 10). Then the proximal phalange vector ($\overrightarrow{PP}$) was calculated by creating a vector in the same direction as the metacarpal vector ($\overrightarrow{MC}$) with the length of the proximal phalange and transforming it with the MCP rotation matrix (Equation 11).

$$R = \begin{bmatrix} \cos(\theta) + u_x^2(1-\cos(\theta)) & u_x u_y(1-\cos(\theta)) + u_z\sin(\theta) & u_x u_z(1-\cos(\theta)) + u_z\sin(\theta) \\ u_y u_x(1-\cos(\theta)) + u_z\sin(\theta) & \cos(\theta) + u_y^2(1-\cos(\theta)) & u_y u_z(1-\cos(\theta)) + u_z\sin(\theta) \\ u_z u_x(1-\cos(\theta)) - u_y\sin(\theta) & u_z u_y(1-\cos(\theta)) + u_z\sin(\theta) & \cos(\theta) + u_z^2(1-\cos(\theta)) \end{bmatrix} \quad (12)$$

$$\overrightarrow{PP} = R_{MCP} * \left(\frac{PP_{length}}{MP_{length}}\overrightarrow{MC}\right) \quad (13)$$

$$\overrightarrow{DP} = R_{PIP} * \left(\frac{DP_{length}}{PP_{length}}\overrightarrow{PP}\right) \quad (14)$$

Similarly, the vector of the distal phalange ($\overrightarrow{DP}$) was calculated by creating a vector in the same direction as the proximal phalange vector ($\overrightarrow{PP}$) with the length of the distal phalange, then transforming it with a rotation matrix calculated using the axis angle formula, the axis of rotation of the IP joint, and the flexion angle of the IP joint (Equation 12).

Finally, the posture of the thumb is calculated by treating the thumb CMC joint as the origin and adding the vectors of the metacarpal, proximal phalanx, and distal phalanx together. This process was repeated 10,000 times with the joint angle combinations from the latin hypercube sampling to create a cloud of fingertip locations of the thumb. These locations are the kinematic space of the thumb.

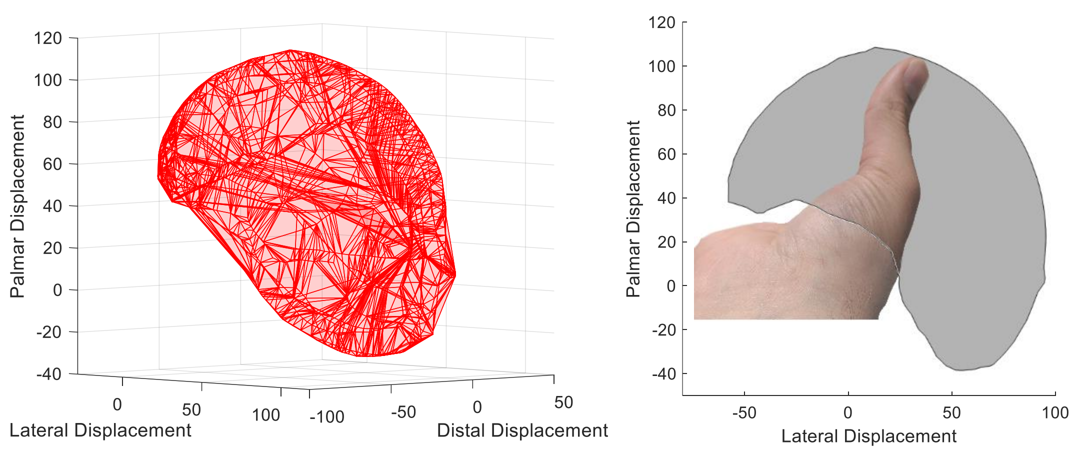

Figure 8.3: Kinematic space of the thumb. Left: Three dimensional view of the kinematic space. Right: Two-dimensional projection looking from the wrist towards the fingers. A transparent thumb has been added to indicate orientation.

The kinematic space of the thumb was visualized both in three dimensions as a volume of space the thumb can reach (Figure 8.3 Left) and in two dimensions as a projection looking from the wrist towards the fingers (Figure 8.3 Right).

8.1.3 Force Measurement

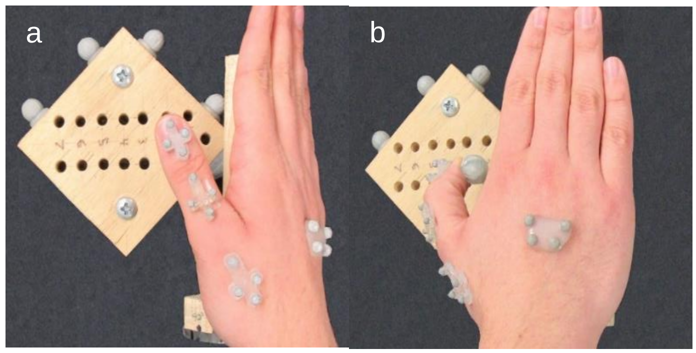

Figure 8.4: Thumb force measurement apparatus. a) Hand is rotated at 60° and thumb is pushing towards the ground. b) Hand is level with the ground and pulling toward the palm.

Thumb strength was measured at 16 positions throughout the kinematic space (Figure 8.4). To start, the participants rested their hand on a support, to limit force to the thumb. In order to collect forces with varied flexions of the thumb, the hand support was rotated in four positions with respect to the ground: 0°, 30°, 60°, and 90°. At each rotation the participant applied forces at two positions: adducted close to the palm and abducted at the furthest position the participant could reach (Figure 8.4). Then at each position, the participant applied forces in two directions: pushing down towards the ground and pulling in towards the palm. Therefore, each participant completed 16 force events: four rotations, two positions (adducted and abducted), two directions (push and pull), and two trials in each combination.

8.1.4 Mapping Forces to the Range of Motion

Finally, the collected force data were mapped to the kinematic space. To do this, the force actions were analyzed to determine the time, direction, and magnitude of the applied force. Motion capture data were analyzed to determine joint angles at the time of maximum force. Then the posture of the thumb and the coordinates for the tip of the thumb were calculated using the same calculations described in equations 6-12. The force vectors (comprised of the position of the tip or the thumb, force direction, and magnitude of the force) and kinematic space (total 3D space the finger can reach) were both transformed to be in the same coordinate system with the origin at the CMC joint of the thumb using the same procedure described in Section 3.2.7. This allowed the force abilities to be mapped to the kinematic abilities (Figure 8.5).

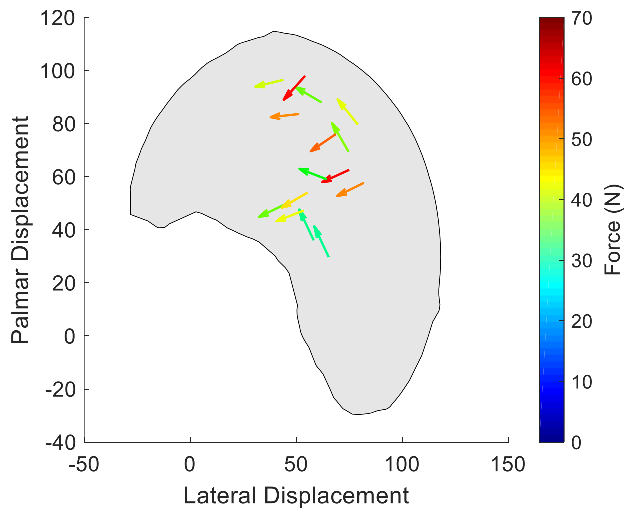

Figure 8.5: Force map of the thumb for an individual. The grey background represents the kinematic space of a participant's thumb. The color scale represents the amount of force that was applied, with each vector representing a 2D projection of the direction of the force and position within the kinematic space where the force was applied.

Appendix B:

MATLAB Codes

Included in this appendix are the key MATLAB codes used to analyze the data in this document. *SubProcessor* was used to analyze the raw data of a participant and utilized the codes *ThumbAngleFunc*, *FingerAngleFunc*, and *FingerForceFunc*. *ThumbOrientation* determined the relationship between the joint angles of the thumb and the axis of rotation of the thumb joints. *ROMplotter* and *ROMplotterThumb* were used to calculate the kinematic space plots of the thumb and *colorquiver* was used to overlay the arrows after the mapping was complete. CompareArthArcs was one of the codes used to develop the regional plots and the code to compare the healthy population to and participant with arthritis.

SubProcessor

```
function [] = SubProcessor(Sub)
%% SubProcessor
%   The goal of this function is to process the raw force and motion data
%   for a subject and save the data as a structure
%
%   Sub = Subject Number
%
%   nROM = [neutral, MCP FE, IP FE, AddAbd, Thumb FE, Big OP, Little OP]
%
%   nforce = [trial;digit;positions,force events]
%
%   Written By Josh Drost 2018

substr=['H',num2str(Sub)];
load([substr,'.mat']);
eval(['Build=',substr,';']);

%% ROM
% Load and name motion capture files files
substr=['H',num2str(Sub)];
ROMstr={'0','0','0','0','0','0','0'};
ROMname = {'Neutral','MCPFE','IPFE','AddAbd','ThumbFE','BigOp','LittleOp'};
nROM=Build.nROM;

for i=1:7
    if nROM(i)<10
        ROMstr{i}=[substr,'_J_000',num2str(nROM(i))];
    else
        ROMstr{i}=[substr,'_J_00',num2str(nROM(i))];
```

```
    end
    load(['R:\Drost\Hand\PA2017\',substr,'\',ROMstr{i},'.mat'])
    eval([ROMname{i},'=',ROMstr{i},';']);
end

ROM=zeros(5,8);

% Thumb ROM
[Tang1,Tmin1,Tmax1]=thumbanglefunc(ThumbFE,Neutral,1);
[Tang2,Tmin2,Tmax2]=thumbanglefunc(BigOp,Neutral,1);
[Tang3,Tmin3,Tmax3]=thumbanglefunc(LittleOp,Neutral,1);

ROM(1,:)=[min([Tmin1';Tmin2';Tmin3']),max([Tmax1';Tmax2';Tmax3'])];

% Relate thumb abduction and flexion
TCMC=[Tang1(3:4,:),Tang2(3:4,:),Tang3(3:4,:)]';
CMCrange=zeros(3,16);
CMCrange(1,:)=linspace(min(TCMC(:,2)),max(TCMC(:,2)),length(CMCrange));
p=CMCrange(1,2)-CMCrange(1,1);

for i=1:length(CMCrange)
CMCrange(2,i)=min(TCMC(and(TCMC(:,2)>CMCrange(1,i)-
p,TCMC(:,2)<CMCrange(1,i)+p),1));
CMCrange(3,i)=max(TCMC(and(TCMC(:,2)>CMCrange(1,i)-
p,TCMC(:,2)<CMCrange(1,i)+p),1));
end

% Finger ROM

fmin=zeros(4,3,2); fmax=zeros(4,3,2);

[~,fmin1,fmax1,~]=fingeranglefunc2(MCPFE,Neutral);
[~,fmin2,fmax2,~]=fingeranglefunc2(IPFE,Neutral);
[~,amin,amax,~]=fingeradabfunc(AddAbd,Neutral,0);

ROM(2:5,:)=[min(fmin1,fmin2),amin,max(fmax1,fmax2),amax]; % ROM = [MCPmin
PIPmin DIPmin AdAbmin MCPmax PIPmax DIPmax AdAbmax

% Save structure

Build.ROM=ROM;
Build.CMCrange=CMCrange;
eval([substr,'=Build;']);
save(substr,substr)

%% Force Offsetter
% This section checks that the force and motion data are properly offset
nforce=Build.nforce;
offseted=Build.Offseted;

if offseted==0
    offset=zeros(length(nforce),2);
    dps=[4,7,10,13,16];
```

```
for i=1:length(nforce(1,:))
    offset(i,1)=nforce(1,i);
    if offset(i,1)<10
    trial=[substr,'_J_000',num2str(offset(i,1))];
    else
    trial=[substr,'_J_00',num2str(offset(i,1))];
    end

    % Load Motion Capture Data
    load(['R:\Drost\Hand\PA2017\',substr,'\',trial,'.mat'])
    eval(['mocap=',trial,';'])
    x=-squeeze(mocap.RigidBodies.Positions(dps(nforce(2,i)),3,:))';
    tx=[1:length(x)]/60;

    % Load Force Data
    force=load(['R:\Drost\Hand\PA2017\',substr,'\',trial,'.txt']);
    if Sub>7
    fmag=sum(sqrt(force(any(force,2),13:15).^2),2);
    else
    fmag=sum(sqrt(force(any(force,2),1:3).^2),2);
    end
    tf=[1:length(fmag)]/360;

    offseti=1;
    while offseti~=0
       plot(tx,x,tf+offset(i,2),fmag)
       title(['Digit ',num2str(nforce(2,i)),' Position
',num2str(nforce(3,i))])
       offseti=input('Offset?');
       offset(i,2)=offset(i,2)+offseti;
    end
end

Build.Offset=offset;
Build.Offseted=1;
eval([substr,'=Build;']);
save(substr,substr)

else
    offset=Build.Offset;

end

%% Forces
% Analyzes the force values for each participant

dat=zeros(1,13);
toffset=[0,0,0,0]; ang=zeros(1,9);

fl=Build.HandSize;
    % Set Trial for pulling data
for i=1:length(nforce(1,:))
    ii=nforce(1,i);
    if ii<10
    trial=[substr,'_J_000',num2str(ii)];
```

```
    else
    trial=[substr,'_J_00',num2str(ii)];
    end

    % Load Motion Capture Data
    load(['R:\Drost\Hand\PA2017\',substr,'\',trial,'.mat'])
    eval(['mocap=',trial,';'])

    % Load Force Data
    force=load(['R:\Drost\Hand\PA2017\',substr,'\',trial,'.txt']);
    if Sub>7
    force=force(any(force,2),13:15);
    else
    force=force(any(force,2),1:3);
    end

    offi=offset(offset(:,1)==ii,2);

    [dati,~,angi] =
fingerforcefunc(mocap,force,nforce(2,i),nforce(3,i),fl(nforce(2,i),:),nforce(
4,i),'datcheck','0','toffset',num2str(offi),'trial',num2str(ii));

    dat=[dat;dati];
    ang=[ang;angi];
end

dat(1,:)=[]; ang(1,:)=[];

% Save structure
Build.Forces=dat;
Build.ForceAngles=ang;
eval([substr,'=Build;']);
save(substr,substr)
end
```

ThumbAngleFunc

```
function [angout,angmin,angmax] = thumbanglefunc(A,N,hand)
%% thumbanglefunc determines thumb angles from motion capture data
%
% min and max: [ip,mcp,the,phi]
%
% the is angle between metacarpals, phi is angle around MC2
%
% hand: 1=right, 2=left

%% Setup
% Accurate way to determine angles, by setting it up, it saves me spelling
% time later
angler=@(u,v) atan2(norm(cross(u,v)),dot(u,v));

% Other setup
nt=size(A.RigidBodies.Rotations,3);
angout=zeros(2,nt);
```

```
nn=size(N.RigidBodies.Rotations,3);
Nang=zeros(2,nn);

for i=1:nn

    mc1RN=vec2mat(N.RigidBodies.Rotations(2,:,i),3);
    pp1RN=vec2mat(N.RigidBodies.Rotations(3,:,i),3);
    dp1RN=vec2mat(N.RigidBodies.Rotations(4,:,i),3);

%% Neutral Angles
% Uses z direction to determine angles
mc1z=mc1RN(:,3);
pp1z=pp1RN(:,3);
dp1z=dp1RN(:,3);

% IP Flexion Extension
Nang(1,i)=angler(pp1z,dp1z);

% MCP Flexion Extension
Nang(2,i)=angler(mc1z,pp1z);
mdist=find(ismember(N.Trajectories.Labeled.Labels,'1m dist'));
mprox=find(ismember(N.Trajectories.Labeled.Labels,'1m prox'));
dati=N.Trajectories.Labeled.Data(mdist,1:3,i)-
N.Trajectories.Labeled.Data(mprox,1:3,i);
dati=vec2mat(N.RigidBodies.Rotations(1,:,i),3)*dati';
if hand==1
[Nang(4,i),Nang(3,i),~]=cart2sph(-dati(1),dati(3),dati(2));
Nang(4,i)=-Nang(4,i);
elseif hand==2
[Nang(4,i),Nang(3,i),~]=cart2sph(dati(1),-dati(3),dati(2));
end

Nang(4,i)=Nang(4,i)-(pi/4);

end

Navg=nanmean(Nang,2);
Navg(isnan(Navg))=0;

for i=1:nt

mc1R=vec2mat(A.RigidBodies.Rotations(2,:,i),3);
pp1R=vec2mat(A.RigidBodies.Rotations(3,:,i),3);
dp1R=vec2mat(A.RigidBodies.Rotations(4,:,i),3);

%% Joint Angles
% Uses x direction to determine angles
mc1z=mc1R(:,2);
pp1z=pp1R(:,2);
dp1z=dp1R(:,2);

% IP Flexion Extension
angout(1,i)=angler(pp1z,dp1z);
% MCP Flexion Extension
```

```
angout(2,i)=angler(mc1z,pp1z);

% CMC Angles
mdist=find(ismember(A.Trajectories.Labeled.Labels,'1m dist'));
mprox=find(ismember(A.Trajectories.Labeled.Labels,'1m prox'));
dati=A.Trajectories.Labeled.Data(mdist,1:3,i)-
A.Trajectories.Labeled.Data(mprox,1:3,i);
dati=vec2mat(A.RigidBodies.Rotations(1,:,i),3)*dati';

if hand==1
[angout(4,i),angout(3,i),~]=cart2sph(-dati(1),dati(3),dati(2));
angout(4,i)=-angout(4,i);
elseif hand==2
[angout(4,i),angout(3,i),~]=cart2sph(dati(1),-dati(3),dati(2));
end
end

% angout(4,:)=angout(4,:)-Navg(4);
angmin=nanmin(angout,[],2);
angmax=nanmax(angout,[],2);
end
```

FingerAngleFunc

```
function [angout,angmin,angmax,Nang] = fingeranglefunc2(A,N)
%% FingerAngleFunc calculates the range of joint anlges for the fingers
% Uses Euler Angles

angler=@(u,v) angdiff(deg2rad(v),deg2rad(u));

% Other setup
outmatsize=[4,4,4];
nt=size(A.RigidBodies.Rotations,3);
nn=size(N.RigidBodies.Rotations,3);
angout=zeros(4,3,nt);
Nang=zeros(4,3,nn);
%% Neutral Angles
% The purpose of this is to get rid of any changes in angles due to pod
% placement

for i=1:nn

pp2RN=N.RigidBodies.RPYs(5,1,i);
pp3RN=N.RigidBodies.RPYs(8,1,i);
pp4RN=N.RigidBodies.RPYs(11,1,i);
pp5RN=N.RigidBodies.RPYs(14,1,i);
mp2RN=N.RigidBodies.RPYs(6,1,i);
mp3RN=N.RigidBodies.RPYs(9,1,i);
mp4RN=N.RigidBodies.RPYs(12,1,i);
mp5RN=N.RigidBodies.RPYs(15,1,i);
dp2RN=N.RigidBodies.RPYs(7,1,i);
dp3RN=N.RigidBodies.RPYs(10,1,i);
dp4RN=N.RigidBodies.RPYs(13,1,i);
dp5RN=N.RigidBodies.RPYs(16,1,i);
% palmRN=N.RigidBodies.Rotations(1,:,i);
```

```
palmRN=0;

    Nang(1,1,i)=angler(palmRN,pp2RN);
    Nang(2,1,i)=angler(palmRN,pp3RN);
    Nang(3,1,i)=angler(palmRN,pp4RN);
    Nang(4,1,i)=angler(palmRN,pp5RN);

    Nang(1,2,i)=angler(pp2RN,mp2RN);
    Nang(2,2,i)=angler(pp3RN,mp3RN);
    Nang(3,2,i)=angler(pp4RN,mp4RN);
    Nang(4,2,i)=angler(pp5RN,mp5RN);


    Nang(1,3,i)=angler(mp2RN,dp2RN);
    Nang(2,3,i)=angler(mp3RN,dp3RN);
    Nang(3,3,i)=angler(mp4RN,dp4RN);
    Nang(4,3,i)=angler(mp5RN,dp5RN);

end
Navg=mean(Nang,2);

%% Range of Motion

for i=1:nt

pp2R=A.RigidBodies.RPYs(5,1,i);
pp3R=A.RigidBodies.RPYs(8,1,i);
pp4R=A.RigidBodies.RPYs(11,1,i);
pp5R=A.RigidBodies.RPYs(14,1,i);
mp2R=A.RigidBodies.RPYs(6,1,i);
mp3R=A.RigidBodies.RPYs(9,1,i);
mp4R=A.RigidBodies.RPYs(12,1,i);
mp5R=A.RigidBodies.RPYs(15,1,i);
dp2R=A.RigidBodies.RPYs(7,1,i);
dp3R=A.RigidBodies.RPYs(10,1,i);
dp4R=A.RigidBodies.RPYs(13,1,i);
dp5R=A.RigidBodies.RPYs(16,1,i);
palmR=0;

    angout(1,1,i)=angler(palmR,pp2R)-Navg(1);
    angout(2,1,i)=angler(palmR,pp3R)-Navg(2);
    angout(3,1,i)=angler(palmR,pp4R)-Navg(3);
    angout(4,1,i)=angler(palmR,pp5R)-Navg(4);

    angout(1,2,i)=angler(pp2R,mp2R)-Navg(1);
    angout(2,2,i)=angler(pp3R,mp3R)-Navg(2);
    angout(3,2,i)=angler(pp4R,mp4R)-Navg(3);
    angout(4,2,i)=angler(pp5R,mp5R)-Navg(4);


    angout(1,3,i)=angler(mp2R,dp2R)-Navg(1);
    angout(2,3,i)=angler(mp3R,dp3R)-Navg(2);
    angout(3,3,i)=angler(mp4R,dp4R)-Navg(3);
    angout(4,3,i)=angler(mp5R,dp5R)-Navg(4);
```

```
end

angout(angout<-100)=0;
angmin=nanmin(angout,[],3);
angmax=nanmax(angout,[],3);

end
```

FingerForceFunc

```
function [angout,angmin,angmax,Nang] = fingeranglefunc(A,N)
%UNTITLED2 Summary of this function goes here
%   Uses Euler Angles between normal vectors to measure joint angles

first=@(a)a(3);
angler=@(u,v) first(rotm2eul((v*u')','ZYX'));

% Other setup
nt=size(A.RigidBodies.Rotations,3);
nn=size(N.RigidBodies.Rotations,3);
angout=zeros(4,3,nt);
Nang=zeros(4,3,nn);
%% Neutral Angles
% The purpose of this is to get rid of any changes in angles due to pod
% placement

for i=1:nn

pp2RN=vec2mat(N.RigidBodies.Rotations(5,:,i),3)';
pp3RN=vec2mat(N.RigidBodies.Rotations(8,:,i),3)';
pp4RN=vec2mat(N.RigidBodies.Rotations(11,:,i),3)';
pp5RN=vec2mat(N.RigidBodies.Rotations(14,:,i),3)';
mp2RN=vec2mat(N.RigidBodies.Rotations(6,:,i),3)';
mp3RN=vec2mat(N.RigidBodies.Rotations(9,:,i),3)';
mp4RN=vec2mat(N.RigidBodies.Rotations(12,:,i),3)';
mp5RN=vec2mat(N.RigidBodies.Rotations(15,:,i),3)';
dp2RN=vec2mat(N.RigidBodies.Rotations(7,:,i),3)';
dp3RN=vec2mat(N.RigidBodies.Rotations(10,:,i),3)';
dp4RN=vec2mat(N.RigidBodies.Rotations(13,:,i),3)';
dp5RN=vec2mat(N.RigidBodies.Rotations(16,:,i),3)';

palmRN=eye(3);

    Nang(1,1,i)=angler(palmRN,pp2RN);
    Nang(2,1,i)=angler(palmRN,pp3RN);
    Nang(3,1,i)=angler(palmRN,pp4RN);
    Nang(4,1,i)=angler(palmRN,pp5RN);

    Nang(1,2,i)=angler(pp2RN,mp2RN);
    Nang(2,2,i)=angler(pp3RN,mp3RN);
    Nang(3,2,i)=angler(pp4RN,mp4RN);
    Nang(4,2,i)=angler(pp5RN,mp5RN);
```

```
    Nang(1,3,i)=angler(mp2RN,dp2RN);
    Nang(2,3,i)=angler(mp3RN,dp3RN);
    Nang(3,3,i)=angler(mp4RN,dp4RN);
    Nang(4,3,i)=angler(mp5RN,dp5RN);

end

Navg=mean(Nang,3);

%% Range of Motion

for i=1:nt

pp2R=vec2mat(A.RigidBodies.Rotations(5,:,i),3)';
pp3R=vec2mat(A.RigidBodies.Rotations(8,:,i),3)';
pp4R=vec2mat(A.RigidBodies.Rotations(11,:,i),3)';
pp5R=vec2mat(A.RigidBodies.Rotations(14,:,i),3)';
mp2R=vec2mat(A.RigidBodies.Rotations(6,:,i),3)';
mp3R=vec2mat(A.RigidBodies.Rotations(9,:,i),3)';
mp4R=vec2mat(A.RigidBodies.Rotations(12,:,i),3)';
mp5R=vec2mat(A.RigidBodies.Rotations(15,:,i),3)';
dp2R=vec2mat(A.RigidBodies.Rotations(7,:,i),3)';
dp3R=vec2mat(A.RigidBodies.Rotations(10,:,i),3)';
dp4R=vec2mat(A.RigidBodies.Rotations(13,:,i),3)';
dp5R=vec2mat(A.RigidBodies.Rotations(16,:,i),3)';

palmR=eye(3);

    angout(1,1,i)=angler(palmR,pp2R)-Navg(1,1);
    angout(2,1,i)=angler(palmR,pp3R)-Navg(2,1);
    angout(3,1,i)=angler(palmR,pp4R)-Navg(3,1);
    angout(4,1,i)=angler(palmR,pp5R)-Navg(4,1);

    angout(1,2,i)=angler(pp2R,mp2R)-Navg(1,2);
    angout(2,2,i)=angler(pp3R,mp3R)-Navg(2,2);
    angout(3,2,i)=angler(pp4R,mp4R)-Navg(3,2);
    angout(4,2,i)=angler(pp5R,mp5R)-Navg(4,2);

    angout(1,3,i)=angler(mp2R,dp2R)-Navg(1,3);
    angout(2,3,i)=angler(mp3R,dp3R)-Navg(2,3);
    angout(3,3,i)=angler(mp4R,dp4R)-Navg(3,3);
    angout(4,3,i)=angler(mp5R,dp5R)-Navg(4,3);

%     angout(1,1,i)=angler(palmR,pp2R);
%     angout(2,1,i)=angler(palmR,pp3R);
%     angout(3,1,i)=angler(palmR,pp4R);
%     angout(4,1,i)=angler(palmR,pp5R);
%
%     angout(1,2,i)=angler(pp2R,mp2R);
%     angout(2,2,i)=angler(pp3R,mp3R);
%     angout(3,2,i)=angler(pp4R,mp4R);
%     angout(4,2,i)=angler(pp5R,mp5R);
%     angout(1,3,i)=angler(mp2R,dp2R);
%     angout(2,3,i)=angler(mp3R,dp3R);
%     angout(3,3,i)=angler(mp4R,dp4R);
```

```
%     angout(4,3,i)=angler(mp5R,dp5R);

end


angmin=nanmin(angout,[],3);
angmax=nanmax(angout,[],3);

end
```

ThumbOrientation

```
%% Thumb Orientation Relation
% The goal of this file is to determine the relationship between the
% orientation of the thumb and the metacarpal positions.
%
% Specifically, what are the axis of rotation of the thumb MCP and IP
% for different orientations of the thumb.
%
% Used w=rxv/r^2;
clear; close all
load thumbinfo

%% Thumb ROM

datorient=zeros(4,6,length(unique(Healthy(:,1))));
subs=unique(Healthy(:,1));
thes2=0; phis2=0; pitchmcs2=0;
MCP=[0;0;0]; IP=MCP; the=0; phi=0;
for i=1:length(subs)
    sub=subs(i);

    if sum(Healthy(:,1)==sub)>0

    file=[0,0,0];
    file(1)=Healthy(and(Healthy(:,1)==sub,Healthy(:,3)==101),2);            %
FlEx
    file(2)=Healthy(and(Healthy(:,1)==sub,Healthy(:,3)==102),2);            %
Lil Op
    file(3)=Healthy(and(Healthy(:,1)==sub,Healthy(:,3)==103),2);            %
Big Op

        if file(1)<10
        trial=strrep(['H',num2str(sub),'_J_000A'],'A',num2str(file(1)));
        else
        trial=strrep(['H',num2str(sub),'_J_00A'],'A',num2str(file(1)));
        end

    thes=0; phis=0; pitchmcs=0;

    for j=1:3

        if file(j)<10
        trial=strrep(['H',num2str(sub),'_J_000A'],'A',num2str(file(j)));
```

```
        else
        trial=strrep(['H',num2str(sub),'_J_00A'],'A',num2str(file(j)));
        end

        load(['R:\Drost\Hand\PA2017\H',num2str(sub),'\',trial,'.mat'])
        eval(['mocapi=',trial,';'])

vecm=zeros(3,length(squeeze(mocapi.Trajectories.Labeled.Data(9,1:3,:))));
        vecdp=vecm; vecpp=vecm; MCPi=vecm; IPi=vecm;
        vdp=vecm; vpp=vecm;
        thei=zeros(1,length(vecm)); phii=thei;

        markernames={'1m dist','1m prox','1pp dist','1pp prox','1dp
dist','1dp prox';'md','mp','pd','pp','dd','dp'};

        for k=1:6

eval([markernames{2,k},'=find(ismember(mocapi.Trajectories.Labeled.Labels,mar
kernames{1,k}));']);
        end

        for k=1:length(vecm)

vecm(:,k)=vec2mat(mocapi.RigidBodies.Rotations(1,:,k),3)*(mocapi.Trajectories
.Labeled.Data(md,1:3,k)'-mocapi.Trajectories.Labeled.Data(mp,1:3,k)');

        % PP and DP vectors are calculated by transforming (dist-prox) into
        % palm then into coordinate system of previous bone. this should
        % control for other rotations of the thumb.

vecpp(:,k)=vec2mat(mocapi.RigidBodies.Rotations(1,:,k),3)*(mocapi.Trajectorie
s.Labeled.Data(pd,1:3,k)'-mocapi.Trajectories.Labeled.Data(pp,1:3,k)');
        vecpp(:,k)=vec2mat(mocapi.RigidBodies.Rotations(2,:,k),3)*vecpp(:,k);

vecdp(:,k)=vec2mat(mocapi.RigidBodies.Rotations(1,:,k),3)*(mocapi.Trajectorie
s.Labeled.Data(dd,1:3,k)'-mocapi.Trajectories.Labeled.Data(dp,1:3,k)');
        vecdp(:,k)=vec2mat(mocapi.RigidBodies.Rotations(3,:,k),3)*vecdp(:,k);
        % Flexions and abduction calcculated by converting cartesion
        % coordinates to spherical
        thei(k)=acos(vecm(2,k)/sqrt(vecm(1,k)^2+vecm(3,k)^2+vecm(2,k)^2));
        phii(k)=-atan2(vecm(3,k),-vecm(1,k));
        if k>1
        vpp(:,k)=(vecpp(:,k)-vecpp(:,k-1))/norm((vecpp(:,k)-vecpp(:,k-1)));
        vdp(:,k)=(vecdp(:,k)-vecdp(:,k-1))/norm((vecdp(:,k)-vecdp(:,k-1)));

        MCPi(:,k)=cross(vecpp(:,k),vpp(:,k-
1))./norm(cross(vecpp(:,k),vpp(:,k-1)));
        IPi(:,k)=cross(vecdp(:,k),vdp(:,k-1))./norm(cross(vecdp(:,k),vdp(:,k-
1)));
        MCPi(:,k)=vec2mat(mocapi.RigidBodies.Rotations(2,:,k),3)'*MCPi(:,k);
        IPi(:,k)=vec2mat(mocapi.RigidBodies.Rotations(3,:,k),3)'*IPi(:,k);
        end

%          if MCPi(3,k)<0; MCPi(:,k)=-MCPi(:,k); end
%          if IPi(3,k)<0; IPi(:,k)=-IPi(:,k); end
```

```
        end
        MCP=[MCP,MCPi]; IP=[IP,IPi]; the=[the,thei]; phi=[phi,phii];

    end

    end
end

% clean up
MCP(:,1)=[];IP(:,1)=[];the(:,1)=[];phi(:,1)=[];
clean=and(any(MCP),and(any(the,1),any(IP)));
clean=and(clean,the<1.7);
datclean=[the(clean)',phi(clean)',MCP(:,clean)',IP(:,clean)'];

[themean,phimean]=meshgrid(linspace(0,1.2,20),linspace(-.5,1.7,20));
space=(themean(1,2)-themean(1,1))*.6;
MCPX=zeros(length(themean)); MCPY=MCPX; MCPZ=MCPX;
IPX=MCPX; IPY=MCPX; IPZ=IPX;

for i=1:length(themean)
for j=1:length(themean)
    spoti=and(and(the>themean(i,j)-
space,the<themean(i,j)+space),and(phi>phimean(i,j)-
space,phi<phimean(i,j)+space));
    MCPX(i,j)=nanmean(MCP(1,spoti)); MCPY(i,j)=nanmean(MCP(2,spoti));
    MCPZ(i,j)=nanmean(MCP(3,spoti)); IPX(i,j)=nanmean(IP(1,spoti));
    IPY(i,j)=nanmean(IP(2,spoti)); IPZ(i,j)=nanmean(IP(3,spoti));
end
end
OrientRel3=struct('MCPx',MCPX,'MCPy',MCPY,'MCPz',MCPZ,'IPx',IPX,'IPy',IPY,'IP
z',IPZ,'the',themean,'phi',phimean);
save OrientRel3 OrientRel3
```

ROMplotter

```
function [pos] = ROMplotter(fl,ROM,varargin)
% This function plots the range of motion of participants in the PA2017
% hand project
%
% fl=[PP,MP,DP]
%
% ROM = [MCPmin PIPmin DIPmin AdAbmin MCPmax PIPmax DIPmax AdAbmax
%
% Program Options (varargin)
%   n: level of detail: number of points in each digit rotation
%   plottype: how I want it plotted
%       1: dots
%       2: outline and constant shade
%       3: Square gradient
%       4:
% Written by Josh Drost

%% Default Options
n=100000; % Default at 10 for speed
```

```
plottype=2; % Default as shape

PP=fl(1); MP=fl(2); DP=fl(3);
if rem(length(varargin),2)==1
    print('Your Input Sucks')
else
    for i=1:length(varargin)/2
       eval([char(varargin(2*i-1)),'=',char(varargin(2*i)),';']);
    end
end

%% Postures over range of motion
% First, the program lists all the joint angles to be tested. Then, it
% determines the finger posture at each joint angle combination.
if n<101
if n==0

MCP=ROM(1):0.0175:ROM(5);
PIP=ROM(2):0.0175:ROM(6);
DIP=ROM(3):0.0175:ROM(7);

else

MCP=linspace(ROM(1),ROM(5),n);
PIP=linspace(ROM(2),ROM(6),n);
DIP=linspace(ROM(3),ROM(7),n);
end

pos=[0,0,0];

for i=1:length(MCP)
for j=1:length(PIP)
for k=1:length(DIP)
    if DIP(k)<=2/3*PIP(j)
    xi=PP*cos(MCP(i))+MP*cos(MCP(i)+PIP(j))+DP*cos(MCP(i)+PIP(j)+DIP(k));
    yi=PP*sin(MCP(i))+MP*sin(MCP(i)+PIP(j))+DP*sin(MCP(i)+PIP(j)+DIP(k));
    pos=[pos;xi,yi,MCP(i)+PIP(j)+DIP(k)];
    end
end
end
end

pos(1,:)=[];
end
%% Postures over range of motion
% First, the program lists all the joint angles to be tested. Then, it
% determines the finger posture at each joint angle combination.

if n>100

XLB=ROM(1:3);
XUB=ROM(5:7);
[thetas] = LHDGenerator(n,XUB,XLB);

pos=zeros(n,3);
```

```
for i=1:n
    if abs(thetas(i,3))<=2/3*abs(thetas(i,2))
    MCP=thetas(i,1); PIP=thetas(i,2); DIP=thetas(i,3);
    xi=PP*cos(MCP)+MP*cos(MCP+PIP)+DP*cos(MCP+PIP+DIP);
    yi=PP*sin(MCP)+MP*sin(MCP+PIP)+DP*sin(MCP+PIP+DIP);
    pos(i,:)=[xi,yi,MCP+PIP+DIP];
    end
end

pos(~any(pos,2),:)=[];

end
%% Plotting time

if plottype==1
    plot(pos(:,1),pos(:,2),'.')
elseif plottype==2
    k=boundary(pos(:,1),pos(:,2),1);
    fill(pos(k,1),pos(k,2),[.7,.7,.7],'EdgeColor',[.7,.7,.7])
elseif plottype==2.5
    k=boundary(pos(:,1),pos(:,2),1);
    fill(pos(k,1),pos(k,2),'w','EdgeColor','k')
elseif plottype==3
    szx=max(pos(:,1))-min(pos(:,1));
    szy=max(pos(:,2))-min(pos(:,2));

    n = hist3(pos,[round(szx/2.5),round(szy/2.5)]); % 2.5 mm
    n1 = n';
    n1(size(n,1) + 1, size(n,2) + 1) = 0;

    xb = linspace(min(pos(:,1)),max(pos(:,1)),size(n1,2));
    yb = linspace(min(pos(:,2)),max(pos(:,2)),size(n1,1));

    h = pcolor(xb,yb,n1);
    set(h,'edgecolor','none')
    colormap(flipud(gray))
elseif plottype==4

    pos2=[round(pos(:,1:2)*4,-1)/4,rad2deg(pos(:,3))];

    xb = [min(pos2(:,1)):2.5:max(pos2(:,1))];
    yb = [min(pos2(:,2)):2.5:max(pos2(:,2))];

    n=50*ones(length(xb),length(yb));

    for i=1:length(xb)
    for j=1:length(yb)
%     any(and(pos2(:,1)==xb(i),pos2(:,2)==yb(j)))
    if any(and(pos2(:,1)==xb(i),pos2(:,2)==yb(j)))
        n(i,j)=range(pos2(and(pos2(:,1)==xb(i),pos2(:,2)==yb(j)),3));
    end
    end
    end

    h = pcolor(xb,yb,n');
```

```
    set(h,'edgecolor','none')
    colormap(gray)
    colorbar
end
end
```

ROMPlotterThumb

```
function [allpoints] = ROMplotterthumb(thumbrange,tsize,points,figtype)

if ~exist('figtype')
figtype=3;
end
tippos=[0,0,0];
mcppos=[0,0,0];
ippos=[0,0,0];

% Latin Hypersquare Point Generator
XUB=[-thumbrange(7),thumbrange(4),thumbrange(2),thumbrange(1)];
XLB=[-thumbrange(3),thumbrange(8),thumbrange(6),thumbrange(5)];
[thetas] = LHDGenerator(points,XUB,XLB);

load OrientRel
MCPpitch=@(the,phi) OrientRel*[1,the,phi,the.^2,the.*phi,phi.^2]';

for i=1:length(thetas)
    the=thetas(i,1); phi=thetas(i,2); mcp=thetas(i,3); ip=thetas(i,4);
    mcpposi=[0;0;0]; mcp2ip=[0;0;0]; ip2tip=[0;0;0]; tipposi=[0;0;0];
    ipposi=[0;0;0];

    [mcpposi(1),mcpposi(2),mcpposi(3)]=sph2cart(the,phi,tsize(1));

    if the<1.4
        the2=the+pi/2;
    else
        the2=the;
    end

    rot=MCPpitch(the2,phi);
    mcpR=rotate3Daxis(mcpposi,rot);

    [mcp2ip(1),mcp2ip(2),mcp2ip(3)]=sph2cart(the,phi+mcp,tsize(2));
    [ip2tip(1),ip2tip(2),ip2tip(3)]=sph2cart(the,phi+mcp+ip,tsize(3));
    mcp2ip2=mcpR*mcp2ip;
    mcp2tip=mcpR*(mcp2ip+ip2tip);
    tipposi=mcpposi'+mcp2tip';
    ipposi=mcpposi'+mcp2ip2';

    mcppos=[mcppos;mcpposi'];
    ippos=[ippos;ipposi];
    tippos=[tippos;tipposi];
end
```

```
% Thumb Positions

    the=-thumbrange(7);phi=0; mcp=0; ip=0;

    if the<1.4
        the2=the+pi/2;
    else
        the2=the;
    end

    [mcpposi(1),mcpposi(2),mcpposi(3)]=sph2cart(the,phi,tsize(1));
    rot=MCPpitch(the2,phi);
    mcpR=rotate3Daxis(mcpposi,rot);

    [mcp2ip(1),mcp2ip(2),mcp2ip(3)]=sph2cart(the,phi+mcp,tsize(2));
    [ip2tip(1),ip2tip(2),ip2tip(3)]=sph2cart(the,phi+mcp+ip,tsize(3));
    mcp2tip=mcpR*(mcp2ip+ip2tip);
    thumbsup=mcpposi'+mcp2tip';

    the=0; phi=thumbrange(8); mcp=0; ip=0;

    [mcpposi(1),mcpposi(2),mcpposi(3)]=sph2cart(the,phi,tsize(1));
    rot=MCPpitch(the,phi);
    mcpR=rotate3Daxis(mcpposi,rot);

    [mcp2ip(1),mcp2ip(2),mcp2ip(3)]=sph2cart(the,phi+mcp,tsize(2));
    [ip2tip(1),ip2tip(2),ip2tip(3)]=sph2cart(the,phi+mcp+ip,tsize(3));
    mcp2tip=mcpR*(mcp2ip+ip2tip);
    thumbsout=mcpposi'+mcp2tip';

%% Plot

mcppos(1,:)=[];
ippos(1,:)=[];
tippos(1,:)=[];

if sum(tsize)<2
allpoints=[tippos*100;mcppos*100;ippos*100];
thumbsup=thumbsup*100;
tumbsout=thumbsout*100;
else
allpoints=[tippos;mcppos;ippos];
end

if figtype==1
figure; hold on
plot3(tippos(:,1),tippos(:,2),tippos(:,3),'.')

elseif figtype==2
    k=boundary(-tippos(:,2),tippos(:,1),1);
    figure; hold on
    fill(-tippos(k,2),tippos(k,1),[.7,.7,.7],'EdgeColor',[.7,.7,.7])

elseif figtype==3
```

```
    pos2=[-tippos(:,2),tippos(:,1)];
    szx=max(pos2(:,1))-min(pos2(:,1));
    szy=max(pos2(:,2))-min(pos2(:,2));

    n = hist3(pos2,[round(szx/5),round(szy/5)]); % 2.5 mm
    n1 = n';
    n1(size(n,1) + 1, size(n,2) + 1) = 0;
    n1(n1==0)=max(max(n1));

    xb = linspace(min(pos2(:,1)),max(pos2(:,1)),size(n1,2));
    yb = linspace(min(pos2(:,2)),max(pos2(:,2)),size(n1,1));

    figure; hold on
    h = pcolor(xb,yb,n1);
    set(h,'edgecolor','none')
    colormap(gray)
    colorbar
elseif figtype==4
figure; hold on
plot3(tippos(:,1),tippos(:,2),tippos(:,3),'.')
plot3([0,thumbsup(1)],[0,thumbsup(2)],[0,thumbsup(3)],'k','LineWidth',3)
plot3([0,thumbsout(1)],[0,thumbsout(2)],[0,thumbsout(3)],'g','LineWidth',3)

elseif figtype==5
%     allpoints=[tippos*100;mcppos*100;ippos*100;-tsize(4),-tsize(5),-20];

    k=boundary(allpoints,0);
    figure; hold on
    plot3([-tsize(4),thumbsup(1)],[-tsize(5),thumbsup(2)],[-
20,thumbsup(3)],'k','LineWidth',3)
    plot3([-tsize(4),thumbsout(1)],[-tsize(5),thumbsout(2)],[-
20,thumbsout(3)],'g','LineWidth',3)

trisurf(k,allpoints(:,1),allpoints(:,2),allpoints(:,3),'Edgecolor','r','Facec
olor','red','FaceAlpha',0.1)
    legend('Radial Abd','Palmar Abd.','ROM')

end

end
```

Color Quiver

```
function [] = colorquiver(X,The,Mag,varargin)
%%colorquiver Color Quiver plots a quiver with small colored arrows
% This function uses quiver to plot data where all arrows are the same
% length and the magnitude is displayed through the c-axis
%
% Required Inputs:
%
% X: the 2D position of the end of the arrow. (n,2) matrix
%
% The: direction of the arrow. This can either be (i,j) coordinates (n,2) or
an
% angle in radians  or (n,1) matrix
```

```
%
% Mag: C values for each arrow, (n,1) matrix
%
% Paired Optional Inputs:
%
% Max Value: sets the top of the color scale. 'MaxValue',scalar
%
% Arrow Length: sets the length of the arrows. 'ArrowLength',scalar
%
% Outputs: Plots arrows on most resent figure.
%
% Written by Josh Drost


%% Set and change default values
% I have set the arrow length and max Value to be what looks best for my
% project. These can be changed through the input.
MaxValue=90;
ArrowLength=15;
Colors=2;

if nargin>3
    for i=1:(nargin-3)/2
        eval([char(varargin(2*i-
1)),'=',num2str(cell2mat((varargin(2*i)))),';'])
    end
end



N=size(X,1);
xrgb=1:1:MaxValue;
x0rgb=linspace(0,MaxValue,5);
if Colors==1
    colorx=parula;
    colort=linspace(0,MaxValue,length(colorx));
    colorname='parula';
elseif Colors==2
colort=linspace(0,MaxValue,5)';
colorx=[0,0,0,1,1;0,1,1,1,0;1,1,0,0,0]';
colorname=interp1(colort,colorx,linspace(0,MaxValue,50));
% plot(x,rgb(3,:),x,rgb(2,:),x,rgb(1,:))
elseif Colors==3
    colorx=gray;
    colort=linspace(0,MaxValue,length(colorx));
    colorname='gray';
% plot(x,rgb(3,:),x,rgb(2,:),x,rgb(1,:))
else
    colorx=hot;
    colort=linspace(0,MaxValue,length(colorx));
    colorname='hot';
end

if size(The,2)==1
Fad2=The;
[The(:,1),The(:,2)]=pol2cart(Fad2,ones(size(Fad2)));
end
```

```
for i=1:N
    if Mag(i)<0
        n=0;
    elseif Mag(i)>MaxValue
        n=MaxValue;
    else
        n=Mag(i);
    end

    if isnan(n)
    else
    quiver(X(i,1),X(i,2),ArrowLength*The(i,1)/norm(The(i,:)),...
        -ArrowLength*The(i,2)/norm(The(i,:)),...
        'Color',interp1(colort,colorx,n),'LineWidth', 1.5,'MaxHeadSize',3)
    end
end
% colormap(colorname)
% h=colorbar;
% ylabel(h, 'Force (N)')
% caxis([0,MaxValue])
end
```

CompareArthArcs

```
%% Compare Healthy Population to Arthritic Participant
clear; close all

load Summary; load AllData2013
fl=Summary.HandSize(:,4:6); axeses=[-.8,1,-.5,1];
ROM=Summary.ROM;
subA=unique(Summary.Arthritic2013.Forces(:,1));

%% Plot Healthy index arc (female)
bins=deg2rad([-90,15,25,35,45,55,65,75,85,95,180]);

meanf=zeros(5,length(bins)-1);
sumf=meanf;
varf=sumf;
vard=sumf;
dirf=meanf;


dig=2;
% Split ROM into regions
figure
[pos]=ROMplotter(fl(dig,:),ROM(dig,:),'n','100000');
close

regs=discretize(cart2pol(pos(:,1),pos(:,2)),bins);

forces=[Summary.Forces(and(Summary.Forces(:,2)==dig,cellfun(@(x)
strcmp(x,'Female'),Summary.Sex(Summary.Forces(:,1)))'),:);...

Summary.Healthy2013.Forces(and(Summary.Healthy2013.Forces(:,2)==dig,cellfun(@
(x)
```

```
strcmp(x,'Female'),Summary.Healthy2013.Sex(Summary.Healthy2013.Forces(:,1)))'
),:)]; % Forces = [dig,pos,time,fmag,fx,fy,fz,x',y',z',x,y,z];
places=[fl(dig,1).*cosd(forces(:,11))+fl(dig,2).*cosd(forces(:,12))+fl(dig,3)
.*cosd(forces(:,13)),...

fl(dig,1).*sind(forces(:,11))+fl(dig,2).*sind(forces(:,12))+fl(dig,3).*sind(f
orces(:,13))];
forces(forces(:,4)>100,4)=100;

regf=discretize(cart2pol(places(:,1),-places(:,2)),bins);

for i=1:max(regs)
   sumf(dig,i)=sum(regf==i);
    if sumf(dig,i)>3
    meanf(dig,i)=mean(forces(regf==i,4));

dirf(dig,i)=cart2pol(nanmean(forces((regf==i),6)),nanmean(forces((regf==i),7)
));
    end
   if sumf(dig,i)>4
   varf(dig,i)=std((forces(regf==i,4)));
   vard(dig,i)=cart2pol(std(forces((regf==i),6)),std(forces((regf==i),7)));
   end
end

titles={'Healthy Motion and Forces','Healthy Motion, Reduced Forces','Reduced
Motion, Healthy Forces','Reduced Motion and Forces'};
subex=[40,36,34,30];

for Ai=1:4
figure
hold on
colorx=hot;
colort=linspace(0,50,length(colorx));
colorname='hot';

for i=1:max(regs)
posi=pos(regs==i,:);
ki=boundary(posi(:,1),posi(:,2),.7);

fill(100*posi(ki,1),100*posi(ki,2),interp1(colort,colorx,meanf(dig,i)),'EdgeC
olor',interp1(colort,colorx,meanf(dig,i)))
end

colormap(colorname)
c=colorbar;
xlabel('Scaled Distal Displacement')
ylabel('Scaled Palmar Displacement')
ylabel(c,'Force (N)')
set(gca,'fontsize',14)
set(c,'fontsize',14)
caxis([0,50])
axis([-60,110,-60,110])
axis square
title(titles{Ai})
```

```
%% Plot Arthritic Participant

% ROM

eval(['ROMi=AllData2013.H',num2str(subex(Ai)),'.ROM(2,:);']);
posA=ROMplotter(100*fl(2,:),ROMi,'plottype','0');
kA=boundary(posA(:,1),posA(:,2),0.7);
plot(posA(kA,1),posA(kA,2),'k')

% forces
forceA=Summary.Arthritic2013.Forces;
forceA=forceA(forceA(:,2)==2,:);
forceA=forceA(forceA(:,1)==subex(Ai),:);
placeA=100*[fl(2,1).*cosd(forceA(:,11))+fl(2,2).*cosd(forceA(:,12))+fl(2,3).*
cosd(forceA(:,13)),...
        -
(fl(2,1).*sind(forceA(:,11))+fl(2,2).*sind(forceA(:,12))+fl(2,3).*sind(forceA
(:,13)))];
dirA=[-forceA(:,6),forceA(:,7)];
colorquiver(placeA,dirA,forceA(:,4),'Colors','4','MaxValue','50')
end
```

REFERENCES

REFERENCES

Altman, R., 2014. Hand Function in Osteoarthritis. Hand Funct.

An, K.N., Chao, E.Y., Cooney, W.P., Linscheid, R.L., 1985. Forces in the normal and abnormal hand. J. Orthop. Res. 3, 202–211. https://doi.org/10.1002/jor.1100030210

An, K.N., Chao, E.Y., Cooney, W.P., Linscheid, R.L., 1979. Normative model of human hand for biomechanical analysis. J. Biomech. 12, 775–788. https://doi.org/10.1016/0021-9290(79)90163-5

An, K.N., Ueba, Y., Chao, E.Y., Cooney, W.P., Linscheid, R.L., 1983. Tendon excursion and moment arm of index finger muscles. J. Biomech. 16, 419–425. https://doi.org/10.1016/0021-9290(83)90074-X

Angelaki, D., Soechting, J., 1993. Non-uniform temporal scaling of hand and finger kinematics during typing. Exp. Brain Res. 95. https://doi.org/10.1007/BF00229789

Assiotis, A., Giannakakis, N., 2017. Trapeziumectomy and Mini Tightrope stabilization of the first metacarpal for thumb carpometacarpal osteoarthritis: a prospective case series. Acta Orthop.

Bae, S., Armstrong, T.J., 2011. A finger motion model for reach and grasp. Int. J. Ind. Ergon. 41, 79–89. https://doi.org/10.1016/j.ergon.2010.11.001

Bagis, S., Sahin, G., Yapici, Y., Cimen, O.B., Erdogan, C., 2003. The effect of hand osteoarthritis on grip and pinch strength and hand function in postmenopausal women. Clin. Rheumatol. 22, 420–424. https://doi.org/10.1007/s10067-003-0792-4

Bashardoust Tajali, S., MacDermid, J.C., Grewal, R., Young, C., 2016. Reliability and Validity of Electro-Goniometric Range of Motion Measurements in Patients with Hand and Wrist Limitations. Open Orthop. J. 10, 190–205. https://doi.org/10.2174/1874325001610010190

Bella, S.D., Palmer, C., 2011. Rate effects on timing, key velocity, and finger kinematics in piano performance. PLoS One 6, e20518. https://doi.org/10.1371/journal.pone.0020518

Bellamy, N., Campbell, J., Haraoui, B., Gerecz-Simon, E., Buchbinder, R., Hobby, K., MacDermid, J.C., 2002. Clinimetric properties of the AUSCAN osteoarthritis hand index: An evaluation of reliability, validity and responsiveness. Osteoarthr. Cartil. 10, 863–869. https://doi.org/10.1053/joca.2002.0838

Bjurehed, L., Brodin, N., Nordenskiöld, U., Björk, M., 2017. Improved Hand Function, Self-Rated Health and Decreased Activity Limitations - results after a two month hand osteoarthritis group intervention. Arthritis Care Res. (Hoboken). https://doi.org/10.1002/acr.23431

Blana, D., Chadwick, E.K., van den Bogert, A.J., Murray, W.M., 2017. Real-time simulation of hand motion for prosthesis control. Comput. Methods Biomech. Biomed. Engin. 20, 540–549. https://doi.org/10.1080/10255842.2016.1255943

Bohannon, R.W., Peolsson, A., Massy-Westropp, N., Desrosiers, J., Bear-Lehman, J., 2006. Reference values for adult grip strength measured with a Jamar dynamometer: a descriptive meta-analysis. Physiotherapy 92, 11–15. https://doi.org/10.1016/j.physio.2005.05.003

Bullock, I.M., Borras, J., Dollar, A.M., 2012. Assessing assumptions in kinematic hand models: A review, in: 2012 4th IEEE RAS & EMBS International Conference on Biomedical Robotics and Biomechatronics (BioRob). IEEE, pp. 139–146. https://doi.org/10.1109/BioRob.2012.6290879

Cerveri, P., De Momi, E., Lopomo, N., Baud-Bovy, G., Barros, R.M.L., Ferrigno, G., 2007. Finger kinematic modeling and real-time hand motion estimation. Ann. Biomed. Eng. 35, 1989–2002. https://doi.org/10.1007/s10439-007-9364-0

Chu, C.Y., Patterson, R.M., 2018. Soft robotic devices for hand rehabilitation and assistance: A narrative review. J. Neuroeng. Rehabil. https://doi.org/10.1186/s12984-018-0350-6

Chung, K.C., Pillsbury, M.S., Walters, M.R., Hayward, R.A., 1998. Reliability and validity testing of the Michigan Hand Outcomes Questionnaire. J. Hand Surg. Am. 23, 575–587. https://doi.org/10.1016/S0363-5023(98)80042-7

Cook, J.R., Baker, N. a., Cham, R., Hale, E., Redfern, M.S., 2007. Measurements of wrist and finger postures: A comparison of goniometric and motion capture techniques. J. Appl. Biomech. 23, 70–78.

Coupier, J., Hamoudi, S., Telese-Izzi, S., Feipel, V., Rooze, M., Van Sint Jan, S., 2016. A novel method for in-vivo evaluation of finger kinematics including definition of healthy motion patterns. Clin. Biomech. 31, 47–58. https://doi.org/10.1016/j.clinbiomech.2015.10.002

Cruz, E.G., Waldinger, H.C., Kamper, D.G., 2005. Kinetic and kinematic workspaces of the index finger following stroke. Brain 128, 1112–1121. https://doi.org/10.1093/brain/awh432

Dahaghin, S., Bierma-Zeinstra, S.M.A., Ginai, A.Z., Pols, H.A.P., Hazes, J.M.W., Koes, B.W., 2005. Prevalence and pattern of radiographic hand osteoarthritis and association with pain and disability (the Rotterdam study). Ann. Rheum. Dis. 64, 682–687. https://doi.org/10.1136/ard.2004.023564

Danion, F., Schöner, G., Latash, M.L., Li, S., Scholz, J.P., Zatsiorsky, V.M., 2003. A mode hypothesis for finger interaction during multi-finger force-production tasks. Biol. Cybern. 88, 91–98. https://doi.org/10.1007/s00422-002-0336-z

Davis Sears, E., Chung, K.C., 2010. Validity and Responsiveness of the Jebsen-Taylor Hand Function Test. J. Hand Surg. Am. 35, 30–37. https://doi.org/10.1016/j.jhsa.2009.09.008

Desai, M.J., Brogan, D.M., Richard, M.J., Mithani, S.K., Leversedge, F.J., Ruch, D.S., 2016. Biomechanical Comparison of Suture-Button Suspensionplasty and LRTI for Basilar Thumb Arthritis. Hand 11, 438–443. https://doi.org/10.1177/1558944716643119

Dipietro, L., Sabatini, A.M., Dario, P., 2003. Evaluation of an instrumented glove for hand-movement acquisition. J. Rehabil. Res. Dev. 40, 181. https://doi.org/10.1682/JRRD.2003.03.0181

Dreiser, R.-L., Maheul-, E., Guillou, G.B., 2000. Sensitivity to change of the functional index for hand osteoarthritis. Osteoarthr. Cartil. 8, 25–28. https://doi.org/10.1053/JOCA.2000.0332

Drost, J., Hong, G., Bush, T., 2019. Mapping together kinetic and kinematic abilities of the hand. J.

Dziedzic, K.S., Thomas, E., Hay, E.M., 2005. A systematic search and critical review of measures of disability for use in a population survey of hand osteoarthritis (OA). Osteoarthr. Cartil. https://doi.org/10.1016/j.joca.2004.09.010

Eguchi, A., Ochi, M., Adachi, N., Deie, M., Nakamae, A., Usman, M.A., 2014. Mechanical properties of suspensory fixation devices for anterior cruciate ligament reconstruction: Comparison of the fixed-length loop device versus the adjustable-length loop device. Knee 21, 743–748. https://doi.org/10.1016/J.KNEE.2014.02.009

Ellis, B., Bruton, A., 2002. A study to compare the reliability of composite finger flexion with goniometry for measurement of range of motion in the hand. Clin. Rehabil. 16, 562–570. https://doi.org/10.1191/0269215502cr513oa

Ellis, B., Bruton, A., Goddard, J.R., 1997. Joint angle measurement: a comparative study of the reliability of goniometry and wire tracing for the hand. Clin. Rehabil. 11, 314–320. https://doi.org/10.1177/026921559701100408

Fair, J.R., Bix, L., Bush, T.R., 2008. Biomechanical Analysis of Opening Glass Jars: Using Kinematics, in: Designing Inclusive Futures. Springer London, London, pp. 45–53. https://doi.org/10.1007/978-1-84800-211-1_5

Fok, K.S., Chou, S.M., 2010. Development of a finger biomechanical model and its considerations. J. Biomech. 43, 701–713. https://doi.org/10.1016/j.jbiomech.2009.10.020

Fowler, N.., Nicol, A.., 2001. Functional and biomechanical assessment of the normal and rheumatoid hand. Clin. Biomech. 16, 660–666. https://doi.org/10.1016/S0268-0033(01)00057-2

Fowler, N.., Nicol, A.., 1999. Measurement of external three-dimensional interphalangeal loads applied during activities of daily living. Clin. Biomech. 14, 646–652. https://doi.org/10.1016/S0268-0033(99)00016-9

Freund, J., Toivonen, R., Takala, E.-P., 2002. Grip forces of the fingertips. Clin. Biomech. 17, 515–520. https://doi.org/10.1016/S0268-0033(02)00043-8

Friebel, T.R., Kleinrensink, E.T.W.G.J., Zuidam, S.R.J.M., 2018. An anatomical study on the effectiveness of Arthrex Mini - TightRope ® ligament reconstruction in an unstable trapeziometacarpal joint. Arch. Orthop. Trauma Surg. 138, 1029–1033. https://doi.org/10.1007/s00402-018-2942-9

Galna, B., Barry, G., Jackson, D., Mhiripiri, D., Olivier, P., Rochester, L., 2014. Accuracy of the Microsoft Kinect sensor for measuring movement in people with Parkinson’s disease. Gait Posture 39, 1062–1068. https://doi.org/10.1016/j.gaitpost.2014.01.008

Gao, F., Latash, M.L., Zatsiorsky, V.M., 2005. Control of finger force direction in the flexion-extension plane. Exp. Brain Res. 161, 307–315. https://doi.org/10.1007/s00221-004-2074-z

Hackel, M., Wolfe, G., Bang, S., Canfield, J., 1992. Changes in hand function in the aging adult as determined by the Jebsen Test of Hand Function. Phys. Ther.

Haugen, I.K., Englund, M., Aliabadi, P., Niu, J., Clancy, M., Kvien, T.K., Felson, D.T., 2011. Prevalence, incidence and progression of hand osteoarthritis in the general population: the Framingham Osteoarthritis Study. Ann. Rheum. Dis. 70, 1581–1586. https://doi.org/10.1136/ard.2011.150078

Haugen, I.K., Mathiessen, A., Slatkowsky-Christensen, B., Magnusson, K., Bøyesen, P., Sesseng, S., van der Heijde, D., Kvien, T.K., Hammer, H.B., 2016. Synovitis and radiographic progression in non-erosive and erosive hand osteoarthritis: Is erosive hand osteoarthritis a separate inflammatory phenotype? Osteoarthr. Cartil. 24, 647–654. https://doi.org/10.1016/j.joca.2015.11.014

Hill, S., Dziedzic, K.S., Ong, B.N., 2010. The functional and psychological impact of hand osteoarthritis. Chronic Illn. 6, 101–10. https://doi.org/10.1177/1742395309345614

Hoffmann, G., Conrad, M.O., Qiu, D., Kamper, D.G., 2015. Contributions of voluntary activation deficits to hand weakness after stroke. Top. Stroke Rehabil. 9357, 1945511915Y0000000023. https://doi.org/10.1179/1945511915Y.0000000023

Hofmann, A., Goebl, W., 2016. Finger forces in clarinet playing. Front. Psychol. 7, 1140. https://doi.org/10.3389/fpsyg.2016.01140

Hooke, A.W., Parry, J.A., Kakar, S., 2016. Mini Tightrope Fixation Versus Ligament Reconstruction - Tendon Interposition for Maintenance of Post-trapeziectomy Space Height: A Biomechanical Study. J. Hand Surg. Am. 41, 399–403. https://doi.org/10.1016/j.jhsa.2015.12.007

Howard, B., Yang, J., Ozsoy, B., 2014. Optimal Posture and Supporting Hand Force Prediction for Common Automotive Assembly One-Handed Tasks. J. Mech. Robot. 6, 021009. https://doi.org/10.1115/1.4025749

Huang, K., Hollevoet, N., Giddins, G., 2015. Thumb carpometacarpal joint total arthroplasty: A systematic review. J. Hand Surg. Eur. Vol. 40, 338–350. https://doi.org/10.1177/1753193414563243

Hudak, P.L., Amadio, P.C., Bombardier, C., 1996. Development of an upper extremity outcome measure: the DASH (disabilities of the arm, shoulder and hand) [corrected]. The Upper Extremity Collaborative Group (UECG). Am. J. Ind. Med. 29, 602–8. https://doi.org/10.1002/(SICI)1097-0274(199606)29:6<602::AID-AJIM4>3.0.CO;2-L

Hume, M.C., Gellman, H., McKellop, H., Brumfield, R.H., 1990. Functional range of motion of the joints of the hand. J. Hand Surg. Am. 15, 240–243. https://doi.org/10.1016/0363-5023(90)90102-W

Igoe, D., Middleton, C., Hammert, W., 2014. Evolution of basal joint arthroplasty and technology in hand surgery. J. Hand Ther. 27, 115–121. https://doi.org/10.1016/j.jht.2013.10.004

Kamper, D.G., Fischer, H.C., Cruz, E.G., 2006. Impact of finger posture on mapping from muscle activation to joint torque. Clin. Biomech. 21, 361–369. https://doi.org/10.1016/j.clinbiomech.2005.11.005

Kapur, S., Friedman, J., Zatsiorsky, V.M., Latash, M.L., 2010. Finger interaction in a three-dimensional pressing task. Exp. Brain Res. 203, 101–118. https://doi.org/10.1007/s00221-010-2213-7

Khalid, M., Jones, M.L., 2012. Index Metacarpal Fracture After Tightrope Suspension Following Trapeziectomy: Case Report. J. Hand Surg. Am. 37, 418–422. https://doi.org/10.1016/J.JHSA.2011.12.017

Kinoshita, H., Obata, S., Nasu, D., Kadota, K., Matsuo, T., Fleisig, G.S., 2017. Finger forces in fastball baseball pitching. Hum. Mov. Sci. 54, 172–181. https://doi.org/10.1016/j.humov.2017.04.007

Kong, Y.-K., Lowe, B.D., 2005. Optimal cylindrical handle diameter for grip force tasks. Int. J. Ind. Ergon. 35, 495–507. https://doi.org/10.1016/j.ergon.2004.11.003

Lawrence, R.C., Felson, D.T., Helmick, C.G., Arnold, L.M., Choi, H., Deyo, R.A., Gabriel, S., Hirsch, R., Hochberg, M.C., Hunder, G.G., Jordan, J.M., Katz, J.N., Kremers, H.M., Wolfe, F., 2008. Estimates of the prevalence of arthritis and other rheumatic conditions in the United States. Part II. Arthritis Rheum. 58, 26–35. https://doi.org/10.1002/art.23176

Lee, K.S., Jung, M.C., 2016. Three-dimensional finger joint angles by hand posture and object properties. Ergonomics 59, 890–900. https://doi.org/10.1080/00140139.2015.1108458

Lee, S.W., Chen, H., Towles, J.D., Kamper, D.G., 2008. Estimation of the effective static moment arms of the tendons in the index finger extensor mechanism. J. Biomech. 41, 1567–1573. https://doi.org/10.1016/j.jbiomech.2008.02.008

Leitkam, S.T., Bix, L., de la Fuente, J., Reid Bush, T., 2015. Mapping kinematic functional abilities of the hand to three dimensional shapes for inclusive design. J. Biomech. 48, 2903–2910. https://doi.org/10.1016/j.jbiomech.2015.04.025

Leitkam, S.T., Bush, T.R., Bix, L., 2014. Determining Functional Finger Capabilities of Healthy Adults: Comparing Experimental Data to a Biomechanical Model. J. Biomech. Eng. 136, 021022. https://doi.org/10.1115/1.4026255

Leitkam, S.T., Reid Bush, T., 2015. Comparison Between Healthy and Reduced Hand Function Using Ranges of Motion and a Weighted Fingertip Space Model. J. Biomech. Eng. 137, 041003. https://doi.org/10.1115/1.4029215

Li, Y.K., White, C., Ignacy, T.A., Thoma, A., 2011. Comparison of trapeziectomy and trapeziectomy with ligament reconstruction and tendon interposition: A systematic literature review. Plast. Reconstr. Surg. https://doi.org/10.1097/PRS.0b013e318217435a

Li, Z.-M., Pfaeffle, H.J., Sotereanos, D.G., Goitz, R.J., Woo, S.L.-Y., 2003. Multi-directional strength and force envelope of the index finger. Clin. Biomech. 18, 908–915. https://doi.org/10.1016/S0268-0033(03)00178-5

Li, Z.M., 2002. The influence of wrist position on individual finger forces during forceful grip. J. Hand Surg. Am. 27, 886–896. https://doi.org/10.1053/jhsu.2002.35078

Lue, S., Koppikar, S., Shaikh, K., Mahendira, D., Towheed, T.E., 2017. Systematic review of non-surgical therapies for osteoarthritis of the hand: an update. Osteoarthr. Cartil. 25, 1379–1389. https://doi.org/10.1016/j.joca.2017.05.016

Magni, N.E., McNair, P.J., Rice, D.A., 2017. The effects of resistance training on muscle strength, joint pain, and hand function in individuals with hand osteoarthritis: a systematic review and meta-analysis. Arthritis Res. Ther. 19, 131. https://doi.org/10.1186/s13075-017-1348-3

Mahendira, D., Towheed, T.E., 2009. Systematic review of non-surgical therapies for osteoarthritis of the hand: an update. Osteoarthr. Cartil. https://doi.org/10.1016/j.joca.2009.04.006

Martin, J., Zatsiorsky, V., Latash, M., 2011. Multi-finger interaction during involuntary and voluntary single finger force changes. Exp. brain Res.

McVeigh, K.H., Murray, P.M., Heckman, M.G., Rawal, B., Peterson, J.J., 2016. Accuracy and Validity of Goniometer and Visual Assessments of Angular Joint Positions of the Hand and Wrist. J. Hand Surg. Am. 41, e21–e35. https://doi.org/10.1016/j.jhsa.2015.12.014

Michalsen, A., Lüdtke, R., Cesur, Ö., Afra, D., Musial, F., Baecker, M., Fink, M., Dobos, G.J., 2008. Effectiveness of leech therapy in women with symptomatic arthrosis of the first carpometacarpal joint: A randomized controlled trial. Pain 137, 452–459. https://doi.org/10.1016/j.pain.2008.03.012

Miller, A., Jones, C., Martin, D., Liss, F., Abboudi, J., Kirkpatrick, W., Beredjiklian, P., 2018. Reliability of Metacarpal Subsidence Measurements after Thumb Carpometacarpal Joint Arthroplasty. J. Hand Microsurg. 10, 022–025. https://doi.org/10.1055/s-0037-1618912

Moe, R.H., Garratt, A., Slatkowsky-Christensen, B., Maheu, E., Mowinckel, P., Kvien, T.K., Kjeken, I., Hagen, K.B., Uhlig, T., 2010. Concurrent evaluation of data quality, reliability and validity of the Australian/Canadian Osteoarthritis Hand Index and the Functional Index for Hand Osteoarthritis. Rheumatology 49, 2327–2336. https://doi.org/10.1093/rheumatology/keq219

Mousavi Hondori, H., Khademi, M., 2014. A Review on Technical and Clinical Impact of Microsoft Kinect on Physical Therapy and Rehabilitation. J. Med. Eng. 2014, 1–16. https://doi.org/10.1155/2014/846514

Nanno, M., Buford, W.L., Patterson, R.M., Andersen, C.R., Viegas, S.F., 2007. Three-dimensional analysis of the ligamentous attachments of the second through fifth carpometacarpal joints. Clin. Anat. 20, 530–544. https://doi.org/10.1002/ca.20426

Nataraj, R., Li, Z.-M., 2013. Robust Identification of Three-Dimensional Thumb and Index Finger Kinematics With a Minimal Set of Markers. J. Biomech. Eng. 135, 091002. https://doi.org/10.1115/1.4024753

Nicolay, C.W., Walker, A.L., 2005. Grip strength and endurance: Influences of anthropometric variation, hand dominance, and gender. Int. J. Ind. Ergon. 35, 605–618.

https://doi.org/10.1016/j.ergon.2005.01.007

Oikonomidis, I., Kyriazis, N., Argyros, A., 2011. Efficient model-based 3D tracking of hand articulations using Kinect, in: Procedings of the British Machine Vision Conference 2011. pp. 101.1-101.11. https://doi.org/10.5244/C.25.101

Parry, J.A., Kakar, S., 2015. Dual mini tightrope suspensionplasty for thumb basilar joint arthritis: A case series. J. Hand Surg. Am. 40, 297–302. https://doi.org/10.1016/j.jhsa.2014.10.057

Peh, W.C.G., Patterson, R.M., Viegas, S.F., Hokanson, J.A., Gilula, L.A., 1999. Radiographic-Anatomic Correlation at Different Wrist Articulations. J. Hand Surg. Am. 24, 777–780. https://doi.org/10.1053/jhsu.1999.0777

Pereira, D., Peleteiro, B., Araújo, J., Branco, J., Santos, R.A., Ramos, E., 2011. The effect of osteoarthritis definition on prevalence and incidence estimates: a systematic review. Osteoarthritis Cartilage 19, 1270–85. https://doi.org/10.1016/j.joca.2011.08.009

Polygerinos, P., Galloway, K.C., Sanan, S., Herman, M., Walsh, C.J., 2015. EMG controlled soft robotic glove for assistance during activities of daily living, in: 2015 IEEE International Conference on Rehabilitation Robotics (ICORR). IEEE, pp. 55–60. https://doi.org/10.1109/ICORR.2015.7281175

Prodinger, B., Stamm, T., Peterson, D., Stucki, G., Tennant, A., 2016. Toward a Standardized Reporting of Outcomes in Hand Osteoarthritis: Developing a Common Metric of Outcome Measures Commonly Used to Assess Functioning. Arthritis Care Res. (Hoboken). 68, 1115–1127. https://doi.org/10.1002/acr.22816

Qin, J., Barbour, K.E., Murphy, L.B., Nelson, A.E., Schwartz, T.A., Helmick, C.G., Allen, K.D., Renner, J.B., Baker, N.A., Jordan, J.M., 2017. Lifetime Risk of Symptomatic Hand Osteoarthritis: The Johnston County Osteoarthritis Project. Arthritis Rheumatol. 69, 1204–1212. https://doi.org/10.1002/art.40097

Qiu, D., Fischer, H.C., Kamper, D.G., 2009. Muscle activation patterns during force generation of the index finger. Conf. Proc. IEEE Eng. Med. Biol. Soc. 2009, 3987–3990. https://doi.org/10.1109/IEMBS.2009.5333525

Qiu, D., Kamper, D.G., 2014. Orthopaedic applications of a validated force-based biomechanical model of the index finger. Conf. Proc. ... Annu. Int. Conf. IEEE Eng. Med. Biol. Soc. IEEE Eng. Med. Biol. Soc. Annu. Conf. 2014, 4013–6. https://doi.org/10.1109/EMBC.2014.6944504

Quaine, F., Paclet, F., Letué, F., Moutet, F., 2012. Force sharing and neutral line during finger extension tasks. Hum. Mov. Sci. 31, 749–757. https://doi.org/10.1016/j.humov.2011.09.001

Ranganathan, V.K., Siemionow, V., Sahgal, V., Yue, G.H., 2001. Effects of Aging on Hand Function. J. Am. Geriatr. Soc. 49, 1478–1484. https://doi.org/10.1046/j.1532-5415.2001.4911240.x

Ruiz-Ruiz, J., Mesa, J.L.M., Gutiérrez, A., Castillo, M.J., 2002. Hand size influences optimal grip span in women but not in men. J. Hand Surg. Am. 27, 897–901. https://doi.org/10.1053/jhsu.2002.34315

Sancho-Bru, J.L., Pérez-González, A., Vergara-Monedero, M., Giurintano, D., 2001. A 3-D dynamic model of human finger for studying free movements. J. Biomech. 34, 1491–1500. https://doi.org/10.1016/S0021-9290(01)00106-3

Sandqvist, G., Eklund, M., 2000a. Hand Mobility in Scleroderma (HAMIS) test: the reliability of a novel hand function test. Arthritis Care Res. 13, 369–374. https://doi.org/10.1002/1529-0131(200012)13:6<369::AID-ART6>3.0.CO;2-X

Sandqvist, G., Eklund, M., 2000b. Validity of HAMIS: a test of hand mobility in scleroderma. Arthritis Care Res. 13, 382–387. https://doi.org/Doi 10.1002/1529-0131(200012)13:6<382::Aid-Art8>3.0.Co;2-9

Sanford, J., Young, C., Popa, D., Bugnariu, N., Patterson, R., 2014. Grip pressure measurements during activities of daily life, in: Popa, D.O., Wijesundara, M.B.J. (Eds.), Proc. SPIE 9116, Next-Generation Robots and Systems, 91160H (June 5, 2014). International Society for Optics and Photonics, p. 10. https://doi.org/10.1117/12.2060167

Scott, J., Huskisson, E.C., 1976. Graphic representation of pain. Pain 2, 185–195. https://doi.org/10.1016/0304-3959(76)90114-7

Seo, N.J., Armstrong, T.J., 2008. Investigation of Grip Force, Normal Force, Contact Area, Hand Size, and Handle Size for Cylindrical Handles. Hum. Factors J. Hum. Factors Ergon. Soc. 50, 734–744. https://doi.org/10.1518/001872008X354192

Seo, N.J., Rymer, W.Z., Kamper, D.G., 2010. Altered digit force direction during pinch grip following stroke. Exp. Brain Res. 202, 891–901. https://doi.org/10.1007/s00221-010-2193-7

Serbest, K., Cilli, M., Yildiz, M.Z., Eldogan, O., 2016. Development of a human hand model for estimating joint torque using MATLAB tools, in: 2016 6th IEEE International Conference on Biomedical Robotics and Biomechatronics (BioRob). IEEE, pp. 793–797. https://doi.org/10.1109/BIOROB.2016.7523724

Sharp, T., Wei, Y., Freedman, D., Kohli, P., Krupka, E., Fitzgibbon, A., Izadi, S., Keskin, C., Robertson, D., Taylor, J., Shotton, J., Kim, D., Rhemann, C., Leichter, I., Vinnikov, A., 2015. Accurate, Robust, and Flexible Real-time Hand Tracking, in: Proceedings of the 33rd Annual ACM Conference on Human Factors in Computing Systems - CHI '15. ACM Press, New York, New York, USA, pp. 3633–3642. https://doi.org/10.1145/2702123.2702179

Shivers, C.L., Mirka, G.A., Kaber, D.B., 2002. Effect of Grip Span on Lateral Pinch Grip Strength. Hum. Factors J. Hum. Factors Ergon. Soc. 44, 569–577. https://doi.org/10.1518/0018720024496999

Simone, L.K., Elovic, E., Kalambur, U., Kamper, D., 2005. A low cost method to measure finger flexion in individuals with reduced hand and finger range of motion, in: The 26th Annual International Conference of the IEEE Engineering in Medicine and Biology Society. IEEE, pp. 4791–4794. https://doi.org/10.1109/IEMBS.2004.1404326

Smaby, N., Elise Johanson, M., Baker, B., Ellen Kenney, D., Marie Murray, W., Rod Hentz, V., 2004. Identification of key pinch forces required to complete functional tasks. JRRD 41, 215–224.

Storey, P., Gadd, R.J., Blundell, C., Davies, M.B., 2012. Complications of Suture Button Ankle Syndesmosis Stabilization with Modifications of Surgical Technique. Foot Ankle Int. 33, 717–721. https://doi.org/10.3113/FAI.2012.0717

Swanson, A.B., 1964. Evaluation of Impairment of Function in the Hand. Surg. Clin. North Am. 44, 925–940. https://doi.org/10.1016/S0039-6109(16)37334-0

Thompson, J.C., Netter, F.H., 2010. Netter's concise orthopaedic anatomy, Netter clinical science. https://doi.org/10.1016/B978-1-4160-5987-5.50014-0

Towheed, T.E., 2005. Systematic review of therapies for osteoarthritis of the hand. Osteoarthr. Cartil. https://doi.org/10.1016/j.joca.2005.02.009

Valero-Cuevas, F.J., 2005. An integrative approach to the biomechanical function and neuromuscular control of the fingers. J. Biomech. https://doi.org/10.1016/j.jbiomech.2004.04.006

Valero-Cuevas, F.J., Zajac, F.E., Burgar, C.G., 1998. Large index-fingertip forces are produced by subject-independent patterns of muscle excitation. J. Biomech. 31, 693–703. https://doi.org/10.1016/S0021-9290(98)00082-7

Venkadesan, M., Valero-Cuevas, F.J., 2008. Neural control of motion-to-force transitions with the fingertip. J. Neurosci. 28, 1366–73. https://doi.org/10.1523/JNEUROSCI.4993-07.2008

Vermeulen, G.M., Slijper, H., Feitz, R., Hovius, S.E.R., Moojen, T.M., Selles, R.W., 2011. Surgical Management of Primary Thumb Carpometacarpal Osteoarthritis: A Systematic Review. J. Hand Surg. Am. 36, 157–169. https://doi.org/10.1016/J.JHSA.2010.10.028

Viegas, S.F., Crossley, M., Marzke, M., Wullstein, K., 1991. The fourth carpometacarpal joint. J. Hand Surg. Am. 16, 525–533. https://doi.org/10.1016/0363-5023(91)90026-8

Viegas, S.F., Patterson, R.M., Hokanson, J.A., Davis, J., 1993. Wrist anatomy: incidence, distribution, and correlation of anatomic variations, tears, and arthrosis. J. Hand Surg. Am. 18, 463–75. https://doi.org/10.1016/0363-5023(93)90094-J

Vieluf, S., Godde, B., Reuter, E.M., Voelcker-Rehage, C., 2013. Age-related differences in finger force control are characterized by reduced force production. Exp. Brain Res. 224, 107–117. https://doi.org/10.1007/s00221-012-3292-4

Villafañe, J.H., Valdes, K., Bertozzi, L., Negrini, S., 2014. Minimal Clinically Important Difference of Grip and Pinch Strength in Women With Thumb Carpometacarpal Osteoarthritis When Compared to Healthy Subjects. Rehabil. Nurs. n/a-n/a. https://doi.org/10.1002/rnj.196

Visser, A.W., Boyesen, P., Haugen, I.K., Schoones, J.W., van der Heijde, D.M., Rosendaal, F.R., Kloppenburg, M., 2015. Instruments Measuring Pain, Physical Function, or Patient's Global Assessment in Hand Osteoarthritis: A Systematic Literature Search. J. Rheumatol. 42, 2118–2134. https://doi.org/10.3899/jrheum.141228

Wohlman, S.J., Murray, W.M., 2013. Bridging the gap between cadaveric and in vivo experiments: A biomechanical model evaluating thumb-tip endpoint forces. J. Biomech. 46, 1014–1020. https://doi.org/10.1016/j.jbiomech.2012.10.044

Wu, J.Z., An, K.-N., Cutlip, R.G., Krajnak, K., Welcome, D., Dong, R.G., 2008. Analysis of musculoskeletal loading in an index finger during tapping. J. Biomech. 41, 668–676. https://doi.org/10.1016/J.JBIOMECH.2007.09.025

Yao, J., Song, Y., 2013. Suture-Button Suspensionplasty for Thumb Carpometacarpal Arthritis: A Minimum 2-Year Follow-Up. J. Hand Surg. Am. 38, 1161–1165. https://doi.org/10.1016/J.JHSA.2013.02.040

Yokogawa, R., Hara, K., 2002. Measurement of Distribution of Maximum Index-Fingertip Force in all Directions at Fingertip in Flexion/Extension Plane. J. Biomech. Eng. 124, 302. https://doi.org/10.1115/1.1468637

Young, J.G., Woolley, C., Armstrong, T.J., Ashton-Miller, J.A., 2010. Hand-Handhold Coupling: Effect of Handle Shape, Orientation, and Friction on Breakaway Strength. Hum. Factors J. Hum. Factors Ergon. Soc. 51, 705–717. https://doi.org/10.1177/0018720809355969

Zhang, Y., Niu, J., Kelly-Hayes, M., Chaisson, C.E., Aliabadi, P., Felson, D.T., 2002. Prevalence of symptomatic hand osteoarthritis and its impact on functional status among the elderly: The framingham study. Am. J. Epidemiol. 156, 1021–1027. https://doi.org/10.1093/aje/kwf141